Mechanistic Studies on AdoCbl-dependent Glutamate Mutase

by

Miri Yoon

A dissertation submitted in partial fulfillment
of the requirements for the degree of
Doctor of Philosophy
(Chemistry)
in The University of Michigan
2009

Doctoral Committee:

Professor E. Neil G. Marsh, Chair
Associate Professor Hashim M. Al-Hashimi
Assistant Professor Kristina Håkansson
Assistant Professor Bruce A. Palfey

ACKNOWLEDGEMENTS

I would like to express my gratitude to all those who helped to complete my doctoral study and this thesis.

Most of all, I would like to thank my advisor, Prof. Neil Marsh. He allowed me an opportunity to study the fascinating enzymology in his group. I always appreciated the way he guided and encouraged me and also amazed with his patience. Without his support and guidance I could had not completed or achieved anything I have done for my doctoral study.

I thank my committee members, Dr. Hakansson, Dr. Al-Hahimi, and Dr. Palfey for their guidance and being so nice to me all the time.

I thank collaborators Natasa and Hangtian in Dr. Hakansson's group, for their great efforts helping me on mass spectrometry and Steven and Ann in Professor Geroge Reed's laboratory for computational simulation work for EPR spectroscopy.

I also would like to thank former and current colleagues in Marsh Lab. Chris, *deceased* Joanne, Lindsey, Yeol, Anjali, Chunhua, Mou-chi, Lei, Roberto, Dustin, Eric, and Ben for their help friendship.

Also special thanks to Namhee, Michael J., and M.D., my best friends over the doctoral years, for always being there for me whenever I need their supports and comfort. Wish them all to be successful in their doctoral studies and future careers.

Finally and most importantly, I would like to thank my parents for everything, their love, support, prayer for me, belief in me, raising me strong enough and allowing me to be ambitious as I wanted. I also thank my brother for visiting this 'full of snow' town to encourage me last winter when I struggled with writing the first chapter of this thesis.

TABLE OF CONTENTS

LIST OF FIGURES

LIST OF TABLES

LIST OF ABBREVIATIONS

13-*(S)* HPOD	13-(*S*)-*hydroperoxy*-9,11-(Z,E)–octadecadienoic acid
2° KIE	Secondary kinetic isotope effect
5’dA	5’deoxyadenosine
AADH	Aromatic amine dehydrogenase
ADH	Alcoholdehydrogenase
AdoCbl	Adenosylcobalamin
ATP	Adenosine-5'-triphosphate
β-NpCbl	β-neopentylcobalamin
Cbl(II)	Cob(II)alamin
cDHFR	Chromosomal DHFR from *E. coli*
Co-C	Cobalt-Carbon
DHFR	Dihydrofolate reductase
DTT	Dithiothreitol
E. coil	Escherichia coli
*Ec*DHFR	*E. coil* Dihydrofolate reductase
EIE	Equilibrium isotope effect
EPR	Electron paramagnetic resonance
F.C. term	Franck-Condon term
FT-ICR MS	Fourier transform ion cyclotron resonance mass spectrometry

GlmES	Glutamate muase ES; fusion protein of glutamate mutase
GS	Ground state
HCl	Hydrochloric acid
His	Histidine
HLADH	Horse liver alcholdehydrogenase
HPLC	High-performance liquid chromatography
HT	Hydrogen tunneling
htADH	Thermophilic alcohol dehydrogenase
HX-MS	Hydrogen-deuterium exchange mass spectrometry
IPTG	Isopropyl-β-D-thiogalactopyranoside
KIE	Kinetic isotope effect
KSI	Ketosteroid isomerase
LA	Linoleic acid
MADH	Methylamine dehydrogenase
MMCM	Methymalnoly-CoA mutase
MR	Morphinone reductase
NAD^+	Nicotinamide adenine dinucleotide
Ni-NTA	Nickel-nitrilotriacetic acid
OD	Optical density
PETNR	Pentaerythritol tetranitrate reductase
PMSF	Phenylmethylsulphonyl fluoride
RQF	Rapid quench flow
SAM	S-adenosyl-L-methionine
SDS PAGE	Sodium dodecyl sulfate polyacrylamide gel electrophoresis

SLO-1	Soybean lipoxygenase-1
TFA	Trifluoroacetic acid
TmDHFR	Thermophilic dihydrofolate reductase
TRS	Tunneling-ready configuration
TS	Transition state
U.V.-vis	Ultraviolet-visible
ZPE	Zero point energy

ABSTRACT

Mechanistic Studies on AdoCbl-dependent Glutamate Mutase

by

Miri Yoon

Chair: E. Neil G. Marsh

Adenosylcobalamin (AdoCbl) serves as a source of free radicals for a group of enzymes that catalyze unusual rearrangements involving hydrogen atom migration and proceed through a mechanism involving carbon-based free radical intermediates. Despite more than 50 years of detailed studies on AdoCbl-dependent enzymes, how enzymes catalyze homolysis of the cobalt-carbon bond of the coenzyme and stabilize the resulting free radicals is not well understood. AdoCbl-dependent glutamate mutase is a one of the simplest enzymes in which radical chemistry is employed.

To better understand how the structure of the substrate influences the energetics of radical formation, the reaction of glutamate mutase with a glutamate analogue, 2-

thiolglutarate has been investigated. 2-Thiolglutarate mimics the reaction with the natural substrate, glutamate however, abstraction of hydrogen from 2-thiolglutarate appears to be irreversible. This is most likely because upon forming the thioglutaryl radical, fragmentation occurs immediately to form the stable thioglycolyl radical which is too stable for the reaction to proceed toward the rearranged product due to delocalization of the unpaired electron on sulfur.

Intrinsic deuterium KIE for hydrogen transfer between substrate and AdoCbl in glutamate mutase was measured by a novel experiment, employing intra-molecular isotope competition with a regio-specifically mono-deuterated substrate followed by analysis by high-resolution mass spectrometry. The intrinsic KIE in glutamate mutase was 7 ± 0.4 at 0 °C. This method was applied to investigate hydrogen tunneling effects in glutamate mutase. Temperature dependence studies on deuterium kinetic isotope effects in glutamate mutase between – 2.5 °C and 7.5 °C found the apparent isotope effects on A_H/A_D ~0.03 and $\Delta Ea_{(D-H)}$ = 2.8 ± 0.5 kcal mol^{-1}. This result demonstrates that hydrogen is extensively tunneling whereas deuterium is not. This is similar to the situation found for other AdoCbl-dependent systems studied previously, however deuterium KIE in glutamate mutase is much smaller. The reduced KIE in glutamate mutase can be explained based on previous secondary KIE studies which suggested coupling of the motions of the primary and secondary hydrogens combined with tunneling.

Chapter 1 Introduction

1.1 Free Radicals in Enzymatic Reactions

Biochemically, the generation of free radicals from stable, closed shell molecules is very challenging because this is highly endothermic. Free radicals are generally highly unstable, short lived species and react very non-specifically in solution. In contrast, when generated at the active site of an enzyme they can be very stable and catalyze remarkably specific reactions. Radicals are potentially useful species in enzymatic catalysis because of their high reactivity and special properties such as the ability to cleave or form non-activated carbon-hydrogen, carbon-carbon, carbon-oxygen, carbon-nitrogen and carbon sulfur bonds. The list of enzymes that employ unpaired electrons, in the form of organic-based free radical intermediates as part of their catalytic cycles continues to expand.

Organic radicals facilitate a variety of unusual and important enzymatic reactions such as isomerizations, nucleotide reduction for DNA biosynthesis, several processes in vitamin biosynthesis, and essential steps in energy transduction. Because free radicals are so reactive and nonselective, they need to be carefully controlled by enzymes to prevent side reactions, enzyme inactivation or damage, unwanted products, or the release of radical intermediates that may result in damage to the cell due to their substantial and unspecific reactivity. Therefore, once a radical is generated, an important function of the enzyme is to guide the very reactive intermediate along the desired reaction path. How enzymes generates and control free radicals is a major topic of investigation within the

field of enzymology. My research has focused on investigating the mechanism of one class of free radical enzymes that uses coenzyme B_{12} to generate free radicals.

1.2 Coenzyme B_{12}

Adenosylcobalamin (AdoCbl) also known as coenzyme B_{12} is a biologically active form of vitamin B_{12} or cyanocobalamin. Vitamin B_{12} deficiency is the cause of pernicious anemia, a disease of unknown etiology that was often fatal. Vitamin B_{12} was discovered 60 years ago in Folkers' and Smith's laboratories from its ability to cure pernicious anemia and identified as the anti-pernicious anemia factor present in the liver. The structure of vitamin B_{12}, the most chemically complex of all the vitamins, was revealed by x-ray crystallographic studies in the Hodgkin laboratory in 1954.

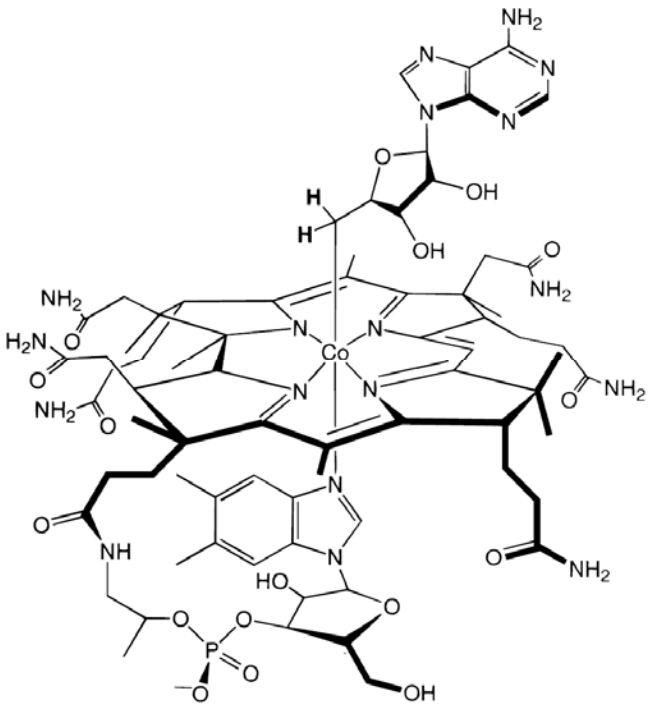

Figure 1.1 Structure of adenosylcobalamin

Vitamin B_{12} is based on a tetrapyrolle-derived corrin ring with a central hexa-coordinated cobalt atom. Four of the six coordination sites are provided by nitrogen atoms in the corrin ring and a fifth by a nitrogen ligand from dimethylbenzimidazole (Figure 1.1). The sixth coordination site, the center of reactivity, is variable, being a cyano group (-CN) or a hydroxyl group (-OH), in the metabolically inactive forms of the coenzyme, or a methyl group (-CH_3) or a 5'-deoxyadenosyl group on the biological active forms. In enzymes such as methylmalonyl-CoA mutase, glutamate mutase and methionine synthase the lower axial dimethylbenzimidazole ligand is not coordinated to the cobalt and is replaced instead by a histidine residue donated by the protein to form ‘‘base-off/His-on’’ conformation. However, in other enzymes, for example diol dehydrases, the dimethylbenzimidazole ligand remains coordinated.

A defined biochemical role for vitamin B_{12} remained unclear until 1958 when researchers in the laboratory of H. A. Barker discovered the first enzyme dependent on adenosylcobalamin. Glutamate mutase catalyzes the mechanistically intriguing the transformation of L-glutamate to L-threo-3-methylaspartate which occurs during fermentation of glutamate by *Clostridium tetanomorphum*. The biologically active cobalamin required in this reaction is known as 5’deoxyadenosylcobalmin (AdoCbl) and is different from the vitamin B_{12} found previously. Historically, the covalent carbon-cobalt bond was the first example of a carbon-metal bond discovered in biology. This cobalt-carbon bond is the key to the biological function of the cofactor, because homolytic cleavage of this bond unmasks the 5’-deoxyadenosyl radical.

1.3 Adenosylcobalamin-dependent Enzymes

1.3.1 General Mechanism of AdoCbl-dependent Isomerases

Adenosylcobalamin (AdoCbl) serves as a source of free radicals for a group of enzymes that catalyze unusual rearrangements involving 1, 2, hydrogen atom shifts. The mechanism of AdoCbl-dependent isomerases may be summarized as the interchange of a hydrogen atom on one carbon with an electron-withdrawing group, *X,* on an adjacent carbon. *X* may be either –OH, $–NH_2$, or a carbon-containing fragment, as in the case of class I mutases (Figure 1.2).

There are now 12 AdoCbl-dependent enzymes that have been identified, which may be grouped into three classes. Class I enzymes are mutases that catalyze carbon skeleton rearrangements: these include glutamate mutase, methylmalonyl-CoA mutase, 2-methyleneglutarate mutase, and isobutyryl-CoA mutase. Class II enzymes are eliminases that catalyze the migration and elimination of a heteroatom, these include ethanolamine ammonia lyase, diol dehydrase, glycerol dehydrase; ribonucleotide triphosphate reductase, which appears to be an exception, is also best included in this class. Class III enzymes are

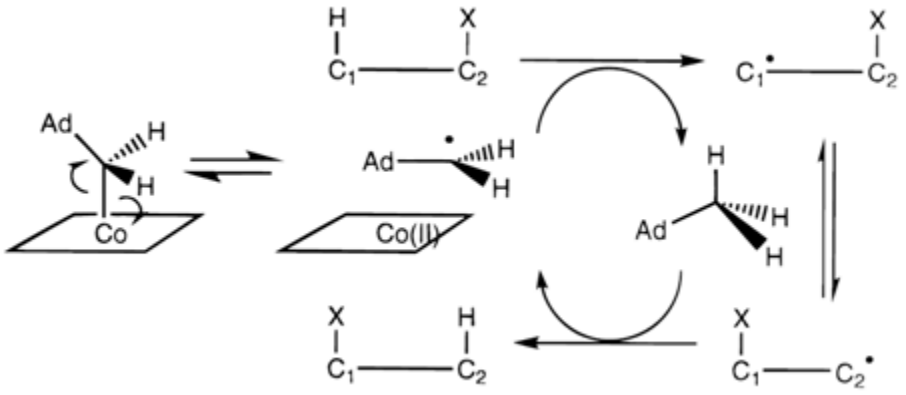

Figure 1.2 AdoCbl-dependent enzymatic carbon skeleton rearrangements

aminomutases that catalyze intermolecular 1,2-amino shifts such as D-α-lysine 5,6-aminomutase, L-β-lysine 5,6-aminomutase, Leucine 2,3-aminomutase and D-Ornithine 4,5-Aminomutase (Figure 1.3).

Class I. Carbon skeleton isomerases

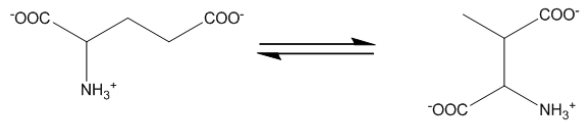

Glutamate mutase

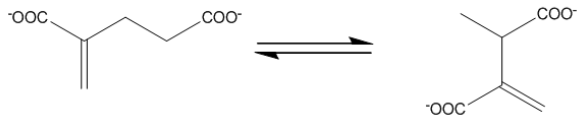

2-Methyleneglutarate mutase

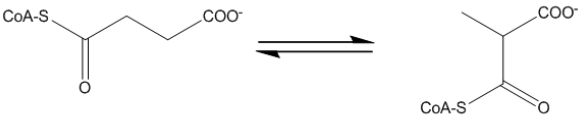

Methylmalonyl-CoA mutase

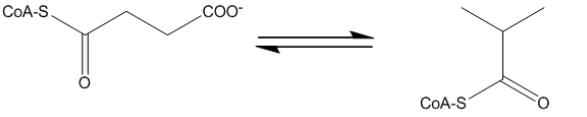

Isobtryl-CoA mutase

Class II. Heteroatom eliminases

Diol dehydrase

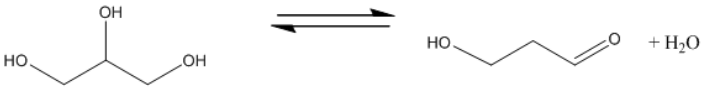

Glycerol dehydrase

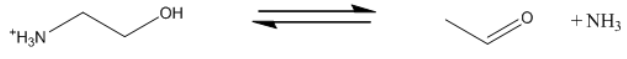

Ethanolamin ammonia lyase

Figure 1.3 AdoCbl-dependent enzyme reactions

Class II Ribonucleotide reductase

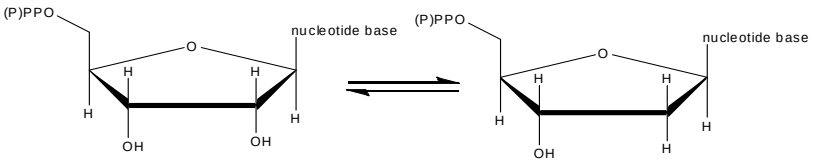

Ribonucleotide reducatse

Class III Aminomutases

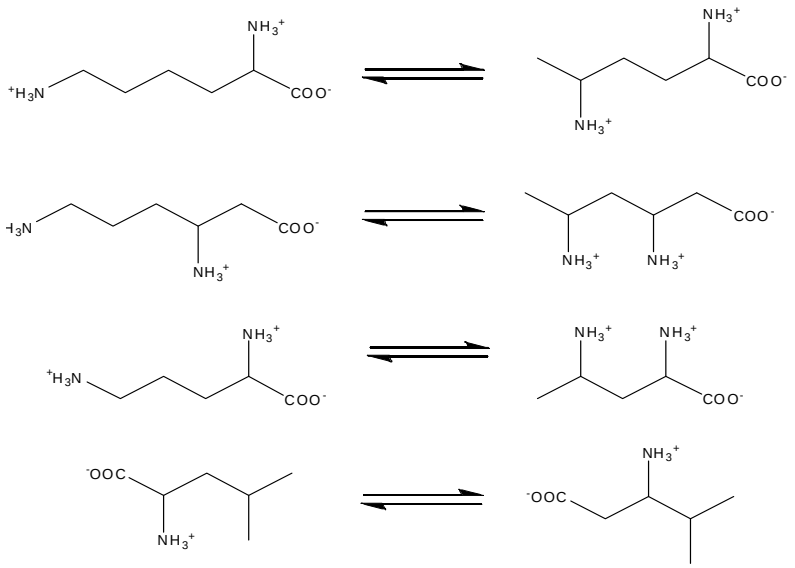

D-α-lysine aminomutase

L-β-lysine aminomutase

D-Ornithine aminomutase

Leucine aminomutase

Figure 1.3(cont.) AdoCbl-dependent enzyme reactions

The rearrangement of a substrate by an AdoCbl-dependent enzyme is a common feature of several bacterial fermentation pathways. In all the enzymes removal of a non-acidic, unreactive hydrogen atom from the substrate by the enzymatic radical is a key step in the mechanism. The only feasible way to activate the non-polar C-H bonds in the substrates of AdoCbl-dependent reactions appears to be by a free radical abstraction of hydrogen atom (Frey, 1990). In this way the substrate is activated towards chemical transformations that would otherwise not be possible.

During the catalytic cycle of such enzymes, homolysis of the Co-C bond of AdoCbl unmasks the 5'deoxyadenosyl radical, which acts as the initiator for the

formation of a substrate radical. The effective manner in which AdoCbl provides a source of 5'dA radical has been described as 'the most elegant and highly perfected radical initiator in the biosphere' (Frey, 1993). The AdoCbl-dependent enzyme must prevent this highly reactive 5'dA radical from undergoing reactions that would normally occur spontaneously in solution. For example, hydrogen abstraction from the solvent or from adventitiously placed amino acid side chains must be strictly avoided. 5'dA radical formed in the reaction of an AdoCbl-dependent enzyme remains harmless since it does not escape, but immediately abstracts a hydrogen from the substrate, which subsequently undergoes the 1, 2-rearrangement. The rearranged radical abstracts hydrogen back from $AdoCH_3$ leading to reforming of AdoCbl and completion of the catalytic cycle. For many AdoCbl-dependent enzymes, it has been demonstrated that there is no exchange of substrate hydrogen with the bulk solvent (Babior & Krouwer, 1979). This implies that the radicals are tightly bound to these enzymes. AdoCbl-dependent enzymes can therefore be regarded as a prime example of enzymatic utilization of an organic radical.

1.3.2 Homolysis of the Co-C Bond

The initial step in the mechanism of all AdoCbl-dependent enzymes is the homolysis of the carbon-cobalt bond of the coenzyme. In cleaving the bond, one electron stays with Co, formally reducing it from +3 to +2 oxidation state, and generating a low-spin cob(II)alamin while the other electron stays with the carbon atom, generating a highly reactive free radical, 5'deoxyadenosyl (5'-dA) radical (Figure 1.4). The efficacy of this process clearly hinges on the Co-ligand dissociation energy, which is apparently tuned by the protein and substrates.

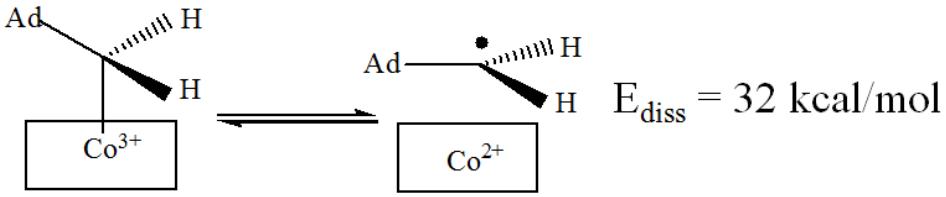

Figure 1.4 Homolysis of the cobalt-carbon bond in AdoCbl

The Co-C bond dissociation energy in AdoCbl is 32 kcal mol $^{-1}$ and the rate constant for uncatalyzed, thermally-induced homolysis is estimated to be 3.8 x 10^{-9} s^{-1}. When this is compared to the rate constant for AdoCbl-dependent enzymes (10-100s^{-1}) the homolysis reaction is accelerated by about 10^{12}-fold by the enzyme. This suggests that enzymes play a significant role in driving this unfavorable equilibrium toward homolysis reaction. However, how the enzymes accomplish the observed acceleration of Co-C bond homolysis remains unclear.

One hypothesis is that a conformational change in the enzyme induced by substrate binding increases steric crowding around the upper ligand of AdoCbl, thus weakening the Co-C bond. This hypothesis is supported by model studies which showed that bulkier upper ligands tend to decrease the bond dissociation energy of the Co-C bond of AdoCbl (Halpern, 1985). The crystal structure of glutamate mutase with AdoCbl and substrate bound has been solved. The crystal structure is especially informative because it appears to have "captured" the enzyme in the act of catalysis. The distance between the 5'-carbon of adenosine and cobalt is too long for it represent in that AdoCbl. Furthermore, the conformations of 5'dA are discernible in the electron density. In one the 5'-carbon is close to the cobalt atom; in the other it points towards the substrate. The two conformations are related by pseudo rotation of the ribose ring (Figure 1.5). These two

observed conformations suggest how glutamate mutase affords an energetically feasible transport of the C5'-radical atom from the cobalt center to the substrate and also provides a mechanism for how the protein may escort the adenosyl radical as it moves from the cobalt to the substrate (Reitzer et al. 2001).

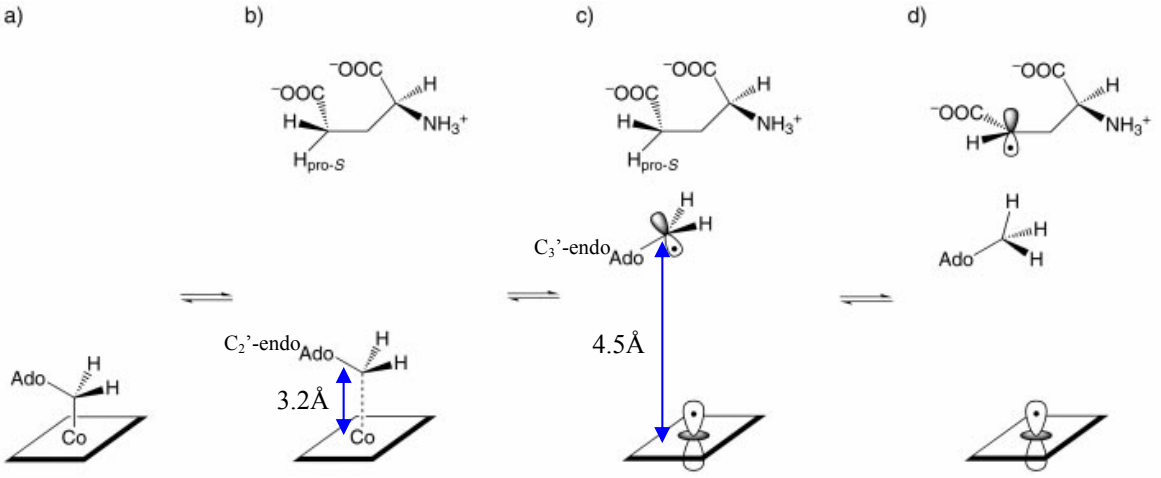

Figure 1.5 The cobalt-carbon homolysis along the reaction sequence catalyzed by glutamate mutase: a) the B_{12} cofactor without substrate; b) substrate binding induces Co-C homolysis through steric strain; c) following homolysis, the 5'-end of the Ado radical is transferred to the substrate; d) abstraction of a hydrogen atom from the substrate by the Ado radical leads to the formation of a 4-glutamyl radical and a protein-associated 5'-desoxyadenosine molecule (Reitzer et al., 2001).

1.4 Glutamate Mutase

1.4.1 Discovery of Glutamate Mutase

Glutamate mutase was the first AdoCbl-dependent enzyme to be characterized through research on the glutamate fermentation pathway in the bacterium *Clostidium tetanomorphum* in 1958. It is used by many anaerobic bacteria in the first step in the metabolic pathway to ferment (*S*)-glutamate as a carbon and energy source. More recently, its activity has been implicated in the biosynthetic pathways of various peptidyl

antibiotics. Glutamate mutase catalyzes the isomerization of L-glutamate to L-*threo*-3-methylaspartate and has been the subject of many mechanistic investigations over the years (Figure 1.6). We have chosen to study glutamate mutase because it is one of the simplest systems in which radical chemistry is employed. Insights gained from glutamate mutase will be applicable to other AdoCbl-catalyzed rearrangements and, more generally, advance our general understanding of how enzymes generate free radicals in a controlled manner at the active site, and how these reactive species are employed to catalyze novel reactions.

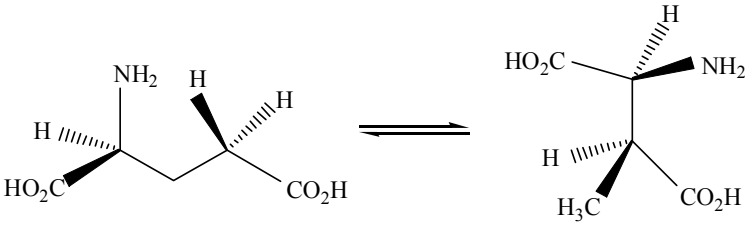

Figure 1.6 Isomerization of L-glutamate to L-threo-3-methylaspartate catalyzed by glutamate mutase

1.4.2 Structure of Glutamate Mutase

Glutamate mutase is a heterotetramer (E_2S_2) consisting of two identical larger subunits, E (*M*r = 54,000), and two identical smaller subunits, S (*M*r = 14,800) (Figure 1.7). The subunits are only weakly associated and readily be separated by gel filtration chromatography. Both subunits are required to bind AdoCbl, and in its active form the enzyme binds two molecules of AdoCbl at the interfaces between the E and S subunits. Crystal structures of the enzyme with the AdoCbl analogs methylcobalamin and cyanocobalamin bound have recently been solved by Kratky's group.

Figure 1.7 Crystal structure of the heterotetramer of glutamate mutase: shown in yellow and blue are the S subunits; shown in red and green are the E subunits

The E subunit of glutamate mutase contains the active site of the enzyme and takes the form of a $(\alpha/\beta)_8$ TIM-(triosphosphate isomerase) barrel. The two E subunits associate together via a hydrophobic contact to form a dimer. The S subunit is the conserved cobalamin binding domain, containing "D-x-H-x-x-G sequence motif that encompasses the cobalt- coordinating histidine residue. To facilitate mechanistic and structural studies on the enzyme, a fusion protein has been engineered in which the S subunit is joined to the C-terminus of the E subunit through an eleven amino acid (Gly-

Gln)$_5$-Gly linker (Figure 1.8). This enzyme, denoted as GlmES, exhibits only three-fold lower catalytic activity than the wild-type two subunit enzyme and binds substrate and coenzyme with similar affinities (Chen and Marsh, 1997).

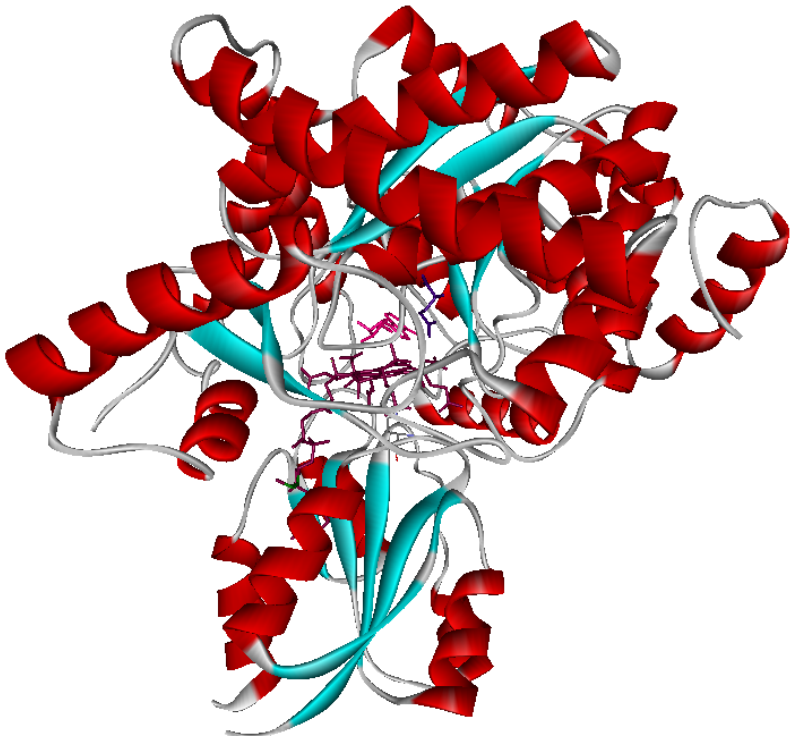

Figure 1.8 Structure of the fusion protein of glutamate mutase, GlmES

1.4.3 The Mechanism of Glutamate Mutase

In the first step of the mechanism, substrate binding to the enzyme-coenzyme complex triggers cobalt-carbon bond homolysis to generate 5'deoxyadenosyl radical. It has been demonstrated that homolysis of AdoCbl is tightly coupled to the formation of substrate-based radical. Thus, the highly reactive 5'dA radical once formed immediately abstracts a non-acidic hydrogen from C-4 position of the substrate to form 5'-

deoxyadenosine and substrate radical. The substrate radical next rearranges: the glycyl group migrates to the neighboring carbon to occupy the position previously occupied by the abstracted hydrogen, thereby producing a product radical. It has been demonstrated that this step occurs through fragmentation and recombination of an intermediate glycyl radical and acrylate. This mechanism is in contrast to the cyclic intramolecular mechanism involving a cyclopropyl carbonyl radical which is proposed for methylmalonyl-CoA and methylene glutarate. Finally, a hydrogen is transferred from the methyl group of 5'-deoxyadenosine, thereby completing the rearrangement and generating 5'-deoxyadenosyl radical which immediately recombines cobalamin(II) to form AdoCbl (Figure 1.9).

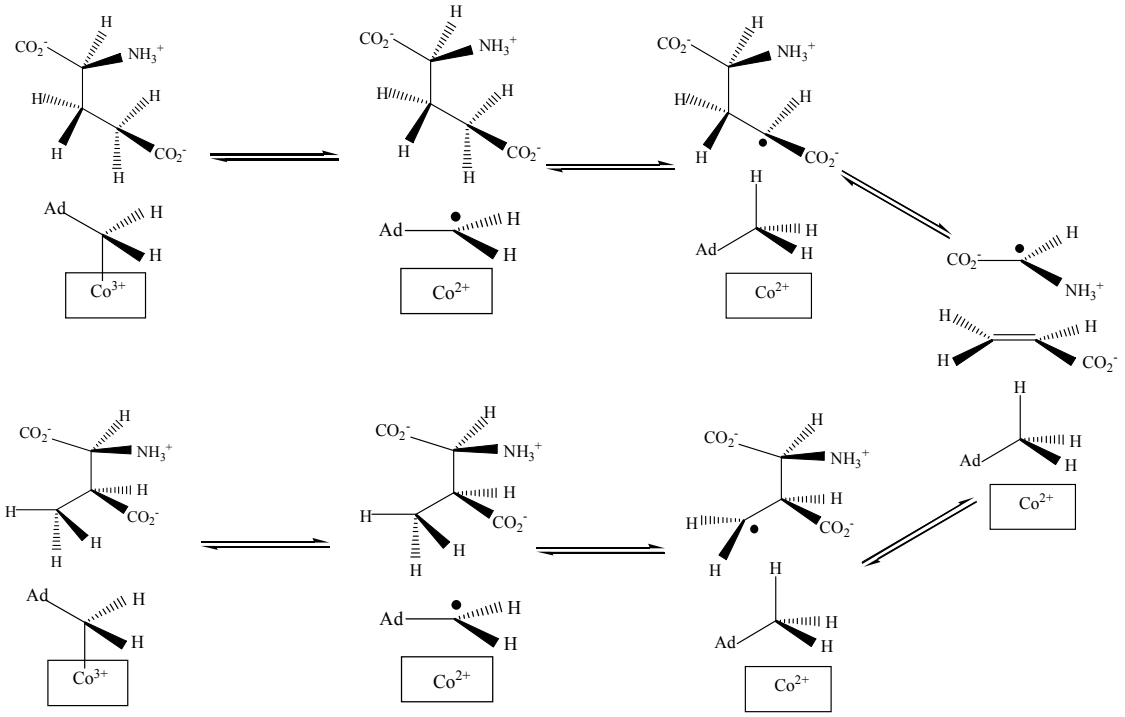

Figure 1.9 Mechanism of the reaction catalyzed by glutamate mutase

1.5 Kinetic Isotope Effects Studies on Enzymatic Reactions

1.5.1 KIE: A Powerful Tool for Studying Enzyme Mechanisms

Enzymes exhibit a remarkable power to catalyze chemically very difficult reactions extremely efficiently. Although a wide range of biochemical and structural studies have been undertaken to gain insights into enzyme catalysis, the origin of the catalytic power of enzymes is not entirely understood. Many enzymes have evolved to catalyze reactions at rates in which $\frac{k_{cat}}{K_M}$ approaches the diffusion limit while preventing unwanted side reactions. However, the key question of how enzymes reduce the activation barriers in the chemical steps is still imperfectly understood. Even site-directed mutation experiments, which are extremely useful in identifying elements of protein structure important for catalysis, cannot unambiguously identify the origin of the catalytic effect. Instead, we need a quantitative tool that is able to determine the individual contributions to the overall catalytic effect and the relationship between the structure and function. Kinetic isotope effects (KIEs) are one of the most powerful quantitative kinetic tools for analyzing enzyme mechanisms as they provide much information on the rate-limiting step in complex reactions and also insight into the microscopic nature of the transition state.

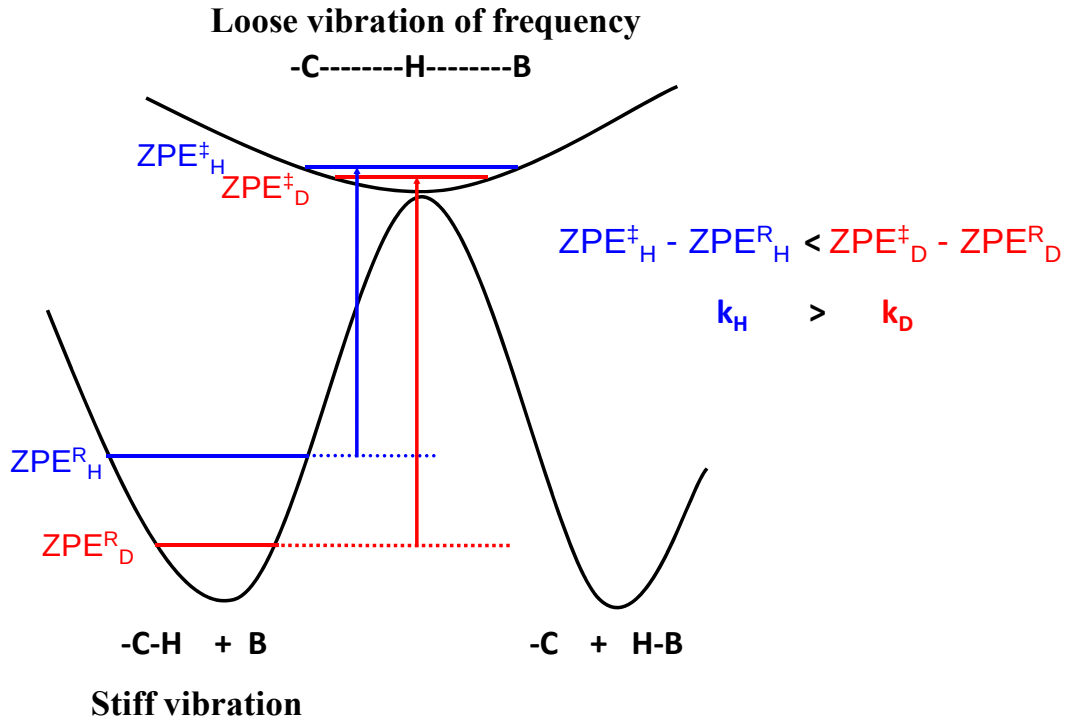

Figure 1.10 The origin of KIEs from transition state theory: ZPE_H^R is ZPE of protium at GS; ZPE_D^R, ZPE of deuterium at GS; $ZPE_H^‡$, ZPE of protium at TS; $ZPE_D^‡$, ZPE of deuterium at TS; k_H, rate of reaction involving carbon-protium bond cleavage; and k_D, rate of reaction involving carbon-deuterium bond cleavage

1.5.2 Origin of KIEs

KIEs are obtained by comparing the rate of reaction between molecules that are unlabeled and those substituted with a heavier isotope. Because of the uncertainty principle, the lowest energy level a particle can occupy is always above the electronic potential minimum (denoted as the zero point energy, ZPE). In the transition state (TS) theory one assumes that the reaction coordinate may be described by a free-energy minimum (the reactant well) and a free-energy maximum that is the saddle point leading to product. The smaller the particle, the less well defined its location and the higher its

ZPE. A major contribution to KIEs is the difference between the ZPEs of ground state (GS) and transition state (TS) among the different isotopes (Figure 1.10). The largest perturbation of the TS occurs when isotopically-labeled atoms are involved in bond breaking or making; these are called primary kinetic isotope effects.

A rapid reversible equilibrium which follows the Boltzman distribution is assumed to be responsible for the distribution of molecules between the ground state reactants and an energy rich complex of the reacting species, i.e. the transition state. For a simple reaction such as proton transfer a linear three-center molecular system can be used.

$A\text{-}H\bullet\bullet\bullet B \Rightarrow A^{-}\bullet\bullet\bullet HB^{+}$

Based on TS theory, the KIEs are exponentially proportional to the reciprocal absolute temperature (1/T) and difference of activation energy as reflected by the Arrhenius equation.

$$k(T) = Ae^{\frac{-\Delta Ea(T)}{RT}} \qquad \text{Eq. 1}$$

where A is the preexponential factor, ΔE_a is the activation energy difference between TS and GS, and R is the gas constant.

For H versus D transfer, the KIE is given by

$$\frac{k_H}{k_D} = \frac{A_H}{A_D}\exp\left(\frac{-(\Delta E_{a,H} - \Delta E_{a,D})}{RT}\right) \qquad \text{Eq. 2}$$

where A_H is Arrhenius factor for H and A_D Arrhenius factor for D.

And the activation energy difference is given as equation 3.

$$\Delta E_{a,H} - \Delta E_{a,D} = ZPE^{\ddagger}_{H} - ZPE^{R}_{H} - (ZPE^{\ddagger}_{D} - ZPE^{R}_{D}) \qquad \text{Eq. 3}$$

where $ZPE^{\ddagger}$ is ZPE of TS, ZPE^{R} the ZPE of reactant.

The reactant ZPE is larger for H than D due to the lower reactant A-H stretch vibration frequency for the more massive D. For a thermodynamically symmetric reaction ($\Delta G_{RXN} = 0$), the reaction path through the TS consists solely of the proton's classical motion over the barrier, so that there is no proton ZPE associated with this motion at the TS. Rather, the TS ZPE is associated with the transverse motion at the TS, which in the collinear model is a symmetric stretch, the heavy particle A-B vibration. Hence, at the TS, $ZPE^{\ddagger}_{H} \approx ZPE^{\ddagger}_{D}$ for such a symmetric reaction. According to quantum theory, the lowest energy level is at a value of $\frac{1}{2}h\nu$ above the zero point energy, where ν is the frequency of vibration. The values of ν for the ZPE of C-H and C-D bonds are 4.15 and 3kcal/mol respectively ($ZPE^{R}_{D} \approx ZPE^{R}_{H}/\sqrt{2}$ and λ=0.5Å for H , λ=0.31Å for D). The net result is the complete "loss" of the ZPE for the proton stretching mode on going from reactant to TS for a symmetric reaction. Typical reactant gives an H vs. D KIE of about 7 at 25°C.

1.5.3 Challenge of Measuring Intrinsic KIEs due to Kinetic Complexity

Most enzymes catalyze reactions via kinetically complex multi-step reactions (Figure 1.11). In an enzyme catalytic cycle, the chemical steps are usually accompanied by substrate binding, product release and protein rearrangement steps, which are rate determining for many enzymes. The resulting multi-barrier reaction path is sometimes very different from the non-enzymatic or uncatalyzed one. This kinetically complex mechanism is a major obstacle for experimental studies of the chemical step. Therefore, kinetic complexity must be carefully considered when investigating KIEs. If there is an isotope effect on a step other than one under investigation or a slow isotopically

insensitive step these will mask the isotope effect, resulting in an observed KIE that is smaller than the intrinsic KIE.

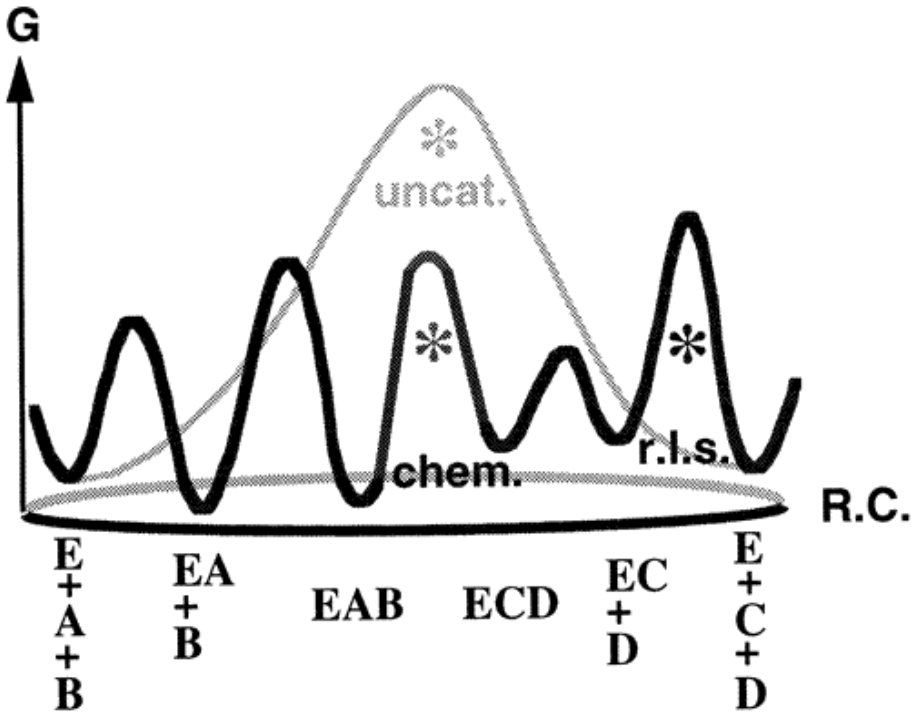

Figure 1.11 Kinetic complexities in enzymatic reactions

Most isotope effect measurements rely on *inter*-molecular competition between labeled and unlabeled molecules to measure the isotope effect on V_{max}/K_m. However, the isotope effect must occur either at or before the rate-determining step. For reactions at methyl groups, this limitation may be overcome by measuring the isotope effect by an *intra*-molecular competition experiment. This requires the synthesis of substrates containing regio-specifically mono-deuterated methyl groups. The isotope effect can be measured, even when the isotopically sensitive step is not rate determining, because it is manifested through *intra*-molecular competition between protium and deuterium atoms,

which remain chemically equivalent even in the enzyme active site due to the rapid rotation of the methyl group. This technique has been used to measure intrinsic KIEs in glutamate mutase, as discussed in Chapter 4. Intrinsic KIEs are directly affected by the reaction potential surface and other physical features so they can be used to study the contribution of tunneling on the reaction and also can be compared to theoretical calculations, which commonly only reflect an effect on a single step.

1.5.4 KIE studies on Glutamate Mutase

An extensive set of KIE measurements on glutamate mutase has been undertaken by the Marsh laboratory. KIE measurements using deuterium- and tritium-labeled substrates and coenzyme have proved especially informative probes of the key steps of Co-C bond homolysis and hydrogen atom abstraction from substrate. Several pre-steady-state kinetic results showed that homolysis of AdoCbl and hydrogen abstraction from the substrate are most likely kinetically coupled to each other in a two-step reaction, as evidenced by the appearance of a kinetic isotope effect on cobalt–carbon bond homolysis when the enzymes are reacted with deuterated substrates, rather than being a concerted reaction with a single transition state. This implies the adenosyl radical can only exist transiently as a high energy intermediate during catalysis.

Initially, KIE on the reaction of glutamate mutase was measured under steady-state condition. Steady-state kinetics is an approximation it only provides information after the reaction reaches the equilibrium. Under steady-state conditions, the enzyme exhibits deuterium isotope effects with both glutamate ($^{D}V\sim 4$) and 3-methylaspartate ($^{D}V\sim 6.3$) initially suggesting that hydrogen transfer between substrate and coenzyme is

significantly rate-limiting in both directions. However, the isomerization catalyzed by glutamate mutase is reversible and it involves two hydrogen transfer steps: one from substrate to coenzyme and the other from coenzyme to product. Therefore, it is very complicate to interpret data and in most case, KIE observed is not the intrinsic KIE. Therefore, Pre-steady state kinetics need to be introduced to measure the intrinsic KIE in H transfer in the reaction of glutamate mutase which follows the kinetics the formation of the intermediate, 5'dA (Figure1.12).

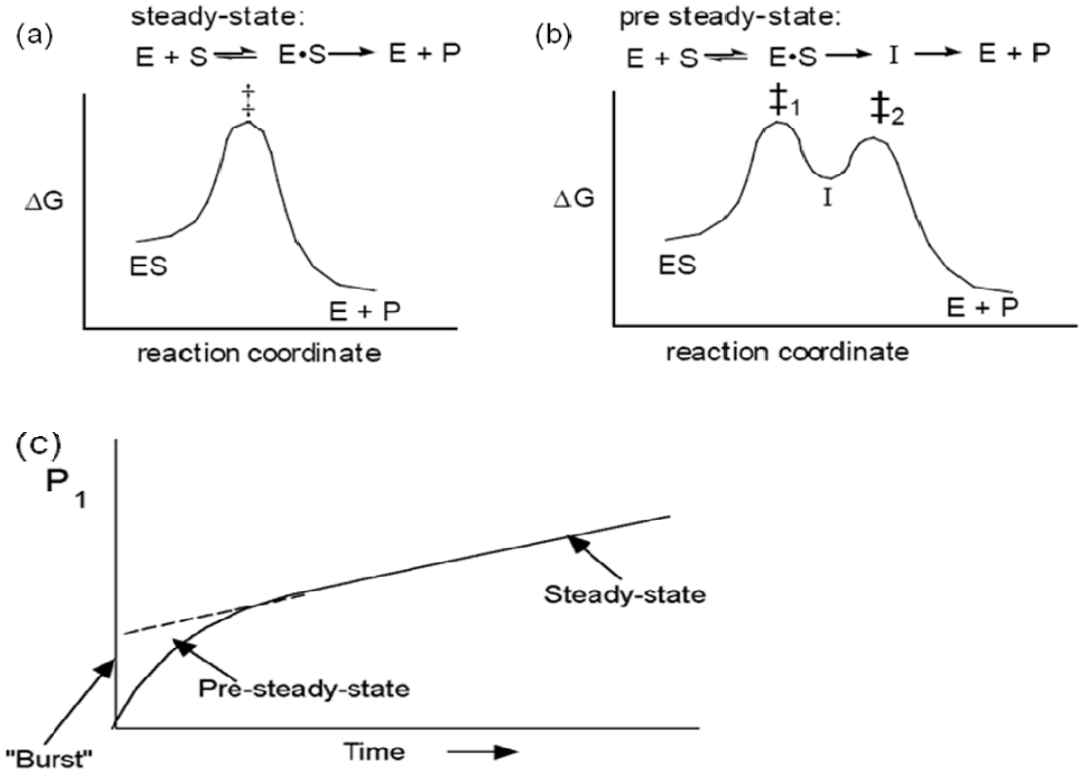

Figure 1.12 Steady-state versus Pre-steady-state studies: (a) reaction coordinate for steady-state kinetics, (b) reaction coordinate for pre-steady-state kinetics, (c) product accumulation as reaction time: steady-state kinetics only provide information about the slowest step (usually product release) in catalytic reaction.

It had also been demonstrated that kinetic complexities partly mask the observed kinetic isotope effects. Large inverse secondary tritium isotope effects ($^{T}V\sim 0.76$) on 5'-dA formation were observed, and led to the primary deuterium isotope effect, which was previously measured indirectly by monitoring Cbl(II) formation to be reinvestigated. Rapid quench kinetic studies of deuterium transfer from deuterated d_5-glutamate to 5'-dA indicated that the overall deuterium isotope effect on AdoCbl homolysis and 5'-dA formation measured by mass spectrometry was much smaller ($^{D}V\sim 2.4$) than previously thought and caused the initial u.v.-visible stopped-flow kinetic measurements to be re-evaluated (Figure 1.13).

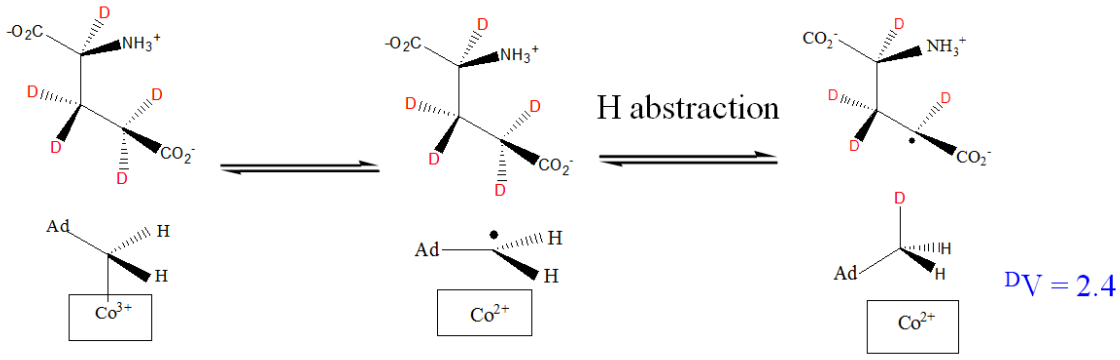

Figure 1.13 Deuterium kinetic isotope effect measured on the formation of 5'dA directly by rapid quench flow.

The origin of this discrepancy is due to misinterpretation of the biphasic kinetics of AdoCbl homolysis observed by stopped-flow spectroscopy when glutamate mutase was reacted with deuterated substrates as rising from negative cooperativity between the two active sites of the dimeric enzyme. This explanation appeared reasonable because the two phases of the reaction had approximately equal amplitudes, and it was previously

observed that binding of the monomeric S subunit to the dimeric E subunit of the wild-type enzyme was weakly cooperative, suggesting the biphasic reaction was due to half-of-sites reactivity. Furthermore, the KIEs calculated before were in general agreement with those reported for other AdoCbl-dependent enzymes. Only in the later experiments did it become apparent that the slower rate was associated with multiple turnovers of the deuterated substrates resulting in di- and tri-deuterated 5'-dA and that it arose from an unexpectedly large inverse equilibrium isotope effect shifting the equilibrium towards homolysis of AdoCbl.

Although the measurement was made in the pre-steady state, the KIE might still be suppressed by nonisotopically sensitive steps prior to homolysis. To evaluate the deuterium isotope effect, given the unexpectedly small value of ^{D}V (~2.4), V/K KIE on the formation of 5'-dA was directly measured by a competition experiment with a mixture of 75% 2,4,4,-d_3-L-glutamtate and 25% *proteo*-L-glutamate. Competition experiments, where the labeled and unlabeled substrates are present at the same time, use the change in the ratio in residual substrate or in product to calculate isotope effect, which is that on V/K of the labeled reactant. The measured $^{D}V/K$ value (~10) was significantly larger than ^{D}V and this suggested an isotopically insensitive step prior to hydrogen, most likely cobalt-carbon bond homolysis, is partially rate-determining and is responsible for suppressing the ^{D}V isotope effect. It was also thought possible that the intrinsic isotope effect on hydrogen transfer could be significantly larger than the $^{D}V/K$ ~10. These findings left the nature of the rate-limiting step, and whether quantum tunneling occurred in glutamate mutase, as open questions.

To gain further insight into this unusual reaction, a novel method needs to be developed to measure the pure intrinsic kinetic isotope effect. *(2S, 3S)*-3-d_1-methylspartate, which has protium and deuterium at the equatorial methyl group has synthesized for the first time in our laboratory. This experiment enables the intra-molecular competition with a specifically labeled compound (Figure 1.14) and also provides the information about the quantum tunneling contribution on the reaction catalyzed by glutamate mutase as it provides more accurate intrinsic isotope effect on hydrogen transfer between substrate and coenzyme. More details will be discussed in Chapter 4.

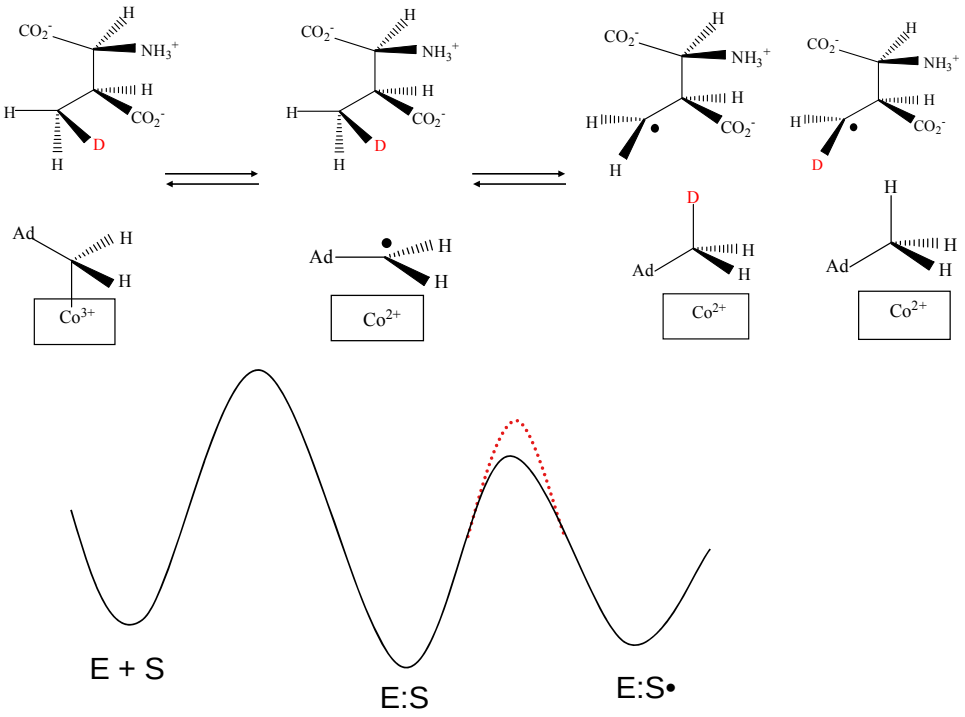

Figure 1.14 Deuterium transfer from (2S, 3S)-3-d_1-methylspartate to 5'-dA under intra-molecular competition condition.

1.6 Quantum Tunneling Effects on Enzymes

1.6.1 Hydrogen Transfer by Quantum Tunneling

Tunneling is a genuine quantum effect, a direct consequence of the phenomenon by which a particle transfers through a reaction barrier by means of its wave-like properties where the wavelength of its particle exceeds the barrier widths. The barrier is assumed to be higher than the kinetic energies of the particle, therefore such a motion is not allowed by the laws of classical dynamics (Figure 1.15). This wavelength for a hydrogen with a zero-point vibrational energy of 10 kJ/mol is calculated to be ~0.5 Å for ^{1}H (protium, H), 0.31 Å for ^{2}H (deuterium, D) and 0.25 Å for ^{3}H (tritium, T). Non-classical behavior is expected for light particles such as hydrogen and deuterium and this positional uncertainty gives rise to a significant probability of H-transfer by tunneling. Hydrogen quantum tunneling has been suggested to play a role in a wide variety of hydrogen-transfer reactions in chemistry and enzymology.

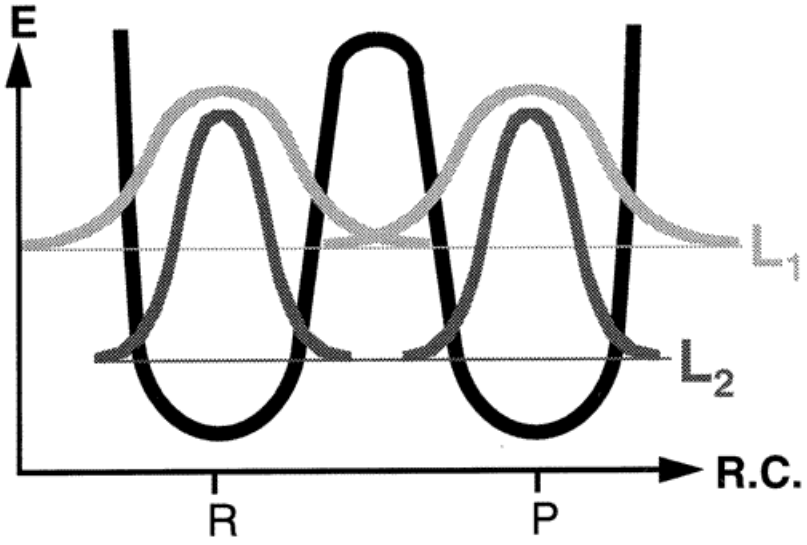

Figure 1.15 Quantum tunneling effect: a particle transfers through a reaction barrier by means of its wave-like properties where the wavelength of its particle exceeds the barrier widths.

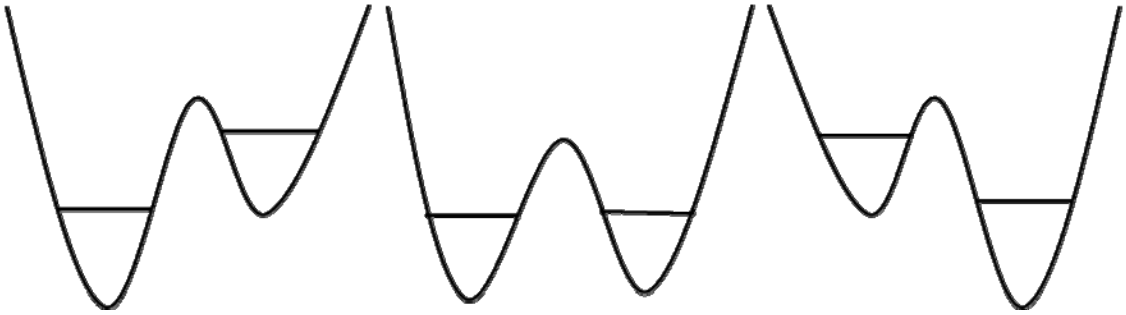

Figure 1.16 Free-energy curves versus proton positions at: (a) initial state (reactant), (b) transition state (intermediate), and (c) final state (product)

On the basis of the currently accepted picture of hydrogen transfer, the quantum mechanical potential-energy surface of the transferring nucleus (hydrogen or its heavier isotopes) is initially characterized by a deep well, and corresponding localization of the hydrogen nucleus, on the donor side. Instead of simple transition state theory, quantum statistical mechanical theory can be introduced to visualize the quantum tunneling clearly. In this approach, the potential energy surface has double wells and a chemical reaction is viewed as a radiationless decay process between an initial state (reactant), metastable intermediate, and a final state (product) (Figure 1.16).

As the donor-acceptor distance decreases through gating motions, which may be facilitated by large-scale rearrangements of the protein, the hydrogen atom starts to perceive a stable minimum on the acceptor side. Once the hydrogen potential surface starts to acquire a double-well character, the donor and acceptor moieties get to close and tunneling can occur (Figure 1.17). Whether tunneling occurs at this stage depends on many factors including the barrier height, curvature, width along the donor-acceptor, orthogonal directions, and the slope and curvature of the potential surface in the region

close to the classical turning point, which is generally where tunneling begins. Thus, the nature of the quantum mechanical potential energy surface has a critical bearing on the tunneling process. (Iyengar et al. 2008)

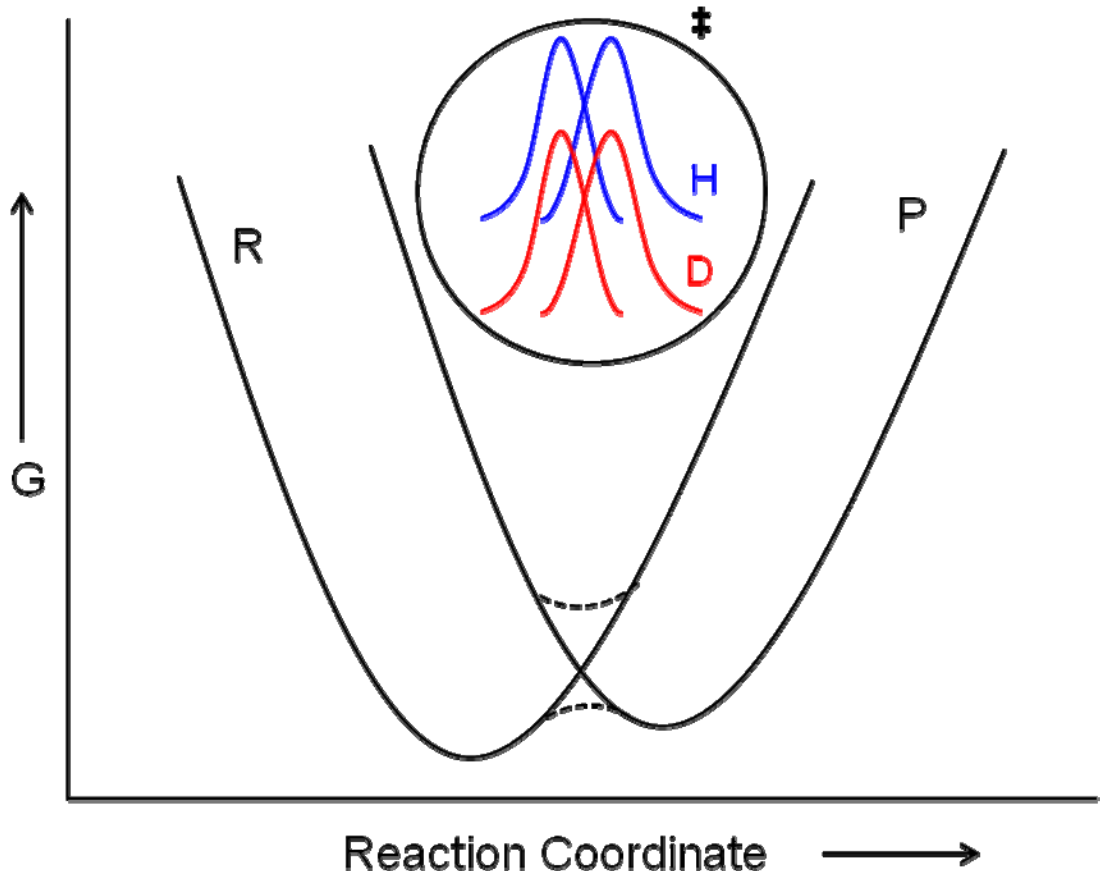

Figure 1.17 Tunneling through double-well character

Deuterium- or tritium- labeling of substrate is an effective way to gather information on enzymatic reactions involving hydrogen transfer. A lighter isotope has a higher tunneling probability than a heavier one, since a heavy isotope has a lower zero-

point energy and its probability function is more localized in its potential energy well. Consequently, an unexpectedly large primary KIE (k_H/k_D >7 at 25°C) is a very good diagnostic tool for tunneling effects.

Classically, the kinetic relationship among the protium, deuterium, and tritium has also widely been used as probes for the mechanisms of enzymes. The Swain-Schaad exponential (SS EXP) relationship is the semiclassical (no tunneling) correlation among the rates of the three isotope of hydrogen. This relationship can be derived from the reduced masses of the isotopes under examination.

$$\frac{\ln(\frac{k_H}{k_T})}{\ln(\frac{k_D}{k_T})} = \frac{\frac{1}{\sqrt{\mu_H}} - \frac{1}{\sqrt{\mu_T}}}{\frac{1}{\sqrt{\mu_D}} - \frac{1}{\sqrt{\mu_T}}} \approx 3.26 \qquad \text{Eq. 4}$$

where k_H, k_D, and k_T are the rates of transfer protium, deuterium and tritium, and μ_H, μ_D, μ_T are the reduced masses of protium, deuterium and tritium, respectively. Therefore, a Swain-Schaad exponent larger than semiclassical limit, 3.26 (in which zero point energies, but not tunneling, have been taken into account) has used as an important experimental criterion for tunneling. The semiclassical (no tunneling) limit was based on simple theoretical considerations of a diatomic cleavage of a stable covalent bond, for example, a C-H bond.

Secondary KIEs result from a change in bonding force constants and vibrational frequencies during the reaction. Quantum tunneling can result in inflated secondary hydrogen isotope effects for systems in which the isotopic hydrogen is coupled to the transferring hydrogen. (Huskey and Schowen, 1983) The relationship between tunneling and coupled motion will be covered in section 1.6.3 and 1.6.4 in detail.

Also, the nonlinear Arrhenius behavior of rate constants provide for the important evidence for tunneling. Particularly, the values of A_H/A_D, and $\Delta E_{a,D}$ -$\Delta E_{a,H}$ that are deviated from semiclassical limit indicate tunneling. Temperature dependence studies diagnostic for tunneling will be covered in detail in the next section.

1.6.2 Temperature-dependence/independence Studies Diagnostic for Tunneling

As mentioned, evidence for tunneling in enzyme reactions has come from the magnitudes of primary and secondary kinetic isotope effects when deuterium or tritium is substituted for a hydrogen species that is transferred in the rate-determining step. The quantum tunneling of hydrogen can be also diagnosed by measuring the temperature dependence of isotope effects as quantum tunneling is not a classical thermodynamic process, and is temperature independent. However, complete temperature independence of a rate of reaction cannot be used as a criterion because the range of temperatures over which enzyme catalyzed reactions can easily be studied is small. Goldanskii has defined a 'tunneling temperature' at which the contribution from tunneling exceeds that from classical barrier crossing (Goldanskii, 1979). For hydrogen as the tunneling species this is about 160 K (recall that room temperature is about 25 °C or 298 K). Therefore, some degree of temperature dependence in the range of experimentally accessible temperatures where enzymes are still active (usually 270~320K) can be expected.

As shown in equation 2, for H versus D transfer, the KIE is given by

$$\frac{k_H}{k_D} = \frac{A_H}{A_D}\exp\left(\frac{-(\Delta E_{a,H} - \Delta E_{a,D})}{RT}\right) \qquad \text{Eq. 2}$$

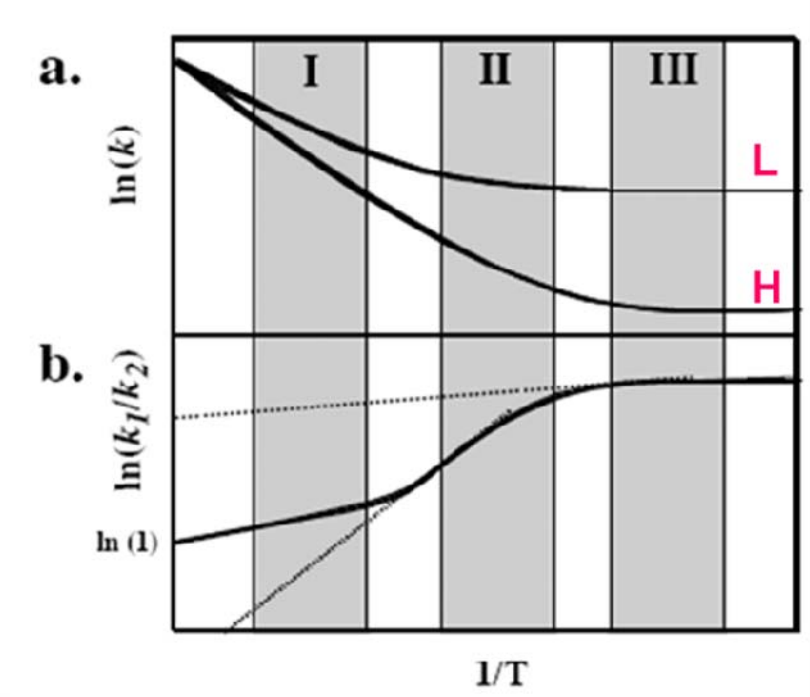

Figure 1.18 An Arrhenius plot of a hydrogen transfer with a tunneling correction to transition state theory: (a) Arrhenius plot of a light isotope (L) and heavy isotope (H), (b) Arrhenius plot of their KIE (L/H). Highlighted are experimental temperature ranges for three systems: I, a system with no tunneling contribution, II, a system with moderate tunneling, and III, a system with extensive tunneling contribution. The dashed lines are the tangents to the plot in each region (Kohen and Klinman, 1999)

The temperature dependence of hydrogen transfer rate constants is usually of curved-Arrhenius form. The curvature arises because the activation energy, E_a, varies from zero for T= 0, where the reaction proceeds entirely by tunneling, to the barrier height for very high temperatures, where classical thermodynamic transfer prevails. However, within the small temperature intervals for which kinetic data of the enzymatic reactions are available, the curvature is usually negligible, so that the standard Arrhenius equation with constant E_a holds.

$$\ln\frac{k_H}{k_D} = \ln\frac{A_H}{A_D} + \left(\frac{-(\Delta E_{a,H} - \Delta E_{a,D})}{RT}\right) \qquad \text{Eq. 5}$$

In the Arrhenius logarithmic plot, the intercept directly indicates the Arrhenius prefactor (A_H/A_D) and the activation energy difference can be obtained from the slope of the plot (Eq. 5), (Figure 1.18). At high temperature, where the tunneling effect will be minimal, the reaction rate is exponentially dependent on the reciprocal absolute temperature as reflected by the Arrhenius equation and the Arrhenius factor will be close to unity. At a very low temperature, where only tunneling contributes significantly to the rate, because no thermal energy is available for the activation, the KIEs will be very large and A_H/A_D will be much larger than 1. Between high and low temperature extremes, the Arrhenius plot of KIE will be curved, as the light isotope tunnels at a higher temperature than the heavy one. At this region, the Arrhenius slope will be very steep and A_H/A_D will be smaller than 1. Deviation from unity with no tunneling seems to be confined to a limited range. With a wide variety of enzyme systems, the Arrhenius behavior of isotope effects had been characterized in great detail for reactions that adhere to semi-classical behavior, establishing semi-classical limits for the isotopic difference in activation energies, and the isotopic Arrhenius prefactors; An A_H/A_D lower than 0.5 indicates tunneling of only the light isotope which also denoted as moderate tunneling while larger than 1.4 indicates tunneling of both isotopes.

Some of the first enzymes studied in which H-tunneling was inferred from measurements of KIEs were bovine serum amine oxidase (Grant and Klinman, 1989), monoamine oxidase (Jonsson and Klinman, 1994) and galactose oxidase (Whittaker et al., 1998) (Table 1.1). These studies were shown to be consistent with the Bell correction model of semi-classical transfer, which invokes tunneling just below the classical transition state and the light isotope tunnels more than the heavy isotope.

Enzyme	k_H/k_D (25 °C)	A_H/A_D	ΔEa(kcal/mol)	Ref.
Bovine serum amine oxidase	11.5	0.24	2.3	[1]
Monoamine oxidase	9.4	0.25	2.2	[2]
Galactose oxidase	16.8	0.25	2.5	[3]

Table 1.1 Enzyme systems for which moderate tunneling was suggested from temperature dependencies: A_H/A_D lower than semiclassical lower limit, 0.5, consistent with the tunnel correction model of semi-classical transfer; [1], Grant and Klinman; 1989 [2], Jonsson and Klinman, 1994; [3], Whittaker et al., 1998

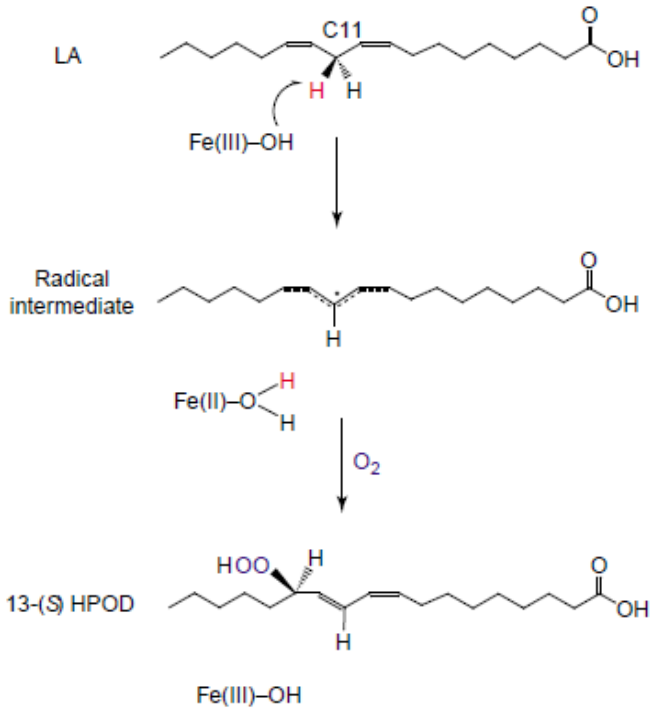

Figure 1.19 Hydroperoxidation of linoleic acid to 13(*S*)-*hydroperoxy-9(Z), 11(E)*-octadecadienoic acid catalyzed by soybean lipoxygenase-1 (SLO-1), (Liang and Klinman, 2004)

Temperature-dependent KIEs in soybean lipoxygenase-1 (SLO-1) have been extensively studied at laboratory of Klinman. SLO-1 is a metallo-enzyme containing a non-heme iron ion that exists as Fe(III) or Fe(II) during the catalysis and it also involves a radical-mediated mechanism. SLO-1 catalyzes the oxidation of linoleic acid to 13-(*S*)-

hydroperoxy-9,11-(Z,E)–octadecadienoic acid via an initial rate-limiting pro-*S* hydrogen radical abstraction from C11 of linoleic acid by the Fe^{+3}–OH cofactor, forming both a substrate-derived radical intermediate and Fe^{2+}-OH_2 (Figure 1.19). KIE measurements for this abstraction show very large deuterium KIEs (~80) and a large temperature independence, A_H/A_D ~20, as well, which suggest tunneling of both isotopes, H and D.

In contrast to the lipoxygenases, some enzymes such as *E.coli* thymidylate synthase and dihydrofolate reductase showed relatively small KIEs (k_H/k_T), 7 and 6 respectively. However when temperature dependence studies were undertaken, A_H/A_T for both systems was ~7, which is much above the semiclassical upper limit (~1.7) and directly indicates tunneling of both isotopes (Table 1.2). These examples suggest that small KIEs cannot be considered definitive evidence against tunneling and that temperature-dependence studies must be undertaken to examine the contribution of the tunneling on reactions as H-transfer can involve environmentally enhanced (coupled) tunneling. This discrepancy in temperature (in)dependencies of the reaction rate and of the KIEs and the concept of the environmentally coupled hydrogen tunneling will be covered in detail in the next section.

Enzyme	**k_H/k_D (25 °C)**	**A_H/A_D**	**ΔEa(kcal/mol)**	**Ref.**
Horse LADH (Phe93 → Trp)	2.4	0.57	0.84	[1]
Morphinone reductase	3.9	0.12	1.96	[2]
Thymidylate synthase	4.0	3.58	0.06	[3]
Pentaerythritol tetranitrate reductase	4.4	4.06	0.05	[2]
Thermophilic dihydrofolate reductase	4.8	0.002	4.61	[4]
Dihydrofolate reductase (*E.coli*)	5.7	4.11	0.20	[5]

Table 1.2 Enzyme systems which have relatively small KIEs (< ~7) but tunneling was suggested from temperature dependencies: [1], Bahnson and Klinman, 1993; [2], Basran and Scrutton, 2003; [3], Agrawal and Kohen, 2004; [4], Maglia and Allemann, 2003; [5], Sikorski and Kohen, 2004.

1.6.3 Protein Dynamics and Tunneling

Protein dynamics has been implicated in the efficiency of hydrogen tunneling in enzymes. Bahnson et al. showed that hydrogen tunneling efficiency was increased in a horse liver alcohol dehydrogenase mutant with a smaller alcohol binding pocket which results in reduction of the distance between the donor and acceptor carbons (Bahnson and Klinman, 1993). This led to the suggestion that flexibility in interdomain movement could influence the catalytic rate by reducing the hydrogen tunneling distance of the native enzyme. Later studies on the thermophilic alcohol dehydrogenase from *Bacillus stearothermophilus* by Klinman's laboratory supported this conclusion.

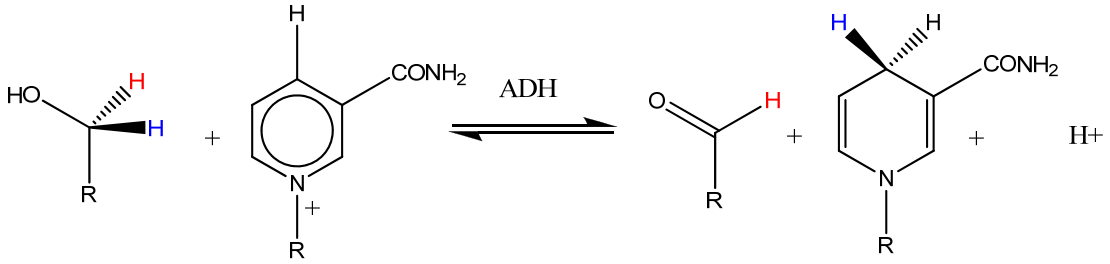

Figure 1.20 Hydrogen transfer from alcohol to the C4 carbon of the nicotinamide ring of NAD+, to produce the corresponding aldehyde catalyzed by ADH.

NADH-dependent thermophilic alcohol dehydrogenase (htADH) catalyzes the reversible oxidation of alcohol by transferring the alcoholic hydride to NAD^+ (Figure 1.20). Klinman et al. extensively studied the relationship between enzyme dynamics and hydrogen tunneling in htADH and investigated whether hydrogen tunneling occurs at elevated temperatures in a biological system that functions physiologically under such conditions (Kohen and Klinman, 1999). The temperature dependence studies in htADH

across a sizeable temperature range (65 – 5 ˚C) suggest a role for protein mobility in C–H-bond cleavage because they showed that the enzyme undergoes a distinct temperature-dependent transition between enzyme forms that differ in their properties for the hydride transfer and accompanying tunneling parameters below and above the transition temperature, ~30˚C. The weak temperature dependence of the KIE in the temperature range 30–65˚C, with A_H/A_D ~2.2, larger than the semiclassical limit (~1.4), suggest a significant hydrogen tunneling contribution under physiological conditions (30 to 65 ˚C). However below 30 ˚C, both isotopes had a much larger energy of activation (31.4 and 23.6 kcal mol^{-1} for D and H, respectively) and large temperature dependence of the KIEs with a relatively small deuterium KIE (~3); this is analogous to previous findings with mesophilic ADH at 25˚C (Cha and Klinman, 1989). The effect of the dynamic transition would be to freeze out certain protein motions that could facilitate hydride transfer (for instance, stretching motions along the reaction coordinate for C–H bond cleavage). Contrary to predictions for tunneling through a rigid barrier, the tunneling with the htADH decreases at and below room temperature. This result was interpreted as ‘‘activity phase transition’’ due to increased rigidity of this thermophilic enzyme at reduced temperatures. This would fit moderate tunneling region under 30 ˚C as both isotopes had a much larger energy of activation and large temperature dependence for KIEs due to the increased rigidity of this thermophilic enzyme at reduced temperature. These findings provide experimental evidence for a role of thermally excited enzyme fluctuations in modulating enzyme catalyzed bond cleavage (Table 1.3), (Kohen and Klinman, 1999); (Kohen and Klinman, 2000).

k_H/k_D	A_H/A_D	$\Delta E_{a,\ D\text{-}H}$ (kcal/mol)	Temperature (˚C)
~4 (5 °C)	1.00E-05	7.8	5~30
~3.4 (60 °C)	2.2	0.5	30~65

Table 1.3 Temperature-dependent transition of tunneling contribution in thermophilic ADH (Kohen and Klinman, 1999)

A hydrogen-deuterium exchange mass spectrometry (HX-MS) study in htADH suggested that a large region in the substrate-binding domain of htADH undergoes a transition from a rigid structure to a more dynamic structure at 30 ˚C. Such motions might be important not only for classical barrier crossing but also for tunneling, because the barrier width depends on the distance between the hydrogen donor and acceptor atoms (Liang et al., 2004). Homologous mesophilic horse liver ADH (HLADH) exhibits temperature-independent KIEs at temperatures above 3°C however it becomes significantly temperature-dependent between 3 °C and -35 °C. The trend in temperature dependent KIEs in HLADH is identical to that has observed in htADH, except it transposed to a lower temperature range. This suggested that protein rigidification occurs at a reduced temperature for a mesophilic protein in relation to a thermophilic protein and, further, that such rigidification will alter the properties of tunneling that become manifest in the temperature dependence of the KIE (Tsai and Klinman, 2001).

The weak temperature dependence of the KIE in the temperature range 30–65˚C, along with a significant activation enthalpy ($\Delta H^{\ddagger}$), has also been observed in other systems, such as trimethylamine dehydrogenase and thermophilic dihydrofolate reductase. This can only be explained by a “Marcus-like” model in which the temperature dependencies of the reaction rate and of the KIE are separated. In Marcus-like model, the

reaction is viewed as having three steps; formation of an encounter complex, hydrogen switch, and departure of products from the complex, and the reaction process can be understood in terms of one-dimensional, overlapping energy wells. The Marcus model was originally designed for electron-transfer reactions and latter applied to hydrogen-transfer processes. Since, in contrast to electron transfer, H-transfer is very sensitive to the donor–acceptor distance, an additional term accounts for fluctuations of that distance. In this model, the efficiency of H-transfer is governed by i) an isotope-independent term (constant), ii) a Marcus-like term that contains λ, the sum of the contribution of inner and local outer reorganization to the reaction barrier and $\Delta G°$, the reaction driving force, and iii) a ‘‘gating’’ term (the Franck-Condon (F.C.) term in equation 7),

$$k = (Const.)\exp[\frac{-(\Delta G° + \lambda)^2}{4\lambda RT}](F.C.Term) \qquad \text{Eq. 6}$$

where R, gas constant; T, absolute temperature.

The Marcus term has a temperature dependence and a weak isotopic dependence that arises when tunneling takes place from vibrationally excited states.

$$k = (Const.)\exp[\frac{-(\Delta G° + \lambda)^2}{4\lambda RT}]\int_{r1}^{r0}\exp[\frac{-m_H w_H {r_H}^2}{2\hbar}]\exp[\frac{-E_x}{k_b T}]dx \qquad \text{Eq. 7}$$

The dominant isotopically sensitive term is the Franck–Condon nuclear overlap along the hydrogen coordinate (F.C. term), that defines the probability of wave function overlap between the H-donor and acceptor as a function of the mass (m_H), frequency (w_H), and distance (r_H) traveled by the transferred hydrogen. This term arises from the overlap between the initial and the final states of the hydrogen’s wavefunction and, consequently, depends on the thermal population of each vibration level. The F.C. term is also expected to be affected by a distance sampling term that reflects the barrier encountered, E_x, in

reducing the distance between the H-donor and acceptor, which is both temperature- and isotope-dependent.

The methylamine dehydrogenase (MADH) reaction displays large primary KIEs (~17), which are almost temperature independent, resulting in a large A_H/A_D of 13.3. However, when enthanolamine is used as the substrate for MADH, the KIE deflated to 14.7, and it becomes temperature dependent, which was interpreted as a switch to a tunneling mechanism modulated by gating motion (Knapp and Klinman, 2002). Calculations including multidimensional tunneling contributions were in good agreement with experiment.

Protein motion also plays an important role in the reactions catalyzed by soybean lipoxygenase-1. For this reaction, a decrease of the proton donor-acceptor distance relative to its equilibrium value is required to enable efficient hydrogen tunneling. In this case, equilibrium thermal motions of the protein strongly impact the reaction, but the dynamical aspects of these motions are not critical. The fast femtosecond to picosecond thermal fluctuations of the protein lead to conformational changes on the slower millisecond time scale of the reaction. These equilibrium conformational changes are averaged over the faster thermal fluctuations and facilitate hydrogen transfer by bringing the donor and acceptor closer, orienting the substrate and cofactor optimally, and providing a favorable electrostatic environment.

1.6.4 Secondary Isotope Effects as Probes for Hydrogen Tunneling Effect: Coupled Motion and Tunneling

When no bond fission to the labeled atom takes place, smaller changes to vibrational modes may still occur and result in a measurable and informative isotope effect, so called secondary isotope effects. Unlike primary isotope effects, secondary isotope effects may be normal (>1) or inverse (<1). A normal isotope effect results when bonding to the labeled atom becomes looser, and an inverse isotope effect results when bonding become tighter. If the isotopic substitution is at an atom directly bonded to the atom undergoing a bonding change, the isotope effect is termed an α-Secondary (2°) KIE. The observed 2° KIEs arise as the consequence of a change in the C-H bond force constant of the primary hydrogen caused by 2°deuteration. Several arguments have been invoked to explain this change in force constant. The most widely accepted is that the force constant is altered due to a change in hybridization state, that is, the rehybridization from sp^3 to sp^2 of a carbon atom adjacent to a 2° deuterium.

In semi-classical theory, the magnitude of the 2° KIE is considered to indicate the progress of reactants to products at the transition state. Therefore 2° KIEs have traditionally been used to report on the nature of the transition state. However, 2° KIE values that are larger than the equilibrium isotope effect (EIE), the fractionation of isotopes between stable states at equilibrium determined by statistical thermodynamics, have been used as evidence for a tunneling contribution to the reaction. The first indication that tunneling may play a role in enzyme-catalyzed hydrogen transfer reactions came from efforts to compute the inflated secondary isotope effects seen in alcohol dehydrogenase reactions (Figure 1.21). A large secondary kinetic isotope effect close to the magnitude of the equilibrium isotope effect suggested a late, product-like transition

state; this in direct contrast to structure reactivity correlations which indicated an early transition state resembling the alcohol.

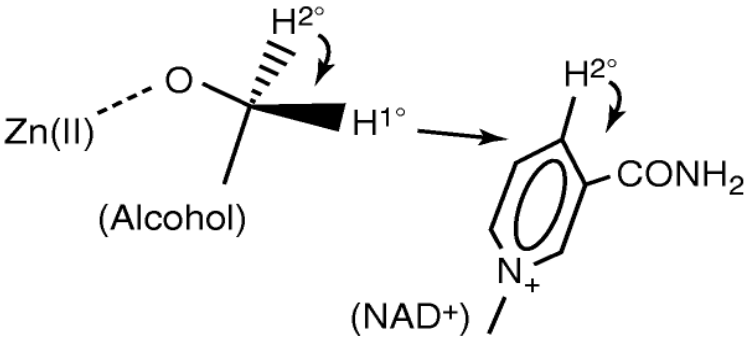

Figure 1.21 Motion of the primary (1°) and secondary (2°) hydrogens in the reaction of alcohol dehydrogenase.

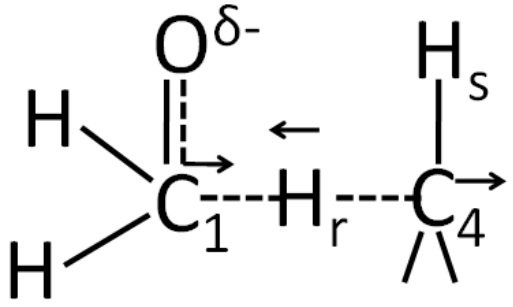

Figure 1.22 Transition state coupling of the primary position of substrate into the secondary position

Later, both Kurz and Freiden and Cook et al. postulated that the origin of inflated secondary kinetic isotope effect was a transition-state coupling of the motion of the primary hydrogen undergoing transfer to the motion of the hydrogen in the secondary position (Kurz and Frieden, 1980); (Cook and Cleland, 1981). As shown, the motion of the H_r hydrogen from cofactor to the carbonyl of substrate is coupled to the bending

motion of the hydrogen which remains bound to C-4 of the cofactor, H_s (Figure 1.22). However, computer simulations of this result indicated that models invoking coupled motion alone were incapable of reproducing the experimental data for yeast alcohol dehydrogenase. It led to the conclusion that both tunneling and coupled motion are required to model the alcohol dehydrogenase reaction.

The concept of coupling can be also applied to describe how the tunneling of the transferred hydrogen is linked to the enzymatic environment. In context of the environmentally coupled model of H-tunneling, the temperature dependence of reaction rates and temperature-independent KIEs arise from collective thermally equilibrated motions that lead to degenerate reactant and product states, i.e., the "tunneling-ready" configuration. Temperature-dependent KIEs are treated as arising from fast (subpicosecond) "gating motions" (motion along the reaction coordinate) that enhance the probability of tunneling by bringing the reactant and product wells closer together.

Scrutton et al. studied two homologous enzymes, morphinone reductase (MR) from *Pseudomonas putida* and pentaerythritol tetranitrate reductase (PETNR) from *Enterobacter cloacae* that catalyze H-transfer by quantum mechanical tunneling. The enzymes have been shown to possess temperature-dependent and temperature-independent KIEs (at least within the limit of experimental detection) respectively. The mechanisms of H-transfer are different; MR, but not PETNR, appears to have a requirement for a promoting motions yet both exhibit identical and inflated 2° deuterium KIEs. These inflated 2° KIEs provide further evidence for hydrogen tunneling in both enzymes. Importantly, 2° KIEs -unlike 1° KIEs - are independent of promoting motions. Such a promoting motion may be considered to reflect the (nonequilibrium) pre-

organization of the cofactor and active-site residues into a “tunneling-ready” configuration (TRC). When coupled with analysis of 1° KIEs, this study emphasizes the utility of 2° KIEs as additional probes of H-transfer within the context of contemporary environmentally coupled frameworks for H-tunneling (Pudney et al., 2006). They also calculated 1° and 2° KIEs in MR and both were in good agreement with the experimental values and the calculations suggest that ~99% of the reaction proceeds via tunneling: which is the first “deep tunneling” reaction observed for H transfer. Their data also supports tunneling being preceded by reorganization: in the reactants, the rings of the nicotinamide and isoalloxazine moieties are stacked roughly parallel to each other, and as the system moves toward a “tunneling-ready” configuration, the nicotinamide ring rotates to become almost perpendicular to the isoalloxazine ring.

Hay et al. investigated 2° deuterium KIE for thermophilic dihydrofolate reductase (TmDHFR) and homologous DHFR from *E. coli* (*Ec*DHFR). They found that the intrinsic 2° KIEs for hydride transfer in both DHFRs are similar despite clear differences in the degree of environmental coupling within these two enzymes. The magnitude of the 2°KIEs in both these enzymes are almost identical - 1.05 and 1.13 for TmDHFR and *Ec*DHFR respectively - and importantly is not significantly exalted than EIE ~1.13 and ~1.08 for TmDHFR and *Ec*DHFR respectively. Yet the 1°KIEs in these two enzymes have significantly different temperature-dependences. The apparent temperature independence of the 2° KIE in TmDHFR provides new evidence that 2° KIEs do not report on dynamical, promoting motions of the protein. This is consistent with them reporting only on tunneling-ready configuration, the donor-acceptor geometry immediately preceding H-transfer. Interestingly, the TRC hypothesis was developed for

deep-tunneling reactions and these results suggest that this proposal may be valid for H-transfers with lower tunneling propensities. It also emphasizes that for environmentally-coupled H-tunneling reactions, the magnitude of the 1° and 2° KIEs can assume values less than the semiclassical limit (~7) and the EIE (1.13), respectively which contrasts with earlier Bell-correction mode. This study also demonstrated the usefulness of α 2° KIEs (their magnitude and temperature dependence) as probes of environmentally-coupled H-transfer reactions in enzyme systems (Hay et al., 2008).

Enzyme	2° k_H/k_D	A_H/A_D	ΔEa(kcal/mol)	Reference
Mesophilic ADH	1.31	1.1	0.79	[1]
BSAO	1.14	0.24	2.32	[2]
HLADH, Phe93 -> Trp	1.27	0.57	0.84	[3]
Monoamine oxidase	1.19	0.25	2.15	[4]
Thermophilc ADH	1.20	1.00E-05	7.8	[5]
Glutamate mutase	0.76 *	~0.03	~3.0	[6]
DHFR (*E.coli*)	1.14	4.11	0.2	[7]
Thermophilic DHFR	1.05	0.002	4.61	[8]
Morphinone reductase	1.18	0.12	1.96	[9]
PETNR	1.17	4.06	0.05	[9]

Table 1.4 Enzyme systems for which environmentally coupled hydrogen tunneling suggested from secondary KIE studies: 2° k_H/k_D calculated from literatures, *, k_H/k_T; [1], Cha and Klinman, 1989; [2], Grant and Klinman, 1989; [3], Bahnson and Klinman, 1993; [4], Jonsson and Klinman, 1994; [5], Kohen and Klinman, 1999; [6], Cheng and Marsh, 2004 and unpublished data; [7], Sikorski and Kohen, 2004; [8], Maglia and Allemann, 2003; [9], Basran and Scrutton, 2003

Hay et al. also have shown that substrate capture is viscosity-dependent, while the following H-transfer step - a well-characterized environmentally coupled quantum tunneling reaction is not. This finding is rationalized in terms of a lack of a network of

long-range motions coupled to the H-transfer reaction in morphinone reductase (MR), similar to the case for aromatic amine dehydrogenase (AADH) (Hay et al, 2008). It has been recently suggested that coupled motions may not be catalytically important in DHFR by computational simulation studies in the laboratory of Warshel (Liu and Warshel, 2007). Their studies argued that the temperature dependence on the KIE does not provide enough support to the proposal that dynamical effects contribute to catalysis. Then, in addition to temperature, other intensive (bulk) properties such as pressure and solution viscosity can be used to probe these reactions. Specifically viscosity studies may be a useful experimental method of identifying long-range motions coupled to H-tunneling in DHFR and LADH (Hay and Scrutton, 2008).

1.6.5 Quantum Tunneling in AdoCbl-dependent Systems

AdoCbl-dependent systems show relatively large KIEs and strong temperature dependence on KIEs so far. Methylmalonyl-CoA mutase (MMCM), which catalyzes the rearrangement of methylmalonyl-CoA to succinyl-CoA, is one of the most extensively studied AdoCbl-dependent enzymes. Chowdhury and Banerjee investigated KIEs on the hydrogen abstraction step catalyzed by MMCM. Under pre-steady-state conditions, experiments were carried out under pseudo first-order conditions in a stopped-flow UV-visible spectrophotometer. These studies were conducted in the temperature ranges of 5-37 °C and 5-20°C with the deuterated and protiated substrates respectively to determine the effect of substrate concentration on k_{obs}, the rate of decay of AdoCbl. Hydrogen transfer reactions catalyzed by MMCM have very large deuterium KIEs of 35.6 at 20 °C suggesting that they proceed by a quantum tunneling mechanism. Temperature

dependence studies were undertaken on the reaction catalyzed by MMCM. The small value (~0.08) of the A_H/A_D ratio and the large value (~3.4 kcal mol^{-1}) of an activation energy difference support that the reaction is dominated by tunneling (Chowdhury and Banerjee, 2000).

The computational study of quantum tunneling dynamics in the MMCM reaction analyzed the molecular mechanism of the tunneling process, which allows one understand the tunneling dynamics in detail. The calculations employing quantized vibrations but classical motion along the reaction coordinate, give a KIE at 5°C of 14.3, much smaller than the experimental value. It was found that multidimensional tunneling increases the magnitude of the calculated intrinsic hydrogen kinetic isotope effect of MMCM at 5°C by a factor of 3.6 from 14 to 51, in excellent agreement with experimental results. Transition state theory calculations with multidimensional tunneling contributions also show large temperature dependence, 20-43%, depending on the size of the model system considered and the potential energy surface. These calculations confirm that tunneling contributions can be large enough to explain even a kinetic isotope effect >50, not because the barrier is unusually thin but because corner-cutting tunneling decreases the distance over which the system tunnels without a comparable increase in either the effective potential barrier or the effective mass for tunneling. Thus, the strength of the interaction driving carbon-centered free radical reaction allows hydrogen transfer to proceed efficiently despite the relatively large tunneling distance (Banerjee and Truhlar 2007).

Doll and Finke studied the KIE for hydrogen abstraction in three different cobalamin analogues (β-NpCbl; AdoCbl; 8-MeOAdoCbl). Their experiments measured

the kinetics of hydrogen abstraction from ethylene glycol (mimicking the diol dehydrase reaction) either by 5'-dA radical, generated by thermolysis of AdoCbl, or neopentyl radical, generated by thermolysis of neopentylcobalamin. In both systems significant hydrogen tunneling was detected from analysis of Arrhenius plots, and furthermore the KIEs measured were much larger than could be accounted for by semi-classical formulation of KIEs. The key data obtained are as follows: deuterium KIEs of 38 at 10 °C; an activation energy difference, $\Delta E_D - \Delta E_H$ of 3.1 kcal mol^{-1}; and a pre-exponential factor ratio A_H/A_D of 0.13 (Doll and Finke, 2003). The isotope effects on Arrhenius pre-exponential factors and activation energies measured in these model systems were very similar to those measured in methylmalonyl-CoA mutase as were the KIEs when corrected for differences in temperature. These results led to the conclusion that tunneling was an intrinsic property of both MMCM and non-enzymatic reaction, and that there was no enhancement of tunneling by at least this B_{12}-dependent enzyme, MMCM (Doll and Finke, 2003).

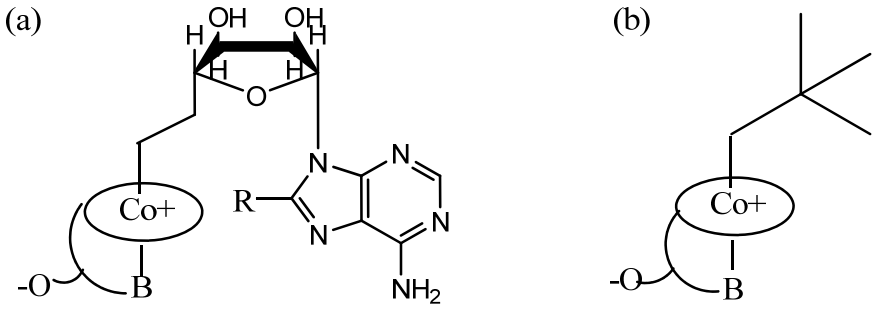

Figure 1.23 Structure of cobalamin analogues: (a) AdoCbl; R=H, 8-MeOAdoCbl; R=MeO (b) β-NpCbl

Chapter 2 Materials and Methods

2.1 Materials

2.1.1 Chemicals and Reagents

Water was deionized and purified by Milli-Q water purification system (Millipore). AdoCbl, L-glutamate, D,L-*threo*-3-methylaspartate were purchased from Sigma Chemical Co. Solutions containing AdoCbl were kept in light-proofed vials and handled in dim light. L-[^{3}H]-glutamate was purchased from Amersham Pharmacia Biotech**.** The media used for bacterial growth (LB and 2TY as broths or agar plate) and the buffers used for protein purification were purchased from commercial suppliers. (*R*, *S*)-2-Thioglutaric acid was synthesized from glutaric acid using a literature procedure (Majer et al., 2003).

2.2 Enzyme Preparation

2.2.1 Glutamate Mutase Expression and Preparation

The glutamate mutase fusion protein, GlmES was overexpressed in a recombinant *Escherichia coli (E.coli) BL21* (Chen and Marsh, 1997). A single *E.coli* bacterial colony was selected from a fresh LB agar plate containing 100 μg/mL of ampicillin. This colony was transferred to a 5mL culture of 2TY containing 100 μg/mL of ampicillin (2TY/amp) and incubated at 37 ºC, overnight, in an orbital shaker at 250 rpm. The overnight culture was then asceptically transferred to a 1L flask containing 500mL of 2TY/amp and

incubated at 37 ºC, with a vigorous shaking at 300 rpm until it reached an A_{600} of 0.8. The 500mL culture was transferred to 22L of 2TY/amp in a Bioflow 4500 fermentor. Cells were grown at 37 °C with constant aeration and stirring at 250 rpm until they reached an A_{600} ~ 0.8 which usually takes about 4-6 hours. A 1mL sample was taken into 1.5mL eppendorf vial before induction to compare protein expression with the induced cells. The sample was centrifuged for 2min at 13,200rpm and supernatant was discarded carefully and the pellet was stored at -20 °C. Proteins were induced by the addition of isopropyl-β-D-thiogalactopyranoside (IPTG) (150 mg/L) and antifoam B (Sigma) was also added to reduce foaming. The cultures were allowed to incubate at 37 °C overnight with a gentle stirring at 150 rpm. The cells were harvested by centrifugation at 6000 rpm for 15min at 4 °C and stored at -20 °C until purification. A small amount of cell paste was taken to check for the presence of the induced protein by SDS PAGE with the sample collected prior to induction as a control sample. Pellets were denatured by heating at 94°C for 5minutes and vortex repeatedly before loaded on the 12% SDS-PAGE gel.

2.2.2 Glutamate Mutase Purification

All the purification steps were conducted on ice or in a 4 °C cold room. Typically, ~ 70 g of cells (damp weight) were collected from 22 L of culture. 50g of cells were resuspended in 100 mL of 1m,M EDTA and 50 mM potassium phosphate buffer, pH 7.0, containing 1 mM DTT and 1 mM phenylmethylsulphonyl fluoride (PMSF). The cells were ruptured by sonication with 16 cycles of 30sec burst at sonication power 7 with a cooling period of 1min and 30sec between each burst. The cell debris was removed by centrifugation at 18000 rpm for 45 min. The supernatant (120 mL) was transferred to a

200mL beaker in an ice box and brought to saturation in 1.4M ammonium sulfate by slow addition of ammonium sulfate with gentle stirring. The precipitate was removed by centrifugation at 18000 rpm for 45 min repeatedly and the cleared supernatant (140 mL) was loaded to hydrophobic phenyl-Sepharose column (Amersham Pharmacia Biotech) which was preequilibrated in 50 mM potassium phosphate buffer, pH 8.0 and 1M ammonium sulfate containing 1 mM DTT. Contaminating proteins were removed and GlmES was eluted by washing the column at a flow rate of 2 mL/min with an ascending gradient of 50 mM potassium phosphate buffer, pH 8.0 containing 1mM DTT according to the following gradients: 0-100 mL, 0%; 100-800 mL, 0-80%; 800-1200 mL, 80-100%; 1200-2400mL, 100%. 25 mL fractions were collected and analyzed by running 12% SDS-PAGE gel. Glutamate mutase usually elutes at the end of the gradient where H_2O is 100%. The fractions containing glutamate mutase were pooled and concentrated to ~50mL by ultrafiltration in a stirred cell fitted with an amicon YM-30 membrane (exclusion limit 30 kDa). Further purification was achieved by an anion-exchange Q-Sepharose column (Amersham Pharmacia Biotech). The column was preequilibrated in 10mM potassium phosphate buffer, pH 8.0 and 1mM DTT sample and the concentrated protein was loaded at a flow rate of 1mL/min. The protein then was eluted at a flow rate of 1mL/min with an increasing gradient of 10mM potassium phosphate, pH 8.0, 0.5M KCI, and 1mM DTT, according to the following gradients: 0-70mM, 0-40%; 70-140mL, 40%; 140-175mL, 40-45%; 175-330mL, 45%; 330-365ml, 45-50%, 365-425mL, 50-60%; 425-450mL, 60-100%; 450-520mL, 100%. 5mL fractions were collected and analyzed by 12% SDS-PAGE. The glutamate mutase fractions were collected and concentrated to ~15mL with YM-30 membrane. The concentrated protein were dialyzed

against 10mM potassium phosphate, pH 8.0 overnight and lyophilized and stored dried at -20 °C.

2.2.3 β-Methylaspartase Expression and Preparation

β-methylaspartase containing a his-tagged N-terminus was overexpressed in a recombinant *Escherichia coli BL21*. A single E. coli bacterial colony was selected from a fresh LB agar plate containing 100 μg/mL of ampicillin. This colony was transferred to a 5mL culture if 2TY containing 100 μg/mL of ampicillin (2TY/amp) and incubated at 37 ºC, overnight, in an orbital shaker at 250 rpm. The overnight culture was then asceptically transferred to a 1L flask containing 500mL of 2TY/amp and incubated at 37 ºC, with vigorous shaking at 300 rpm until it reached an OD_{600} of 0.8. The 500mL culture was equally transferred to six of 2L flask containing 1L of 2TY/amp. Cells were grown at 37 °C with constant aeration and stirring at 250 rpm until they reached an A_{600} of 0.8. Proteins were induced by the addition of IPTG (150 mg/L) and antifoam B (Sigma) was also added to reduce foaming. The cultures were allowed to incubate at 37 °C overnight with a gentle stirring at 150 rpm. The cells were harvested by centrifugation at 6000 rpm for 15min at 4 °C and stored at -20 °C until purification. Typically, ~ 20 g of cells (damp weight) were collected from 6 L of culture.

2.2.4 β-Methylaspartase Purification

~20g of cells were suspended in 50mL of 50mM potassium phosphate, pH 8.0 and 2mM imidazole. The resuspended cells were ruptured by sonication with 16 cycles 30sec burst at sonication power 7 with a cooling period of 1min and 30sec between each

burst. The cell debris was removed by centrifugation at 18000 rpm for 45 min. The supernatant was then applied to 30mL of Ni-NTA His-Bind resin (Novagen) which was preeauilibritaed in 50mM potassium phosphate, pH 8.0 and 2mM imidazole buffer, and allowed to incubate with the resin overnight. The resin was poured into a glass column and step gradient of 2, 20, 50, 250mM imidazole in potassium phosphate, pH 8.0 was applied in sequence. 5mL fractions were collected and OD_{280} of each fraction was checked. Once an OD_{280} reached less than 0.01, the eluting buffer was changed to a higher concentration of imidazole. Typically, β-methylaspartase was eluted in the early fractions of 250mM imidazole buffer. 5mL fractions were collected and analyzed by 12% SDS-PAGE. β-Methylaspartase fractions were concentrated with an amicon with YM-10 filter membrane and stored at -20 ºC in 50% glycerol.

2.3 Enzyme Assay

Glutamate mutase activity was measured using the aerobic spectrophotometric assay. In this assay, the β-methylaspartate formed from glutamate is converted by an excess of β-methylaspartase to mesaconate. The accumulation of mesaconate can be monitored by the increase in absorbance at 240nm. A typical assay solution contained 0.3nM GlmES, 25 μM AdoCbl, 2 units of β-methylaspartase, 10 mM KCl, and 1 mM $MgCl_2$ in 50 mM potassium phosphate, pH 7.0 in a total volume of 1 mL. Reactions were initiated by addition of L-glutamate. The measurements were repeated three times and the averaged value was used for the kinetic calculations. It was not possible to use AdoCbl concentration above 30 μM in assay because the high absorbance of the coenzyme interfered with the spectrophotometric assay.

2.4 UV-Vis Spectroscopy under Anaerobic Condition

U.V.-visible spectroscopy was used to examine whether 2-thiolglutarate binding to the holo-enzyme initiates homolysis of AdoCbl and formation of Cbl(II). Homolysis of AdoCbl results in extensive change to the u.v.-visible spectrum of the coenzyme which is associated with a change in the oxidation and coordination state of cobalt. 1 mL of a 50 μM solution of GlmES in 50 mM potassium phosphate (pH 7.0) was introduced into an cuvette and made anaerobic by repeated evacuation and flushing with argon gas. Stock solutions of AdoCbl and 2-thiolglutarate (pH 7.0) were prepared separately and purged with argon gas for at least 30 min. The holoenzyme was reconstituted by addition of the sAdoCbl solution to the cuvette to give a final concentration of 35 μM holoenzyme. After incubation for several minutes, the spectrum of the holoenzyme was recorded. D, L-2-Thiolglutarate, at a final concentration of 2-8mM, was then added via an airtight syringe to initiate the reaction, and spectra were recorded. A decrease of absorbance at 530nm and an increase at 470nm was clearly observed which indicates the formation of Cbl(II).

2.5 Tritium Partitioning Experiment

The partitioning of tritium from an enzyme-bound intermediate to substrates provides a good way to investigate the reversibility of the hydrogen transfer. 5'-tritium-labeled AdoCbl (specific activity of ~5000 dpm/nmol) was prepared enzymatically through the exchange of tritium from tritium-labeled glutamate. In a septum-sealed vial, the mixture of 50 μM glutamate mutase, 10 mM (S)-thiolglutarate and 5mM DTT in 150 mM potassium phosphate buffer (pH 7.0) was made anaerobic by repeated evacuation and purging with argon. Tritium-labeled AdoCbl, at a final concentration of 26 μM, was

introduced into the mixture using an airtight syringe, and the solution was incubated in the dark for 30 min at room temperature under argon gas. AdoCbl and 5'-dA were recovered by reverse phase HPLC and their tritium contents were determined by scintillation counting. Control reactions were performed in which either glutamate was substituted for 2-thiolglurate, or the enzyme omitted. When enzyme, tritium-labeled AdoCbl, and 2-thiolglutarate were incubated, almost the entire radioactivity was accounted for in the peaks corresponding to 5'-dA and AdoCbl. A small number of counts ~ 5 % of total were found in the flow-through fraction from the HPLC column containing 2-thiolglutarate. However, a control experiment in which the enzyme was omitted resulted in a similar number of counts being present in the flow-through fraction; otherwise radioactivity was only associated with AdoCbl. A further control in which enzyme, tritiated AdoCbl and L-glutamate were incubated together under similar conditions confirmed that almost all the tritium was, as expected lost from the coenzyme.

2.6 EPR Spectrometry

2.6.1 Sample Preparation under Anaerobic Conditions

EPR samples were prepared in a glove box at 4 °C, in dim light. 1 mg of solid 2-thiolglutaric acid was added to an EPR tube and covered with a rubber cap. The EPR tube was purged repeatedly with argon and vacuum prior to be placed in glove box. 0.26 mL of 0.35 mM GlmES in 250 mM potassium phosphate buffer (pH 7.0) and 12 μL of a 1 M solution of DTT were purged with argon prior to be placed in glove box as well. The enzyme mixture was added to an argon-purged EPR tube containing 2-thioglutaric acid in glove box. The 2-thiolglutaric acid was dissolved by gentle pipetting, and the solution

was incubated for 1 min; argon-purged 30 μL of a 10 mM solution of AdoCbl was added to initiate the reaction, and the solution was gently mixed by pipetting. The sample was frozen in dry ice in the glove box and then removed and stored, protected from light, in liquid nitrogen. The final concentrations of GlmES, thioglutaric acid, and AdoCbl were 0.30, 20, and 1.0 mM, respectively. A sample containing 0.30 mM GlmES, 1 mM AdoCbl, and 20 mM L-glutamate was prepared in a similar manner, except that the reaction was initiated by addition of glutamate last.

2.6.2 Recording EPR

EPR spectra were recorded in the dark using a Bruker EMX EPR spectrometer equipped with a liquid nitrogen Dewar system. The conditions for obtaining spectra were as follows: temperature, 115 K; microwave power, 20 mW; microwave frequency, 9.2 GHz; modulation frequency, 100 kHz; modulation amplitude, 3 G. The data were analyzed using the Bruker Win-EPR data manipulation program. The spectrum of the enzyme reacted with 2-thiolglutarate is considerably more complex than that of the enzyme reacted with glutamate, and is unlike that seen previously for any AdoCbl enzyme.

2.6.3 Power Saturation

The series of spectra also recorded over a wide range of microwave powers, 20, 2, 0.2, 0.02, 0.002mW with microwave frequency, 9.2GHz; modulation frequency, 100kHz; modulation amplitude, 0.3mT under 115K to investigate whether this very complicated EPR spectrum arises from a single species or is the result of mixture of species.

2.7 Synthesis of *(2S, 3S)*-3-d_1-Methylspartate from Mono-deuterated Mesaconate

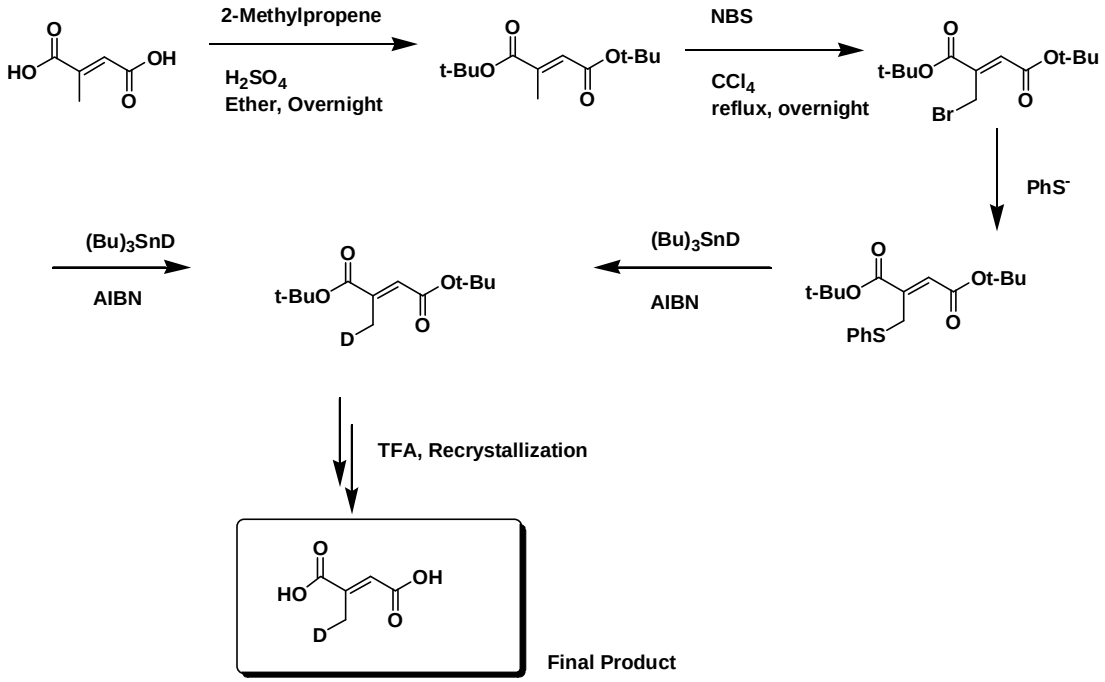

Figure 2.1 Scheme for synthesis of mono-deuterated mesaconate

The synthesis of mono-deuterated mesaconate (Figure 2.1) is based on the regio-specific deuteration of mesaconic acid (methylfumaric acid), which is an intermediate in the fermentation of glutamate by many anaerobic bacteria. Mesaconate is a versatile intermediate that can be readily converted to 3-methylaspartate through the action of β-methylaspartase, an enzyme that has been used to synthesize a variety of aspartic acid analogs.

(2S, 3S)-3-d_1-methylaspartate was synthesized from mono-deuterated mesaconate by enzymatic reaction of β-methylaspartase (Figure 2.2). ~40mg of *(2S, 3S)*-3-d_1-methylspartic acid was dissolved in 250 mM potassium phosphate buffer, pH 8.0, 20 mM potassium chloride, 2 mM magnesium chloride and approximately 1.1 M ammonium

hydroxide and converted to the diammonium salt. 60 units of β-methylaspartase were added and the reaction mixture was incubated at 37°C for 6 hours. An additional 27 units of β-methylaspartase and 80 µL of 2 M ammonium chloride were added to drive the equilibrium toward methylaspartate and the incubation was continued at 37°C for 12 hours. 50 µL of 12N HCl was added to the reaction mixture and heated at 94°C for 5 min to precipitate the β-methylaspartase. The precipitated protein was removed by repeated centrifugation of the suspension (13,200 rpm x 10 min). The supernatant solution was extracted five times with 4 mL water and 24 mL ethyl ether mixture to remove unreacted mesaconate. The decrease in 240 nm absorbance of the reaction mixture indicated that 105 mmoles of mesaconate had disappeared. By assay the activity of β-methylaspartase with the prepared product, the concentration of the mono-deuterated methylaspartate was determined to be 18 mM in a final volume of 4.8 mL. The pH of d_1-methylasprtate was adjusted to pH 7 by 250mM potassium phosphate buffer, pH 7.8.

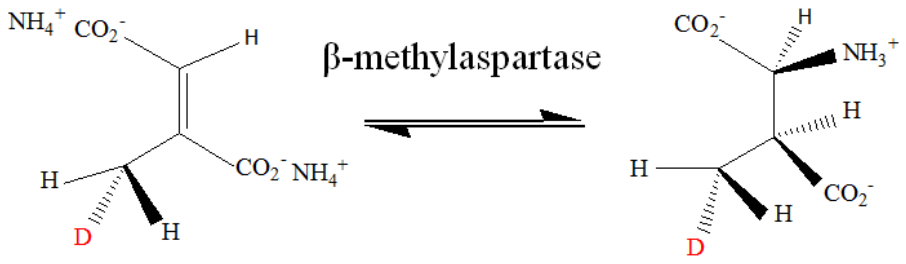

Figure 2.2 Synthesis of d_1-methyl-*threo*-methylasprtate from mono-deuterated mesaconate

2.8 HPLC Analysis of 5'dA

5'-dA was recovered and quantified by Alltech® Alltima™ HPLC reversed-phase C_{18} column, 4.6 x 250mm. Solvents for HPLC were prepared as follows: buffer A: 100% water, buffer B: 10% water and 90% acetonitrile. For better mass spectrometry signals, trifluoroacetic acid (TFA) was not used in the HPLC solvents although the resolution of the HPLC column was lower without TFA. Enzymes remaining in samples were removed by repeated centrifugation (13,200rpm x 5min). A 500 µL injection loop was used and the injection loop was cleaned with four times volume of de-ionized water prior to injection of sample each time. The C_{18} column was preequilibrated in buffer A and the mixture was eluted with an ascending gradient of buffer B as follows: 0 to 5min, 0% B; 5 to17 min, 0 to 40% B; 17 to 18 min, 40 to 100% B, 18 to 23 min, 100% B, 23 to 24 min, 100 to 0% B, 24 to 29 min, 0% B. The flow rate was 1 mL/min and compounds were detected by monitoring absorbance at 260nm.

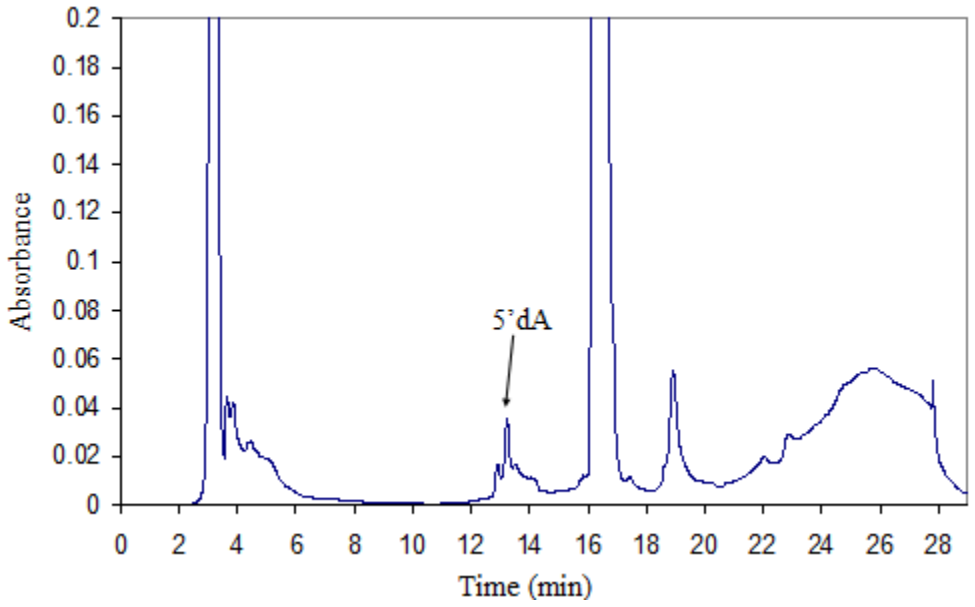

Figure 2.3 Purification and Quantification of 5'-dA by HPLC

The peak around 12-13 min (Figure 2.3), which was previously confirmed by running standard 5'-deoxyadenosine mixed with real enzyme samples from Rapid quench flow, was collected and concentrated to complete dryness by lyopholizer for mass spectrometry. Peaks were present before and after 5'dA peak, and those peaks were also collected as the 5'dA peak varies slightly depending on the column pressure and the amounts of samples loaded. All the procedures were conducted in the dark and dried samples were stored at -20 °C covered by aluminum foil prior to mass spectrometry analysis.

2.9 Rapid Quench Flow

Rapid quench experiments were performed using a Hi-Tech RQF-63 apparatus. Rapid quench-flow is a well established kinetic technique where the experimentalist can isolate intermediates and products within a reaction mechanism and analyze them by analytical methods. It has three separate syringes A, B and Q. The enzyme solutions are injected to syringe A, substrate to syringe B and strong quenching acid injected to syringe Q (Figure 2.4). 73.5µL of 275 µM glutamate mutase in 5mM potassium phosphate buffer, pH 7.0 was mixed with 6.5µL of 358µM AdoCbl immediately before the experiment to the final effective concentration of 285 µM holoenzyme. Although AdoCbl was kept in a dried form in the dark at -20 °C, AdoCbl contains small amount of 5'dA (1nmol/20nmol AdoCbl). AdoCbl was purified by HPLC and concentrated to complete dryness by lyopholizer and stored at -20 °C covered by aluminum foil prior to the rapid quench reaction to remove the 5'dA present in AdoCbl. For better mass spectrometry signal, a minimal amount of potassium phosphate buffer was used

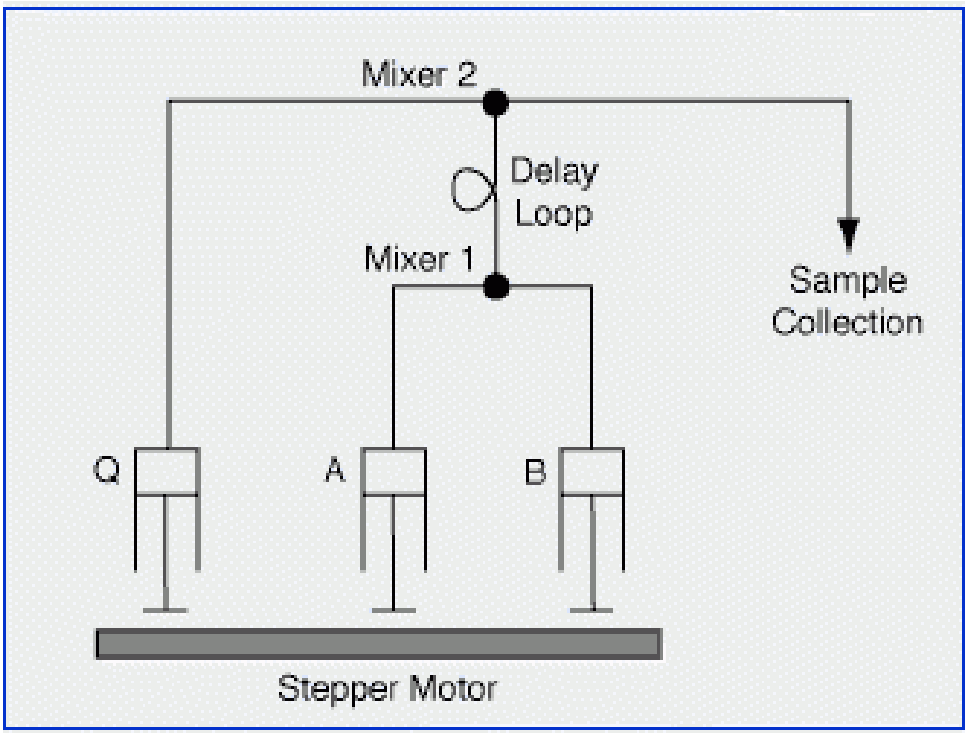

Figure 2.4 Rapid chemical quench flow apparatus

The holoenzyme mixture was rapidly mixed with 80mL of 2.2 mM d_l-methyl-*threo*-methylasprtate in 250 mM potassium phosphate buffer, pH 7.8. To enhance the mixing with the more viscous enzyme solution, a small amount of glycerol (0.1% in final) was added to d_l-methyl-*threo*-methylasprtate to adjust the viscosity close to the enzyme solution. Small volumes of solutions are driven through a high-efficiency mixer and flow into a delay loop. The reactions were quenched with 80 μL of 2.5% trifluoroacetic acid, after aged for various times (12.9~161.9 ms). The reaction solution was recovered at the collect loop by injecting ~500 μL of potassium phosphate buffer. Reaction temperatures were controlled by the water bath connected to RQF-63. The actual temperature in the reaction chamber is slightly (~0.5 ˚C) higher at -2.5 ˚C ~ 12.5 ˚C and slightly lower at 25 ˚C ~ 30 ˚C.

It is known that multiple turnovers will cause 5'-dA to become multiply deuterated at longer times and this will complicate the mass spectrometry measurements and calculations of KIEs as well. To avoid this complication, the reactions were quenched at very short times. It was determined that the relative amounts of di-deuterated 5'dA were less than 1% of non-deuterated 5'dA in shorter than 23.6ms reaction time.

2.10 High-resolution FT-ICR Mass Spectrometry

The direct measurement of 5'-dA kinetics also enable the analysis of the deuterium content of 5'-dA as a function of reaction time by electrospray mass spectrometry. Ultrahigh-resolution FT-ICR mass spectrometry was used to measure the kinetic isotope effect of the reaction between d_1-methyl-*threo*-methylaspartate and glutamate mutase. The presence of natural abundance of ^{13}C and ^{15}N complicates the accurate analysis of deuterium kinetic isotope effects as the peaks for deuterated intermediates and $^{13}C/^{15}N$ containing molecules overlap. To resolve 5'dA containing deuterium and natural abundance of ^{13}C and ^{15}N, a resolution of 70,000 is required (the masses $^{12}C_9\,^{1}H_{13}\,^{13}C_1\,^{14}N_5\,^{16}O_3$ and $^{12}C_{10}\,^{1}H_{12}\,^{2}H_1\,^{14}N_5\,^{16}O_3$ are detected at 253.11716 and 253.12012, respectively: a mass difference of ~3.0 mDa) and, therefore, use of Fourier transform ion cyclotron resonance mass spectrometry (FT-ICR MS) instrument is essential (Figure 2.5).

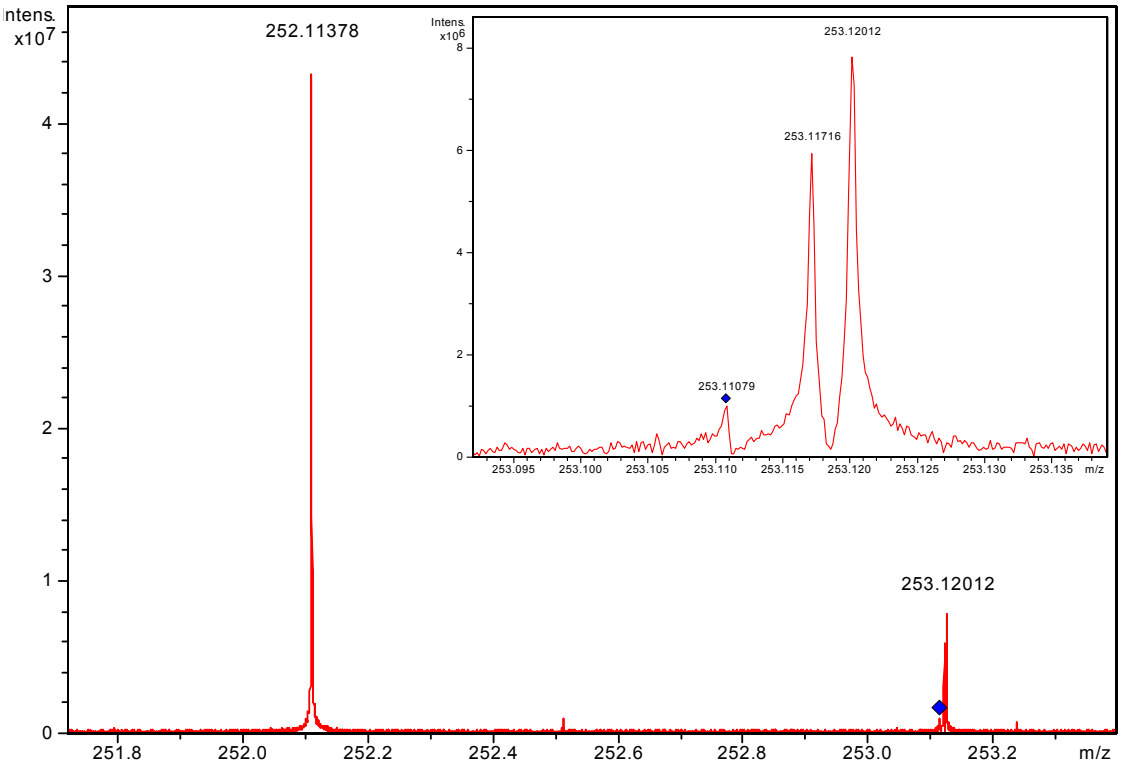

Figure 2.5 High-resolution FT-ICR MS of 5'-dA: the peaks due to ^{13}C, ^{2}H-labeled and unlabeled 5'-dA are indicated. Inset: Expansion of the region around 253.117 amu showing the ^{13}C-labeled and ^{2}H-labeled ions clearly resolved (the small peak at 253.111 is due to natural-abundance [^{15}N] 5'-dA)

5'dA was re-dissolved in an electro-spray solvent containing 50% MeOH and 0.1% formic acid (Acros Organics, Morris Plains, NJ). Experiments were performed in positive ion mode at 50 µL/h with a 7 T Q-FT-ICR mass spectrometer (Bruker Daltonics, Billerica, MA). Assignments for the observed two peaks were confirmed by running commercially available 5'-deoxyadenosine under the same experimental conditions. Only the lower m/z peak corresponding $^{12}C_9\,^{1}H_{13}\,^{13}C_1\,^{14}N_5\,^{16}O_3$ was observed for non-deuterated 5'-deoxyadenosine whereas two peaks ($^{12}C_9\,^{1}H_{13}\,^{13}C_1\,^{14}N_5\,^{16}O_3$ and $^{12}C_{10}\,^{1}H_{12}\,^{2}H_1\,^{14}N_5\,^{16}O_3$) were seen following incubation in 0.5 or 1% D_2O.

Broadband detection and narrowband detection mode were compared using commercially available 5'-dA and samples from enzymatic reactions. For broadband mode date was collected using 512K data points, whereas 128K data points were used for narrowband mode. Higher mass resolving power (m/Δm, where m represents the ionic mass and Δm is the mass spectral peak width at half maximum peak height) is obtained in narrowband mode, which was about 560,000 for $^{12}C_9\ ^{1}H_{13}\ ^{13}C_1\ ^{14}N_5\ ^{16}O_3$ peak while the resolving power of 106,000 was obtained in broadband band mode. Similarly higher resolving power obtained in narrowband mode trends with the enzymatic real sample collected after 55.8ms reaction times and 5'dA incubated in 1% D_2O. For example, in broadband mode, a mass resolving power of ~87,000 is obtained for the $^{12}C_9\ ^{12}C_{10}\ ^{1}H_{12}\ ^{2}H_1\ ^{14}N_5\ ^{16}O_3$ peaks while in narrowband mode a mass resolving power of ~299,000 is obtained for the deuterated peak. Furthermore, the two peaks of interest $^{12}C_9\ ^{1}H_{13}\ ^{13}C_1\ ^{14}N_5\ ^{16}O_3$ (252.10436Da) and $^{12}C_{10}\ ^{1}H_{12}\ ^{2}H_1\ ^{14}N_5\ ^{16}O_3$(252.10799Da) are better baseline-resolved in narrowband mode detection. Therefore, the rest of experiments were performed in narrowband mode and the incorporation of deuterium into 5'-dA from the reaction between d_1-methyl-*threo*-methylaspartate and holoenzyme were precisely followed.

For all experiments, the instrument was tuned to ensure that the detected relative abundance of $^{13}C_1$ versus the monoisotopic peak is as close as possible to the calculated ratio of ~0.1324 before the ratio of mono- to non-deuterated 5'-dA was determined. The center of the mass, Q_{mass} and the width of the window, $Q_{resolution}$ were slightly modified to correct the ratio of ^{13}C to ^{12}C. However a $Q_{resolution}$ larger than 4 was used for most of the measurements to monitor the di-deuterated 5'dA as well.

Chapter 3 Substrate Analog Studies on Glutamate Mutase

3.1 Introduction

To better understand how the structure of the substrate influences the energetics of radical formation, the reactions of glutamate mutase with several glutamate analogues have been investigated. Glutamate mutase recognizes its substrates, L-glutamate and L-*threo*-3-methylaspartate, with a well-designed hydrogen bond network to control the very active radical intermediates. Glutamate mutase therefore is highly specific for its substrates and it has been found that the enzyme will bind only molecules that are substituted slightly at the α-carbon of glutamate (Figure 3.1).

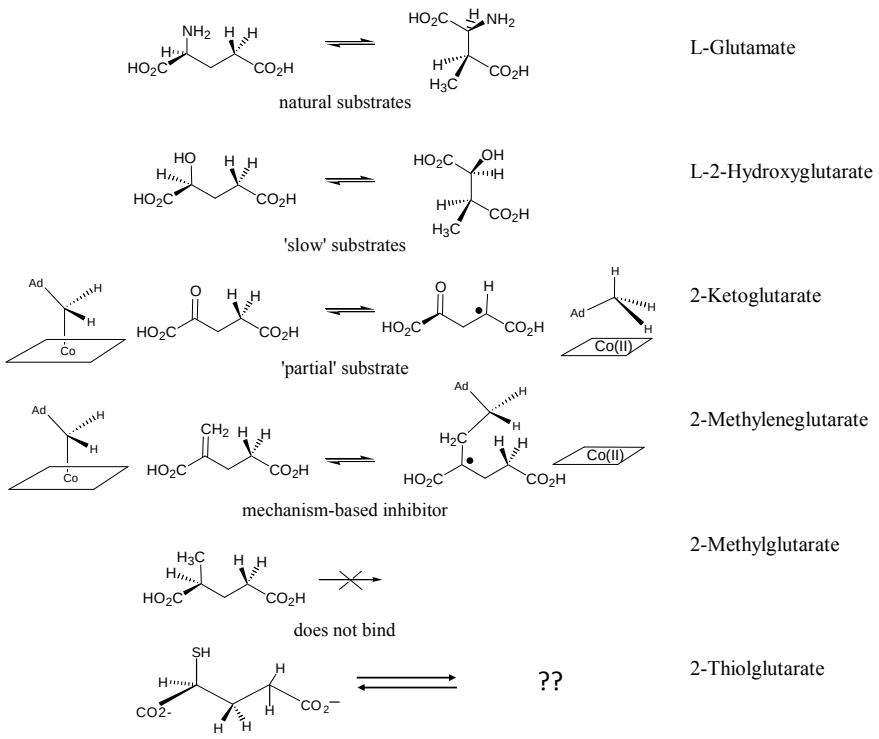

Figure 3.1 Substrate analogs and their reactions catalyzed by glutamate mutase

In contrast to the class II eliminases, diol dehydrase and ethanolamine ammonia-lyase, which have been shown to be fairly promiscuous in their substrate selectivity and has resulted in the identification of substrates that exhibit various degrees of complete and irreversible inactivation, class I mutases such as glutamate mutase showed a much lower susceptibility to inactivation. When the substrate is glutamate, the amino group stabilizes the intermediate glycyl radical such that it is only 1 – 2 kcal/mol higher in energy than the initially formed glutamyl radical.

If the amino group is substituted by a hydroxyl group, the energy of the intermediate glycolyl radical is higher and catalysis is expected to be slower. This has been shown to be the case for the rearrangement of 2-hydroxyglutarate. This substrate turns over about 100 times slower than the reaction with glutamate due to the slow rearrangement, which is the rate-limiting step (Roymoulik, 2000). With glutamate the migrating carbon bears nitrogen that can better stabilize the intermediate glycyl radical than oxygen can stabilize the corresponding glycolyl radical. This result demonstrates that a functional group which can stabilize the migrating carbon radical is essential for facilitating the carbon skeleton rearrangement.

On the other hand, 2-ketoglutarate is bound by the holoenzyme and activates the coenzyme to allow tritium exchange between AdoCbl and carbon-4 of 2-ketoglutarate. However, it does not undergo rearrangement and there is no turnover from 2-ketoglutarate to 3-methyloxalacetate. Therefore this analog can be called a "partial" substrate (Roymoulik, 1999).

2-methyleneglutarate, which is a substrate for the related B_{12} enzyme methyleneglutarate mutase, reacts quite differently with glutamate mutase. It initiates

homolysis of the coenzyme, however the adenosyl radical attacks the exomethylene group to generate a stable adduct between 5'dA and methyleneglutarate. In this respect 2-methleneglutarate behaves like a mechanism-based inhibitor (Huhta, 2002).

The effect of substituting the glutamate nitrogen with oxygen and carbon functionality leads us to examine the reactivity of the enzyme with the sulfur-containing analog, 2-thiolglutarate. This compound might react with enzyme to generate radical intermediates; in particular the putative thioglycolate radical that would arise by fragmentation of the initially formed 2-thiolglutaryl radical would be stabilized by the sulfur atom.

3.2 Results

3.2.1 Inhibition of Glutamate Mutase Activity by 2-Thiolglutarate

To determine whether 2-thiolglutarate was capable of binding at the enzyme active site, the possibility that this substrate analog was a competitive inhibitor was examined. In these and all other experiments 2-thiolglutarate was used as the racemic mixture. Glutamate mutase is specific for the S-enantiomer of its substrates, and the R-enantiomer does not bind to the enzyme. Therefore the presence of the R-enantiomer of 2-thiolglutarate should not interfere, and the concentrations of 2-thiolglutarate referred to here are those of the S-enantiomer only. Initial velocity measurements of glutamate mutase activity were performed at a fixed concentration of AdoCbl (25 μM) in the presence of various substrate concentrations and 2-thiolglutarate concentrations. Using the KaleidaGraph program (Abelbeck Software), the data were fitted to the Michaelis-Menten equation to determine $K_{m,app}$. The plots of $\frac{1}{[S]}$ vs. $\frac{1}{v}$ clearly showed intersecting

lines diagnostic for competitive inhibition, consistent with the inhibitor binding at the same site as the substrate (Figure 3.2). When an inhibitor competitively binds to the enzyme active site, it will reduce the free enzyme available for substrate. The competitive inhibitor binds to the enzyme but not to the enzyme-substrate complex. Therefore, the inhibitor only changes the K_m but does not affect the turnover number of the enzyme.

$$K_{m,app} = K_m(1+\frac{[I]}{K_I}) \qquad \text{Eq. 8}$$

Computer fitting of the data yielded values for K_I = 0.055 ± 0.004 mM for (S)-2-thiolglutarate and K_m = 0.54 ± 0.05 mM for glutamate.

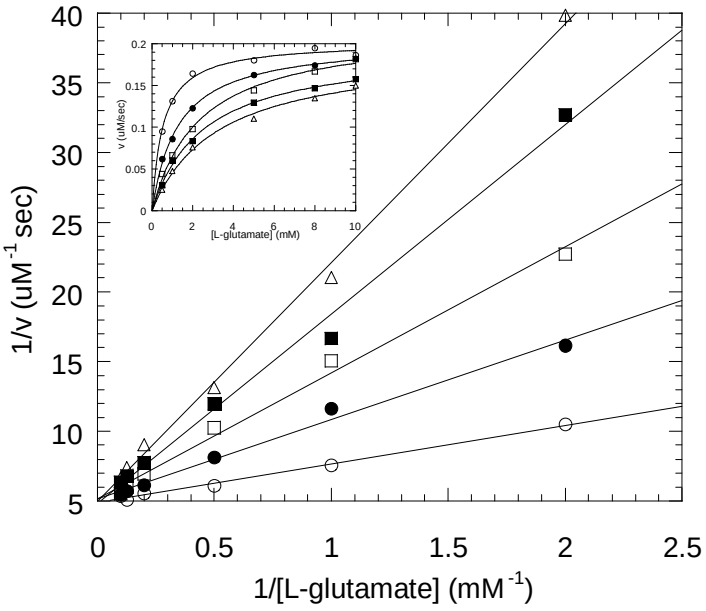

	2-thiolglutrate (mM)	$K_{m,app}$ (mM)
○	0	0.5
●	0.05	1.3
□	0.125	2.3
■	0.25	2.5
△	0.5	3.2

Figure 3.2 Kinetics of enzyme inhibition by 2-thiolglutarate: Double-reciprocal plots of initial velocity vs. glutamate concentration at various concentrations of 2-thiolglutarate: 0.0 (○), 0.05 (●), 0.125 (□), 0.25 (■), and 0.5 mM (△). The inset is a linear plot of the same data.

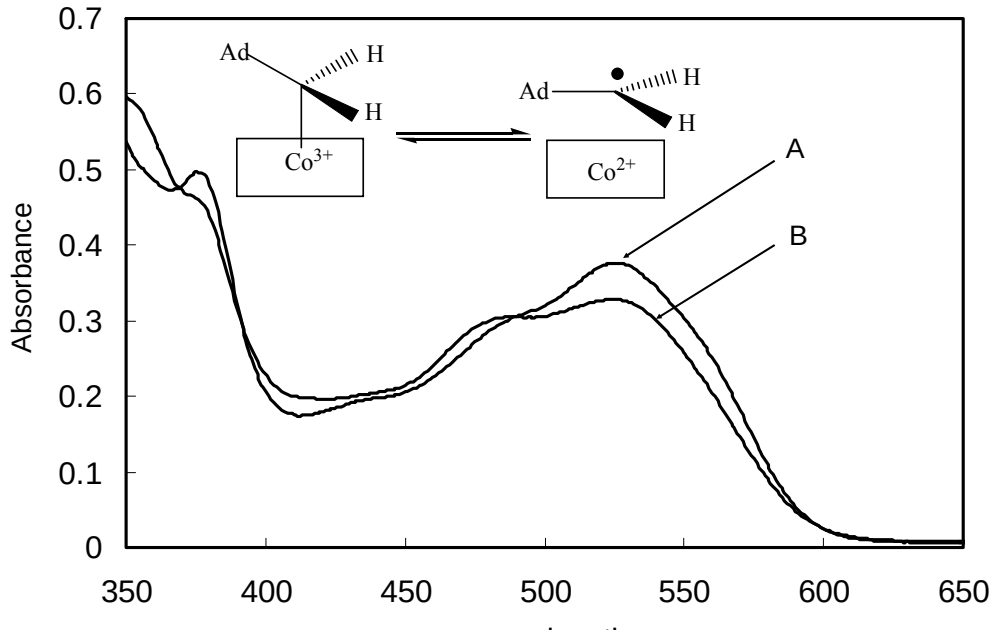

Figure 3.3 UV-visible spectral changes associated with the binding of 2-thiolglutarate to holoenzyme (glutamate mutase + AdoCbl): A; Spectrum of the holoenzyme (35 μM) in the resting state, B; Spectrum of the holoenzyme recorded 20 sec after addition of 2-thiolglutarate (final concentration of 1 mM).

3.2.2 Homolysis of AdoCbl by 2-Thiolglutarate

The kinetic data indicated that 2-thiolglutarate was binding in the active site of the enzyme. Therefore, UV-visible spectroscopy was used to examine whether 2-thiolglutarate binding to the holo-enzyme would initiate homolysis of AdoCbl and the formation of Cbl(II). Addition of 1 mM (S)-2-thiolglutarate to holo-glutamate mutase (35 μM) resulted in significant changes to the u.v.-visible spectrum of the holo-enzyme. In particular, a decrease of absorbance at 530 nm and an increase at 470 nm, indicative of formation of Cbl(II) on the enzyme were evident (Figure 3.3). The spectral changes were almost identical to those that occurred when the holo-enzyme was incubated with 10 mM L-glutamate. Assuming $\Delta\varepsilon_{530}$= 4000 M^{-1} cm^{-1} for the homolysis of AdoCbl, the fraction of enzyme in Cbl(II) form after 30 s incubation with 2-thiolglutarate was 34 %, whereas,

with L-glutamate it was 37 %. With longer incubation times (up to 30 min), with either 2-thiolglutarate or L-glutamate, the slow conversion of the Cbl(II) species to hydroxocobalamin was observed, presumably due to adventitious oxidation of Cbl(II) despite the precautions to make the reaction anaerobic.

3.2.3 Investigation of Turnover Products

Because 2-thiolglutarate appeared to initiate coenzyme cleavage, an investigation was undertaken to decide whether the enzyme might catalyze the rearrangement of 2-thiolglutarate to the methylaspartate analogue, 2-thiol-3-methylsuccinate. A sample was prepared in D_2O buffered with 50mM potassium phosphate, pD 7.0, containing 36 μM glutamate mutase, 30 μM AdoCbl and 20 mM (S)-2-thiolglutarate. The solution was incubated at 25 ºC for 30 min in the dark. For comparison, a control sample that omitted AdoCbl was also prepared. The sample was transferred to an NMR tube and the proton NMR spectrum recorded at 400 MHz. The proton NMR spectrum contained only peaks attributable to 2-thiolglutarate or AdoCbl. In particular, there was no evidence for a characteristic doublet at ~ 0.6 ppm that would correspond to the methyl hydrogens of 2-thio-3-methylsuccinate.

3.2.4 Origin of Hydrogen in 5'-dA

If 2-thioglutrate behaved in an exactly analogous fashion to glutamate one would expect hydrogen to be abstracted from the C-4 carbon. However, if the substrate was bound in a slightly different orientation in the active site it might be feasible for hydrogen to be removed from the thiol group (Figure 3.4). This reaction has precedent in the

generation of a thiyl radical by Class II (AdoCbl-dependent) ribonucleotide reductase (Licht and Stubbe, 1996) (Figure 3.5). Similarly an unexpected reaction was observed when 2-methyleneglutarate was incubated with the enzyme in which the adenosyl radical undergoes addition to the exomethylene double bond to give a radical adduct between the coenzyme and substrate analog. To determine the origin of the hydrogen transferred to 5'-dA the reaction in D_2O buffered with potassium phosphate (pD = 7.0) was conducted.

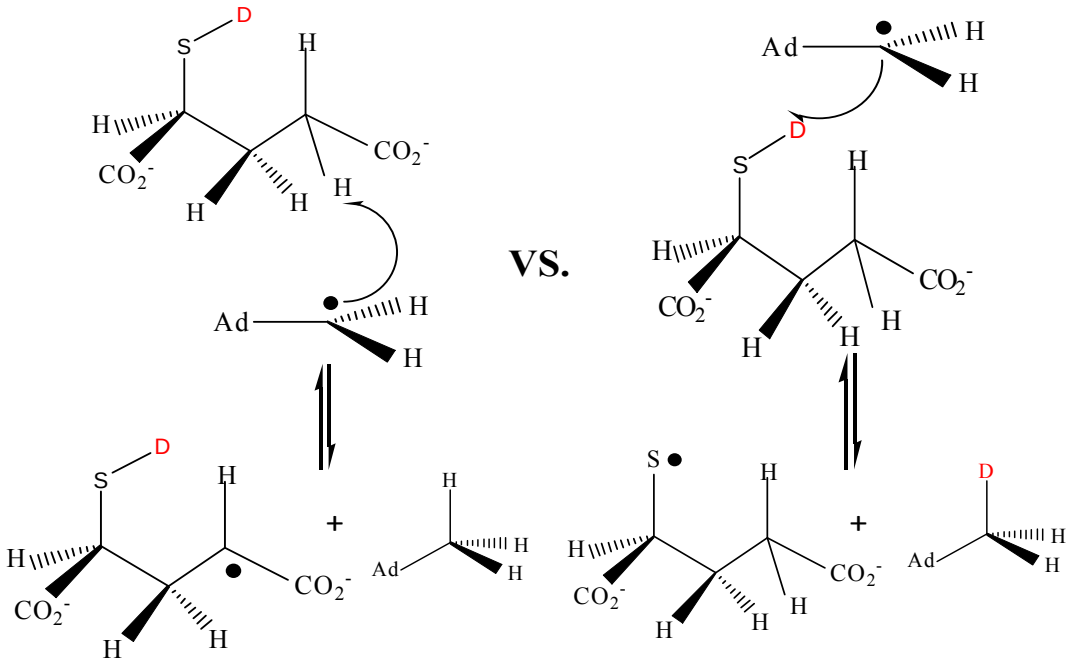

Figure 3.4 Origin of the hydrogen transferred to 5'-dA

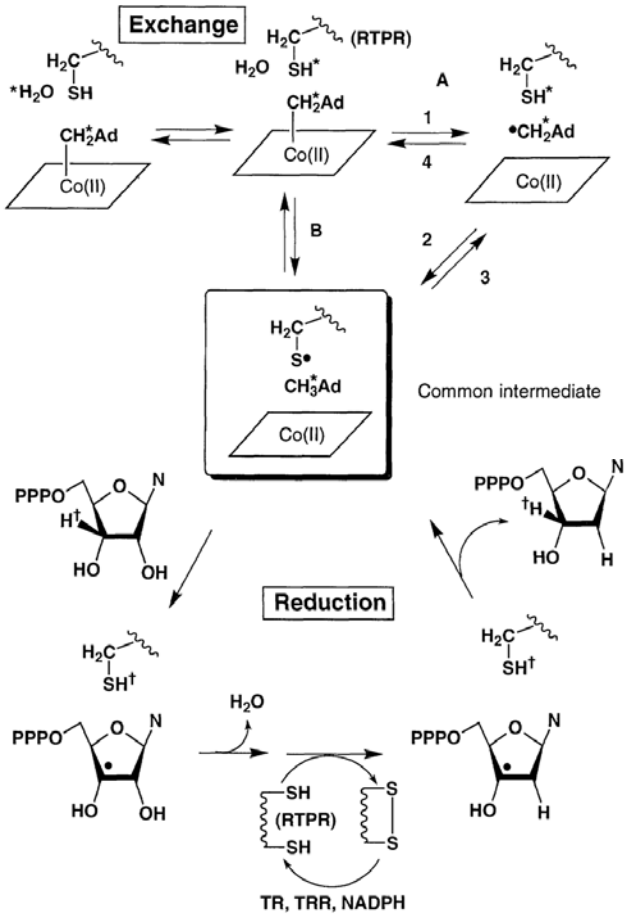

Figure 3.5 Generation of a thiyl radical by ribonucleotide reductase (Licht and Stubbe, 1996)

A solution containing 50 μM glutamate mutase, 98 μM AdoCbl, 10 mM (S) 2-thiolglutarate and 5 mM DTT was incubated at room temperature in the dark for 5 min. 5'-dA was recovered from the reaction mixture by reverse-phase HPLC. The peak corresponding to 5'-dA was collected and analyzed by electrospray mass spectrometry to confirm its identity. If hydrogen abstraction was occurring from C-4 of 2-thiolglutarate then 5'-dA should contain only protons in the 5'-methyl group resulting in a peak at [m+1] = 252 for 5'-dA. On the other hand, if abstraction occurred from the thiol group, then deuterium should be incorporated into 5'-dA resulting in a peak at [m+1] = 253.

The mass spectrum showed no evidence that deuterium was incorporated into 5'-dA, the major peak was at [m+1] = 252, with a peak of about 10 % the intensity at [m+1] = 253 which could be attributed to the ^{13}C-content of 5'-dA (Figure 3.6).

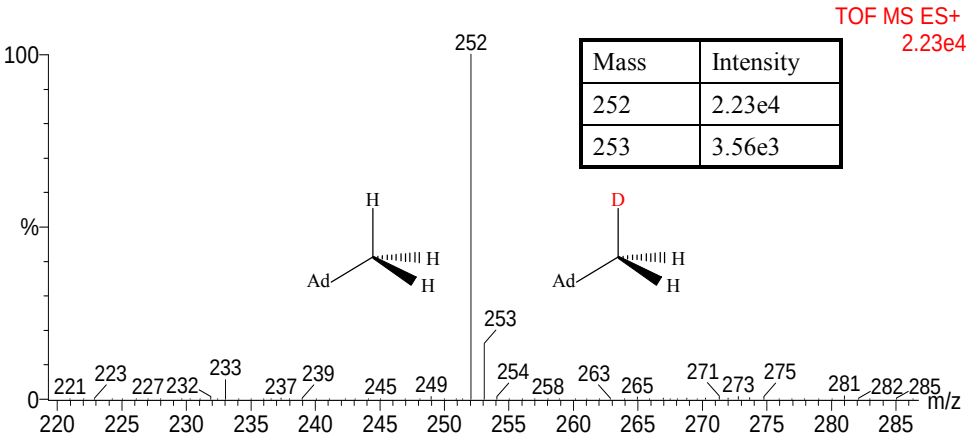

Figure 3.6 Analysis of deuterium contents of 5'dA by mass spectrometry

3.2.5 Tritium Exchange between AdoCbl and 2-Thiolglutarate

To determine whether hydrogen transfer between AdoCbl and 2-thiolglutarate was reversible, the ability of the enzyme to catalyze the transfer of tritium at the 5'-carbon of AdoCbl to 2-thiolglutarate was examined. Previously it was shown that the transfer of tritium from AdoCbl to glutamate and methylaspartate is essentially complete after 15 s (k_{app} = 0.67 ± 0.05 s-1) (Marsh, 1995). Even after prolonged incubation (30 min) of 2-thiolglutarate with holo-enzyme reconstituted with tritiated AdoCbl, almost all of the radioactivity was accounted for in the peaks corresponding to 5'-dA and AdoCbl.

A small number of counts ~ 5 % of total were found in the flow-through fraction from the HPLC column containing 2-thiolglutarate, however, a control experiment in which the enzyme was omitted resulted in a similar number of counts being present in the flow-through fraction; otherwise radioactivity was only associated with AdoCbl. A

further control in which enzyme, tritiated AdoCbl and L-glutamate were incubated together under similar conditions confirmed that almost all the tritium was, as expected lost from the coenzyme (Figure 3.7). Therefore it can be concluded that hydrogen transfer from 2-thiolglutarate to 5'-dA is essentially irreversible.

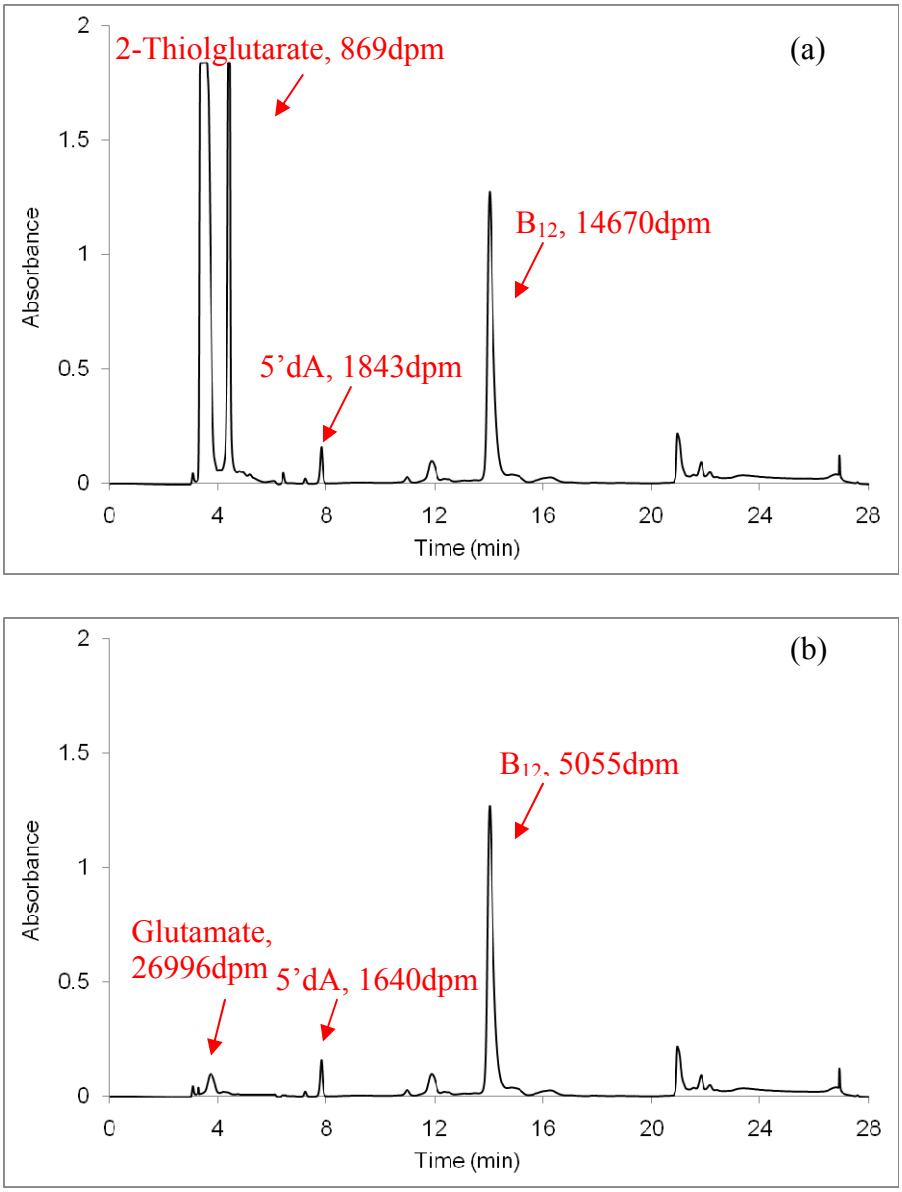

Figure 3.7 Tritium exchange between AdoCbl and (a) 2-thiolglutarate, (b) glutamate: numbers next to peaks are tritium counts with a unit of dpm.

3.2.6 EPR Spectroscopy

To better characterize the radical species generated by the reaction of 2-thiolglutarate with the enzyme, EPR spectrum of glutamate mutase in the presence of 2-thiolglutarate was recorded. For comparison, a sample of the enzyme reacted with L-glutamate was prepared in parallel and the EPR spectrum recorded under the same conditions. The spectrum of the enzyme reacted with glutamate has been well-characterized and shown to arise through the interaction of the C-4 glutamyl radical and Cbl(II). The EPR spectrum of the enzyme-glutamate complex recorded is identical to that which has been analyzed previously. In contrast, the EPR spectrum of the enzyme-thiolglutarate complex is particularly unusual: more complex than that of the enzyme reacted with glutamate, and very different from spectra that have been obtained for any other AdoCbl enzymes. For example, the spectrum of the enzyme reacted with hydroxyglutarate, which is a slow substrate, is very similar to that obtained with glutamate, as is the spectrum of the enzyme reacted with 2-methyleneglutarate, which is a mechanism-based inhibitor. In each of these cases there is good evidence that the unpaired electron resides on a carbon atom.

Preliminary analysis of the enzyme-thiolglutarate EPR spectrum suggests the presence of a cob(II)alamin species interacting with an organic radical with the characteristic EPR features of g_z = 2.04 and A_{avg} = 54 G. The eight-fold hyperfine coupling feature arising from the nitrogens in the corin ring that ligate cobalt, which is clearly seen in the enzyme-glutamate complex, appears also to be present in the spectrum; but is obscured by the presence of other radical species. The superhyperfine structure, arising from the interaction with the axial histidine, is not clearly resolved in

either spectrum, possibly due to broadening by the interaction with the organic radical species. Most evident are additional features in the lower magnetic field region (2600-3100 G) and one at higher field strength with g = 1.85 (Figure 3.8).

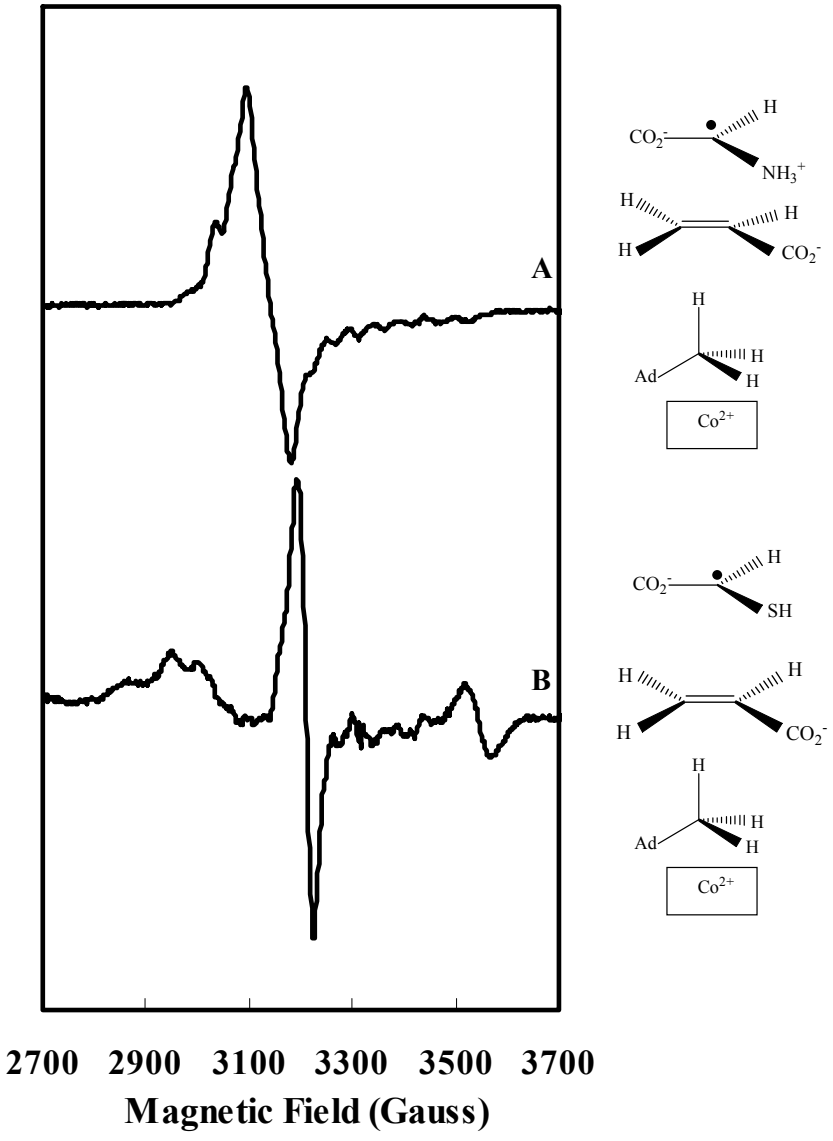

Figure 3.8 EPR spectra of glutamate mutase holoenzyme with A: glutamate, and B: 2-thiolglutarate: microwave power, 10dB; microwave frequency, 9.2GHz; modulation frequency, 100 kHz; modulation amplitude, 3mT; temperature, 115K

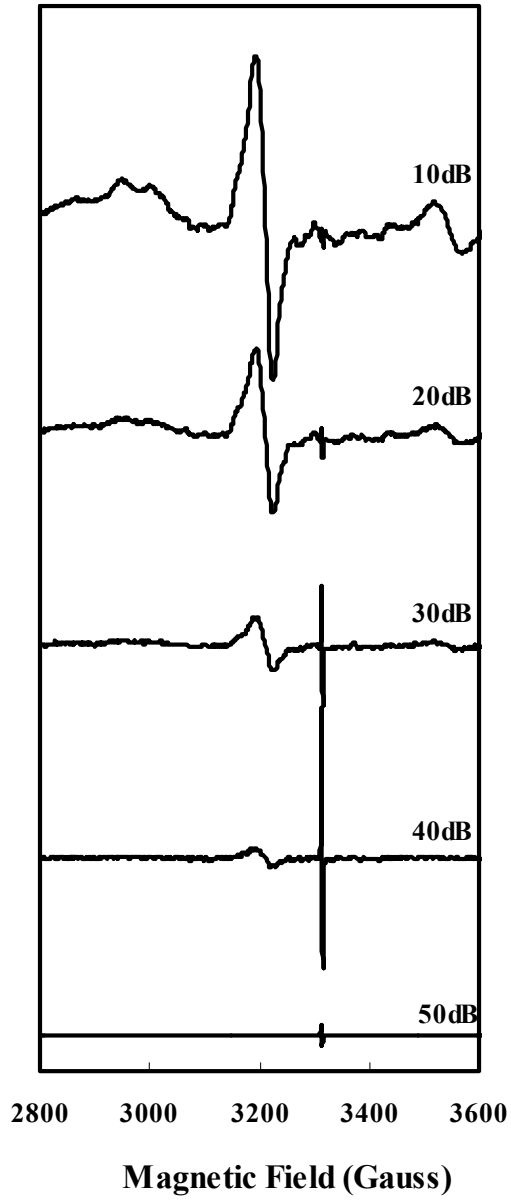

Figure 3.9 Series of EPR spectra of glutamate mutase holoenzyme with 2-thiolglutarate recorded over a wide range of microwave powers:
Microwave power, 10, 20, 30, 40, 50dB; microwave frequency, 9.2GHz; modulation frequency, 100 kHz; modulation amplitude, 0.3mT; temperature, 115K

To examine whether this very complicated EPR spectrum arises from a single species or is the result of mixture of species, a power saturation study was undertaken. The series of spectra recorded over a wide range of microwave powers indicates the

presence of a single species with identical power dependence, with the exception of the very sharp singlet at g = 1.98 that is most likely due to traces of oxygen in the sample (Figure 3.9). The single species is expected to be based mostly or entirely on sulfur, and this presumably accounts for the additional complexity of the spectrum.

The unusual appearance of the spectrum leads to speculate that the complex spectrum arises from the interaction of cob(II)alamin with most likely a thioglycolyl radical derived from the fragmentation of thioglutaryl radical. Computational simulation of the spectrum was undertaken by Steven Mansoorabadi and Ann Menefee in Professor George Reed's laboratory assuming a spin-coupled interaction between low-spin Co2+ in cob(II)alamin and a thioglycolyl radical. The simulation result is consistent with the spectrum recorded and it confirms the formation of thioglycolyl radical (Figure 3.10).

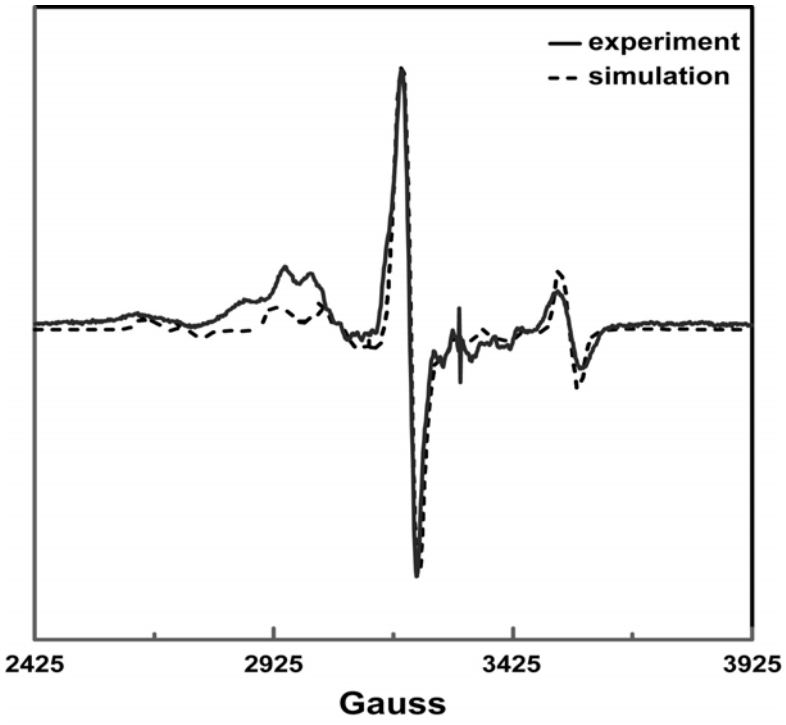

Figure 3.10 Comparison of the simulated and experimental EPR spectra for glutamate mutase reacted with 2-thiolglutarate.

Because the p*K*a of the sulfur atom is close to that of the pH at which the spectrum was recorded, the spectrum was simulated assuming that the sulfur atom was either protonated or deprotonated. However, the simulation values varied very slightly between two states and the protonation state of sulfur from the spectrum could not be determined.

From the zero-field splitting parameters and the Euler angles aligning the zero-field splitting tensor with the Co^{2+} **g**-tensor, the cobalt atom and the thioglycolyl radical are calculated to be ~10 Å apart, with the thioglycolate radical lying at an angle of ~70° (sulfur protonated) or ~60° (sulfur deprotonated) from the normal to the plane of the corrin ring. Inspection of the crystal structure of the enzyme-substrate complex (Reitzer, et al., 1999 and Gruber et al., 2001) suggests that these geometrical constraints for the Co^{2+} -thioglycolyl radical pair are quite consistent with the enzyme active site.

3.3 Discussion

From the results presented so far, the reaction of 2-thiolglutarate with glutamate mutase can be summarized as follows. 2-Thiolglutarate binds to the enzyme active site and triggers homolysis of AdoCbl. The adenosyl radical then reacts to abstract hydrogen from C-4 of 2-thiolglutarate, to generate a radical at C-4 of 2-thiolglutarate. The thioglutaryl radical next undergoes fragmentation to generate acrylate and a thioglycolyl radical (Figure 3.11). These steps mimic the reaction with the natural substrate, glutamate. However, abstraction of hydrogen from 2-thiolglutarate appears to be irreversible as the lack of tritium exchange suggests. This is most likely because upon forming the thioglutaryl radical, fragmentation occurs immediately to form the stable thioglycolyl radical and acrylate.

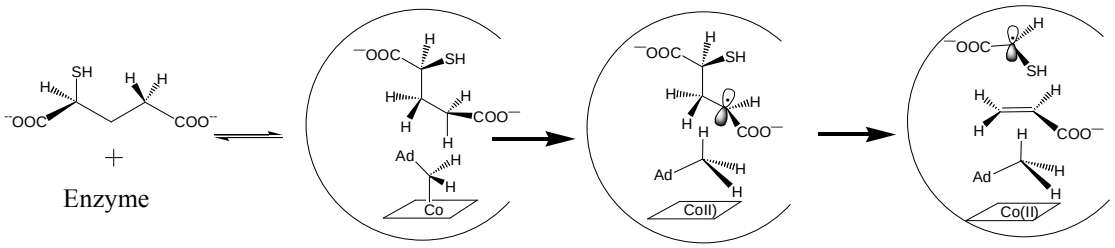

Figure 3.11 Proposed mechanism for the reaction of 2-thiolglutarate with glutamate mutase, resulting in the formation of Cbl(II), 5'-dA, and the thioglycolyl radical.

The selective stabilization of radical intermediates by sulfur has been used to probe the mechanism of the radical-SAM-dependent enzyme, lysine-2,3-aminomutase. Here the sulfur-containing lysine analog 4-thia-lysine was used to stabilize the radical initially formed by abstraction of hydrogen at C-3 of lysine, allowing it to be observed by EPR. In this case 4-thia-lysine is still turned over by the enzyme, albeit at only about 1 % of the rate of lysine. 2-thio-3-methylsuccinate is the expected product of the rearrangement of 2-thiolglutarate. However, the equilibrium constant most likely disfavors the rearrangement of 2-thiolglutarate to 2-thio-3- methylsuccinate and the product may be prone to decomposition. Therefore, we cannot rule out the possibility that 2-thiolglutarate is turned over by the enzyme very slowly.

The EPR spectrum of the enzyme reacted with glutamate has been characterized and is well-simulated by assuming the exchange-coupled interaction between the C-4 glutamyl radical and Co^{2+} in Cbl(II). From this simulation, it was concluded that the two unpaired electrons were 6.6 ± 0.9 Å apart, a distance latter found to be in good agreement with that expected from analysis of the crystal structure of the enzyme-substrate complex. Assuming that 2-thiolglutarate binds to the enzyme in the same orientation as glutamate, fragmentation of the initially formed 2-thiolglutaryl radical to produce the thioglycolyl

radical and acrylate would move the radical ~3 Å farther from the cobalt atom. Therefore, an ~10 Å separation between the cobalt and thioglycolyl radical that was derived from the simulation appears to be quite reasonable.

The thiyl radical associated with the mechanism of AdoCbl-dependent ribonucleotide reductase has been extensively characterized by EPR. The spectrum is well simulated by assuming the interaction of a sulfur based organic radical with cob(II)alamin. The corresponding g values required for reasonable fits in simulations for the thiyl radical of the ribonucleotide reductase are 2.2, 2.0, and 1.99 (Licht et al., 1996). However, the EPR spectrum of ribonucleotide reductase is too different from that of the glutamate mutase-2-thiolglutarate complex for inferences to be drawn. Further experiments with isotopically-labeled compounds and detailed simulations of the spectra of the enzymatic sample should allow the radical species to be definitively identified and spatial relationship to the cobalt atom to be calculated.

Recently, Toraya et al. investigated reactions of diol dehydrase with thioglycerol. Holodiol dehydrase underwent rapid and irreversible inactivation by thioglycerol without catalytic turnovers. In the inactivation, the Co–C bond of adenosylcobalamin underwent irreversible cleavage forming unidentified radicals and cob(II)alamin that resisted oxidation even in the presence of oxygen. Two moles of 5'-deoxyadenosine per mol of enzyme was formed as an inactivation product from the coenzyme adenosyl group. Inactivated holoenzymes underwent reactivation by diol dehydrase-reactivating factor in the presence of ATP, Mg^{2+} and adenosylcobalamin. It was thus concluded that thioglycerol served as mechanism-based inactivators. In the inactivation by thioglycerol, a product radical may be lost by the elimination of sulphydryl group, producing acrolein

and unidentified sulphur compound(s). The loss or stabilization of product radicals would result in the inactivation of holoenzyme, because the regeneration of the coenzyme becomes impossible (Toraya, 2008).

Sandala et al. calculated the radical stabilization energies for a variety of substituted glycyl radical analogues and they demonstrated that modifications at the radical center can profoundly affect the relative stability of the resulting radical, leading to important mechanistic consequences. Furthermore, they also found that the formation of a thioglycolyl radical, derived from (S)-2-thiolglutaric acid, is highly dependent on the protonation state of sulfur. The neutral thioglycolyl radical is found to be of stability similar to that of the glycolyl radical generated from reaction with a slow substrate, (*S*)-2-hydroxyglutaric acid and to be expected to rearrange to product on the basis of energy requirements, whereas the S^-, deprotonated form of the thioglycolyl radical is much more stable; ~45 KJ mol $^{-1}$ lower than neutral radical and ~32 KJ mol $^{-1}$ lower than glycyl radical. The relatively high forward barrier for recombination of the cleavage products associated with the anion fragment radical and the disproportionate equilibrium in favor of these cleavage products can rationalize the inhibition of the enzyme by the substrate analogue 2-thiolglutarate (Sandala, 2008).

One aspect of the reaction of thiolglutarate with the enzyme remains unclear. If the formation of the thioglycolyl radical is sufficiently favorable for it to effectively be irreversible, as the lack of tritium exchange suggests, then one might expect that all of the enzyme active sites would be converted to this radical form. However, it appears that only ~35% of the enzyme active sites undergo homolysis upon reaction with 2-thiolglutarate, a proportion similar to that observed with glutamate. Indeed, none of the

substrate analogues that have been investigated with the enzyme seem to elicit more than 50% cleavage of the coenzyme. It is possible that the lack of observed tritium exchange is simply a consequence of very slow exchange kinetics coupled with a large isotope effect discriminating against the transfer of tritium to 2-thiolglutarate. Another possibility is that some of the protein is inactive, although previous binding measurements indicate a 1:1 stoichiometry for AdoCbl binding to the coenzyme. It is also possible that this may be the result of 'half-of-sites' or negative cooperativity between the two active sites of the glutamate mutase dimer.

3.4 Conclusion

Previous substrate analog studies as mentioned at the beginning of this chapter, together with the data presented here, highlight the importance of the structure of the substrate in optimizing the stability of radical intermediates for efficient catalysis. The functional group at C-2 of the substrate plays a critical role in the fragmentation-recombination pathway by which the carbon skeleton undergoes rearrangement by stabilizing the transiently formed radical on C-2. When the substrate is glutamate, the amino group stabilizes the intermediate glycyl radical such that it is only 1 – 2 kcal/mol higher in energy than the initially formed glutamyl radical (Chih and Marsh, 2000). With a thiol group at C-2 it appears that the resulting thioglycolyl radical is too stable for the reaction to proceed toward the rearranged product due to delocalization of the unpaired electron on sulfur.

Chapter 4 Investigation of the Intrinsic Deuterium Kinetic Isotope Effects and Hydrogen Tunneling Effects for Hydrogen Transfer between AdoCbl and Substrate in Glutamate Mutase

4.1 Introduction

Our interest in the mechanisms by which enzymes generate free radicals, as exemplified by dependent glutamate mutase led us to undertake an extensive set of kinetic isotope effect (KIE) measurements to examine how hydrogen abstraction from the substrate and coenzyme homolysis are coupled together. Pre-steady-state kinetic studies are required to investigate the intrinsic isotope effect on hydrogen transfer, which is a very early step in the glutamate mutase reaction. Rapid chemical quench techniques are essential to monitor the accumulation of intermediate, 5'dA and to obtain the microscopic rate information on the mechanism. The kinetic isotope effect for hydrogen transfer was previously measured by comparing the separately measured reaction rate of labeled and unlabeled substrates. However, the isotopically insensitive step of coenzyme homolysis, which is kinetically coupled to the hydrogen abstraction, may mask the intrinsic kinetic isotope effect for hydrogen abstraction.

To avoid this complexity, and obtain the accurate intrinsic kinetic isotope effect, *(2S, 3S)*-3-d_1-methylspartate, a substrate molecule containing both hydrogen and deuterium in the methyl group was synthesized. This compound allows the intra-molecular competition for hydrogen transfer from the methyl group to be investigated.

The experiment takes advantage of the fact that the intrinsic deuterium KIE can be measured by specifically labeling the methyl carbon with one deuterium atom and analyzing the isotopic composition of the reaction products. The KIE can be measured, even when the isotopically sensitive step is *not* rate determining, because it is manifested though *intra*-molecular competition between protium and deuterium atoms, which remain chemically equivalent even in the enzyme active site. The deuterium content of 5'-dA was directly analyzed by high-resolution mass spectrometry which can resolve 5'-dA containing deuterium and natural abundance of ^{13}C or ^{15}N. An important assumption in this experiment is that hydrogen and deuterium have the same probability of occupying the abstractable position in the methyl group of the substrate; i.e. that the methyl group can rotate completely freely. The C-D bond is slightly shorter than a C-H bond so even this most conservative of substitutions introduces a slight asymmetry into the methyl group that could, in principle, lead to one rotational conformation being preferred over another. However, this possibility is extremely unlikely as the differences in energies between such conformations are undoubtedly very small relative to thermal energies at room temperature. Indeed, there is no demonstration of restricted rotation of a methyl group in the active site for an enzyme.

Hydrogen tunneling has increasingly been found to contribute to enzyme reactions in hydrogen transfer reactions including in AdoCbl-dependent reactions. The quantum tunneling of hydrogen can be diagnosed by measuring the temperature dependence of isotope effects. Chowdhury and Banerjee have measured the KIE of this hydrogen abstraction step in the reaction catalyzed by AdoCbl-dependent methylmalonyl-CoA mutase. More recently Doll and Finke studied the same step in three

different cobalamins, including coenzyme B_{12} (AdoCbl), dissolved in ethylene glycol, no protein being present. They showed that the KIEs of all three tested ligands fit the same linear Arrhenius plot as the KIEs of Chowdhury and Banerjee, from which they concluded that the presence of the protein has no significant effect on the hydrogen transfer rate. The combination of well-designed intra-molecular competition experiment and high resolution mass spectrometry techniques provides a very accurate method for measuring intrinsic isotope effects in glutamate mutase. This novel method can be applied to investigate the hydrogen tunneling effects in glutamate mutase. Intrinsic deuterium isotope effects in glutamate mutase are measured at various temperatures (-2.5˚C ~ 30 ˚C) to determine whether hydrogen tunneling makes an important contribution in glutamate mutase reaction.

4.2 Results

4.2.1. Intrinsic Kinetic Isotope Effect in Glutamate Mutase

The intrinsic KIE in an AdoCbl-dependent enzyme was measured for hydrogen atom transfer from substrate to coenzyme, which is a key step in the mechanism of this class of enzymes. Glutamate mutase enzyme was reacted 10˚C with (*2S, 3S)*-3-d_1-methylspartate and quenched at various reaction times (12.9ms ~161.9ms) and the ratio of protiated and deuterated 5'-dA were analyzed by high resolution mass spectrometry. During the reaction 5'-deoxyadenosyl radical, generated by homolysis of AdoCbl, is confronted with the choice of abstracting either protium or deuterium from the methyl group of the same substrate molecule. Hydrogen or deuterium abstraction generates methylaspartyl radical that rapidly rearranges to the much more stable glutamyl radical so

that at sufficiently short times (< 100 ms) the reaction is effectively irreversible and the intrinsic isotope effect is manifested.

Figure 4.1 shows a representative mass spectrum from an experiment in which the reaction was stopped after 161.9ms (the longest reaction time spectrum was taken to clearly exhibit ^{13}C, ^{2}H-labeled and $^{2}H_2$-labeled ions) and the 5'-dA peaks were analyzed by electrospray FT-ICR MS in positive-ion mode. The $[M+H]^+$ peaks due to naturally occurring ^{13}C- and ^{2}H-labeled 5'-dA molecules are baseline-resolved and are of similar abundance.

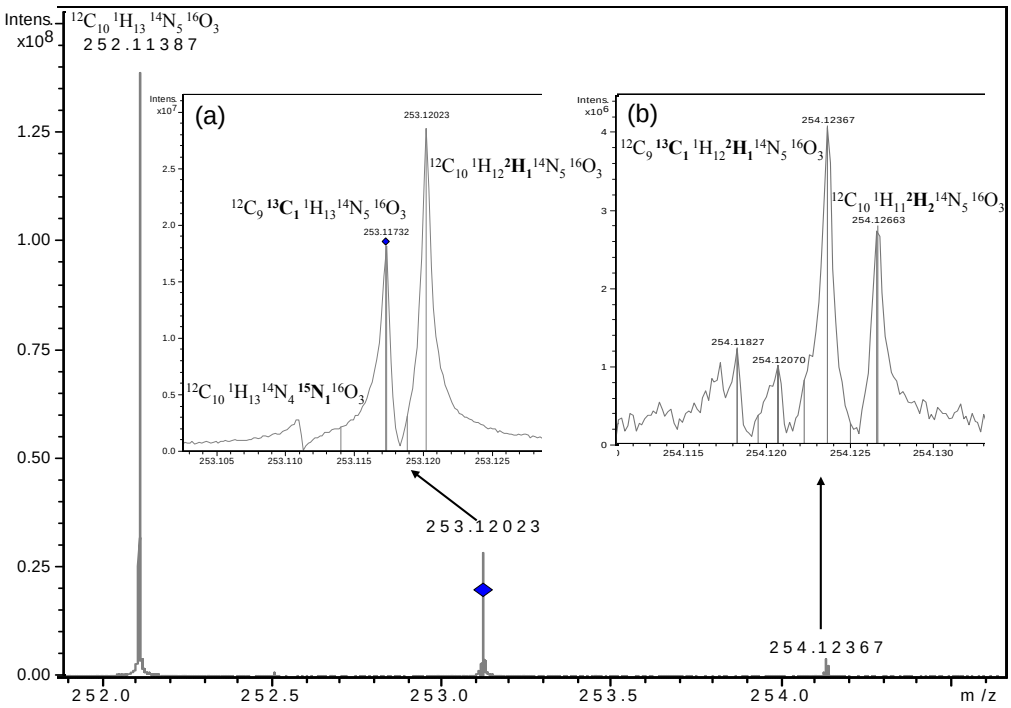

Figure 4.1 High-resolution FT-ICR MS of 5'-dA isolated from glutamate mutase after reaction with [$^{2}H_1$]methylaspartate for 161.9 ms: the peaks due to unlabeled, ^{13}C, and ^{2}H, ^{15}N labeled 5'-dA are indicated. Inset: (a) Expansion of the region around 253.120amu showing the ^{13}C-labeled and ^{2}H-labeled ions clearly resolved at 253. 117amu and 253.120 (the small peak at 253.111 is due to natural-abundance [^{15}N] 5'-dA). (b) Expansion of the region around 254.123amu showing the ^{13}C, ^{2}H-labeled and $^{2}H_2$-labeled ions clearly resolved at 254.1236 and 254.1266

From the well-resolved mass spectrum, the KIE can simply be calculated by comparing the peak height for non-deuterated peaks, sum of [^{12}C] 5'-dA and [^{13}C] 5'-dA and mono-deuterated peaks [^{12}C, ^{2}H]5'-dA and [^{13}C,^{2}H]5'-dA according to equation 9. Because there are two protium atoms and one deuterium atom in the methyl group of *2S, 3S)*-3-d_1-methylaspartate, the KIE must be corrected by a factor of 2.

$$KIE = \frac{1}{2}\left(\frac{[^{12}C]-5'dA+[^{13}C]-5'dA}{[^{12}C,{}^{2}H]-5'dA+[^{13}C,{}^{2}H]-5'dA}\right) \qquad \text{Eq. 9}$$

Alternatively, because the natural abundance of ^{13}C is known to great precision, the intrinsic KIE can also be calculated by comparing the ratio of [^{13}C]5'-dA to sum of [^{12}C,^{2}H]5'-dA [^{13}C,^{2}H]5'-dA and correcting the result for the natural abundance, n, (~0.1324) using equation 10 which derived from equation 11.

$$KIE = \frac{1}{2}\left(\frac{[^{13}C]-5'dA}{[^{12}C,{}^{2}H]-5'dA+[^{13}C,{}^{2}H]-5'dA}\right)\left(\frac{1+n}{n}\right) \qquad \text{Eq. 10}$$

$$KIE = \frac{1}{2}\left(\frac{[^{13}C]-5'dA}{[^{12}C,{}^{2}H]-5'dA+[^{13}C,{}^{2}H]-5'dA}\right)\left[\left(\frac{[^{12}C]-5'dA}{[^{13}C]-5'dA}\right)+\left(\frac{[^{13}C]-5'dA}{[^{13}C]-5'dA}\right)\right] \qquad \text{Eq.11}$$

The deuterium KIE values obtained from two equations are very similar within the error of 10% as the instrument is tuned to ensure that the detected relative abundance of $^{13}C_1$ versus the monoisotopic peak is as close as possible to the calculated ratio of ~0.1324 for all measurements as mentioned earlier. Deuterium KIE for hydrogen transfer from the substrate, *(2S, 3S)*-3-d_1-methylaspartate, to 5'-dA in glutamate mutase is ~3 under 10 ˚C between the reaction times 12.9ms and 112.2ms. These values are lower than ~4.1, the value published in 2007 (Yoon et al., 2007), varying slightly (~10~30%) at different reaction times. There are two main reasons that cause the recent data to exhibit lower

KIEs. First, more highly purified AdoCbl was used only in recent experiment; as mentioned in the material and methods chapter, commercially available AdoCbl contains small amount of 5'dA (1nmol/20nmol AdoCbl) that can be purified by HPLC. Furthermore, we revised the method of calculation to take [^{13}C, ^{2}H]5'-dA peaks into account for the calculation, which will increase the amount of deuterated 5'-dA by ~ 13% and reduce the KIEs accordingly. This value is well within the semi-classical limit for a deuterium isotope effect and is much smaller than the anomalously large KIEs previously measured in other AdoCbl enzymes and non-enzymatic model reactions, which were attributed to extensive hydrogen tunneling. This argues strongly for a role for glutamate mutase in modulating the transition state for hydrogen transfer and thereby changing the KIEs. The result is in surprising contrast to those measured for methylmalonyl-CoA mutase and non-enzymatic model systems which are both of similar magnitude and much larger than the semi-classical limit.

4.2.2 Temperature Dependence Studies on Kinetic Isotope Effects

KIEs, their temperature dependences, and the internal relationships between them are important tools in studying the nature of H-transfer. Glutamate mutase reactions with *(2S, 3S)*-3-d_1-methylspartate were quenched after aging for various reaction times (12.9~161.9ms) under various temperatures (-2.5˚C ~ 30 ˚C) to determine the intrinsic kinetic isotope effect at various temperatures and investigate hydrogen tunneling effects in the reaction of glutamate mutase. Generally deuterium KIEs decrease as the temperature gets higher because the reaction tends to go faster at higher temperature as there is more thermal energy available. And interestingly, the deuterium KIEs seem to

increase more as the reaction time gets shorter at relatively lower temperature (Figure 4.2).

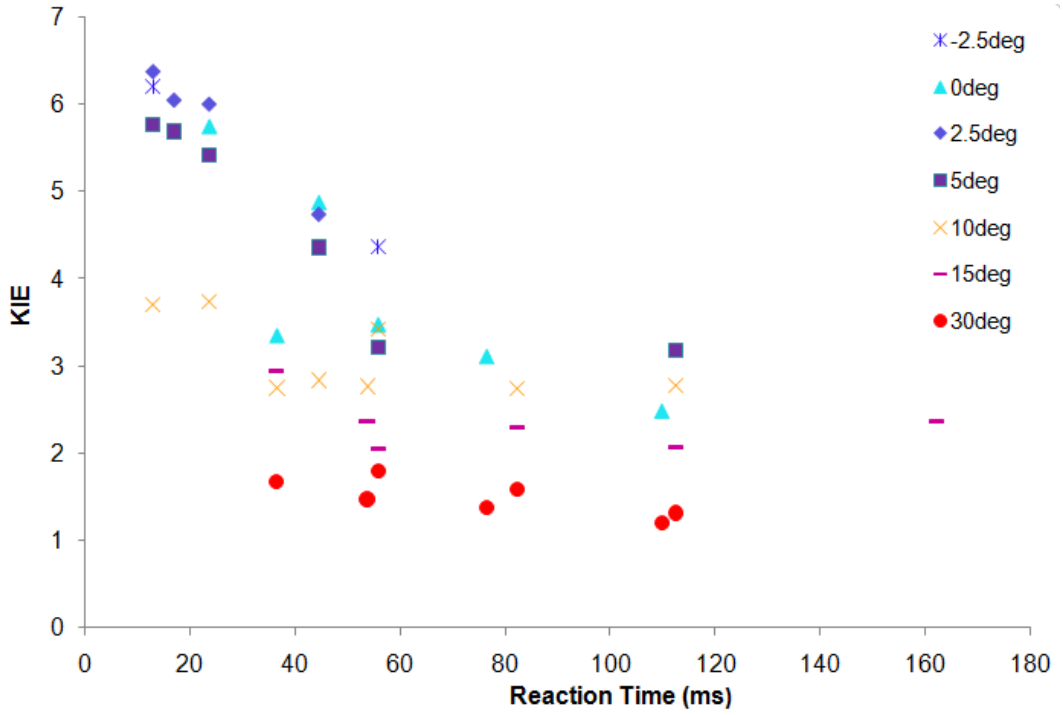

Figure 4.2 Deuterium KIE at various temperatures: ✳, -2.5˚C; ▲, 0˚C;◆, 2.5˚C; ■, 5˚C; X, 10˚C; —, 15˚C; ● , 30˚C

The plot of deuterium KIEs vs. temperature at various reaction times clearly exhibits a complex pattern of temperature dependence as the dependency varies at different reaction time ranges and temperature ranges (Figure 4.3). Deuterium KIEs is more temperature-dependent at lower temperature while it becomes almost temperature independent at temperatures above 15˚C. At short reaction times, 12.9ms and 23.6ms, deuterium KIEs increased significantly at temperature below 7.5˚C showing biphasic pattern.

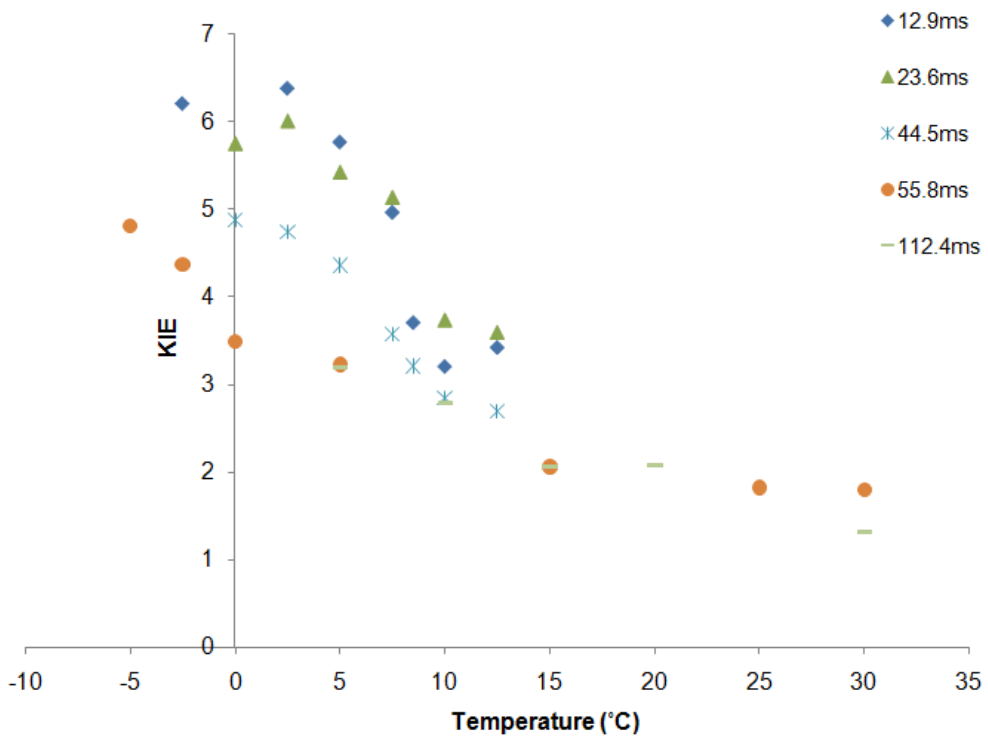

Figure 4.3 Temperature dependence of deuterium KIEs at various reaction times: ◆, 12.9ms; ▲, 23.6ms; ∗, 44.5ms; ● , 55.8ms; —, 112.4ms

Previously, the rate of 5'-dA formation by glutamate mutase was determined using rapid quench method. For the formation of 5'-dA from L-*threo*-3-methylaspartate and AdoCbl was 15.6 ms ($k_{obs} \approx 64\ s^{-1}$) (Chih, and Marsh, 1999). The rate of substrate-induced cleavage of AdoCbl by glutamate mutase was also determined previously by monitoring the Co-C homolysis by stopped-flow spectroscopy. With protiated methylaspartate, the relaxation time is 12.5ms ($k_{obs} \approx 80\ s^{-1}$). However with L-*threo*-[3-$^{2}H_3$-methyl]aspartate, the formation of Cbl(II) appeared to be biphasic; the relaxation times for the first and second phases were ~45ms ($k_{obs} \approx 22\ s^{-1}$) and 430 ms ($k_{obs} \approx 2.3 s^{-1}$), respectively (Marsh and Ballou, 1998). This phenomenon was explained when it was shown that the second slower phase was associated with multiple turnovers of the

deuterated substrates resulting in di- and tri-deuterated 5'-dA and that it arose from an unexpectedly large inverse equilibrium isotope effect shifting the equilibrium towards homolysis of AdoCbl. Although the reactions were quenched at very short times (<162ms), multiple turnovers result in significant amounts (> 2%) of di-deuterated 5'dA at reaction times longer than ~36 ms (Figure 4.1 (b)) or higher temperatures (Figure 4.4). This accounts for the complex temperature dependence of KIEs at various temperatures and reaction times. The formation of 5'-dA containing more than one deuterium must arise from multiple hydrogen abstraction reactions which could occur if the methylaspartate radical either rearranges to produce glutamate or partitions back to form methylaspartate, which, after diffusion from the enzyme, would allow another molecule of deuterated substrate to react with the enzyme.

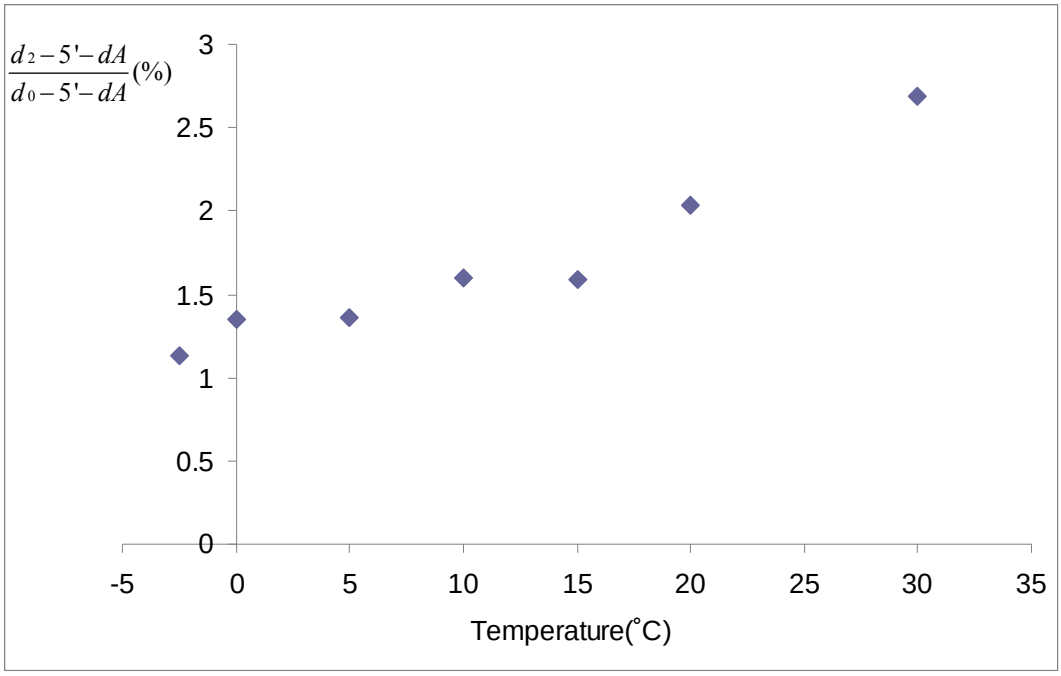

Figure 4.4 Relative amount of di-deuterated 5'-dA at reaction times (36.5ms ~ 55.8ms) under various temperatures

Figure 4.5 shows the mole fractions of non-, di- and tri-deuterated 5'dA in the reaction of AdoCbl with *(2S, 3S)*-3-d_1-methylspartate. When the reaction is quenched at very short time before the multiple turnover occurs, no di-deuterated 5'dA would be generated and ratio between non- and mono-deuterated 5'dA is indeed an "intrinsic" deuterium KIE. However, as the reaction is quenched at a longer reaction times, deuterated AdoCbl would be generated which in a second catalytic cycle generate the di-deuterated 5'dA. It is impossible to express exact mole fractions as a function of reaction time due to the complexities of the kinetics. However based on the KIE obtained at the shortest reaction time (assuming that is an intrinsic KIE) at each temperature, that KIE value can be used to estimate the mole fraction equations of isotopically labeled species in table 4.1 and mole fractions will be determined at each round. The actual fractions will lie between either the values obtained from first and second round or second and third round of turnover, depending on the reaction time, informing the relationship between the reaction times and turnovers numbers.

	Round I	Round II	Round III
Fraction (d_0-5'dA)	$\frac{2x}{(1+2x)}$	$\frac{8x^3+4x^2+2x}{(1+2x)^3}$	$\frac{32x^5+32x^4+32x^3+8x^2+2x}{(1+2x)^5}$
Fraction (d_1-5'dA)	$\frac{1}{(1+2x)}$	$\frac{8x^2+2x+1}{(1+2x)^3}$	$\frac{48x^4+24x^3+16x^2+4x+1}{(1+2x)^5}+\frac{8x^2}{(2+x)(1+2x)^4}$
Fraction (d_2-5'dA)	0	$\frac{2x}{(1+2x)^3}$	$\frac{16x^3+4x^2+2x}{(1+2x)^5}+\frac{4x^3+4x}{(2+x)(1+2x)^4}$
Fraction (d_3-5'dA)	0	0	$\frac{4x^2}{(1+2x)^4(2+x)}$

Table 4.1 Estimated Mole fractions of d_0-5'-dA d_1-5'-dA d_2-5'-dA d_3-5'-dA at each turnover rounds as a function of KIE = x

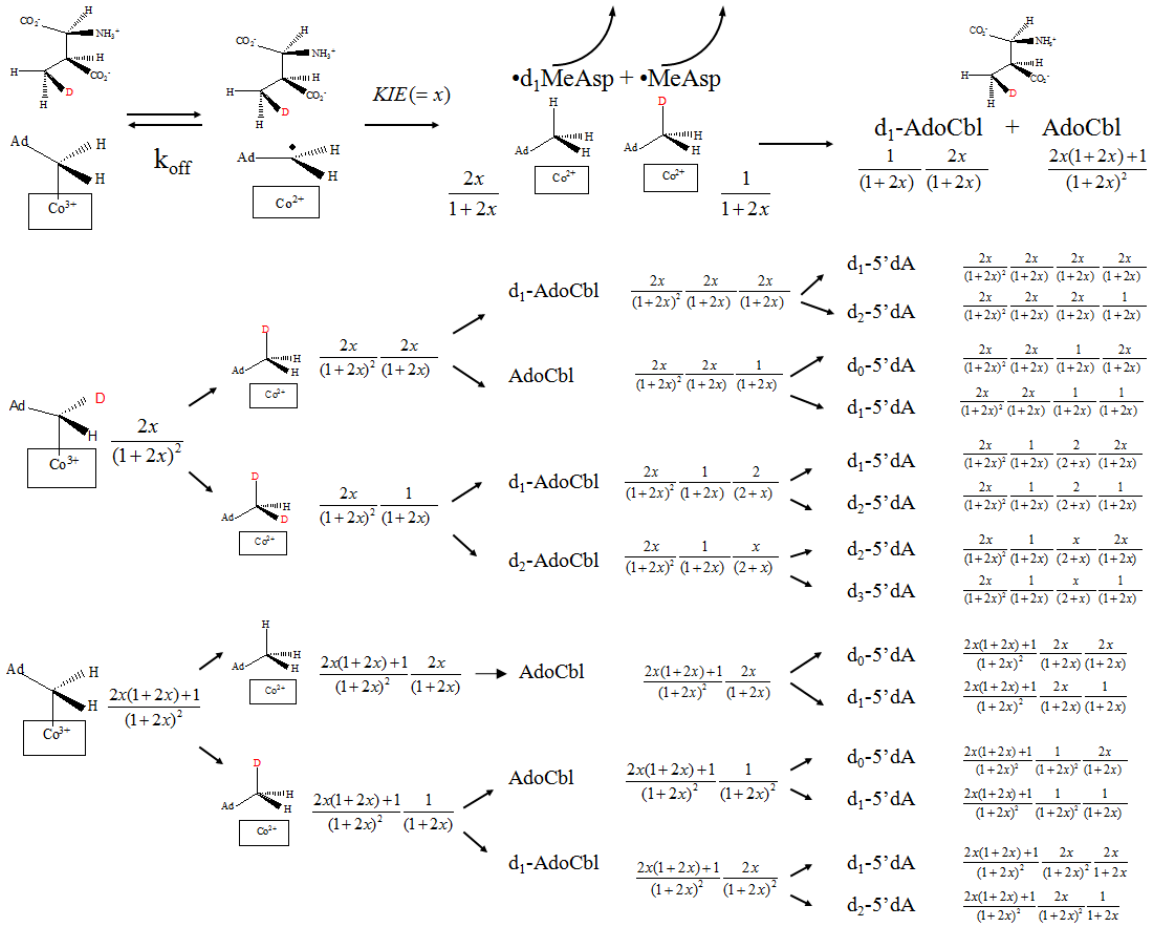

Figure 4.5 Mechanism for generating multiple turnover products; mole fractions were obtained when the KIE is given as x.

As expected, the deuterium KIEs measured at lower reaction times (11.9ms ~ 23.6ms) are almost constant. Very low amounts of di-deuterated 5'-dA are formed (<1%) and much larger deuterium KIEs measured than at longer time reactions in which more di-deuterated 5'dA is formed. Arrhenius logarithmic plots of only the reactions with much shorter reaction times (11.9ms ~ 23.6ms) at lower temperatures (-2.5˚C ~ 7.5˚C) were taken for the data fitting to determine the temperature dependency on KIEs. As mentioned, the intercept directly indicates the Arrhenius prefactor (A_H/A_D) and the activation energy difference is obtained from the slope (Eq. 5).

$$\ln\frac{k_H}{k_D} = \ln\frac{A_H}{A_D} + \left(\frac{\Delta E_{a,(D-H)}}{RT}\right) \qquad \text{Eq. 5}$$

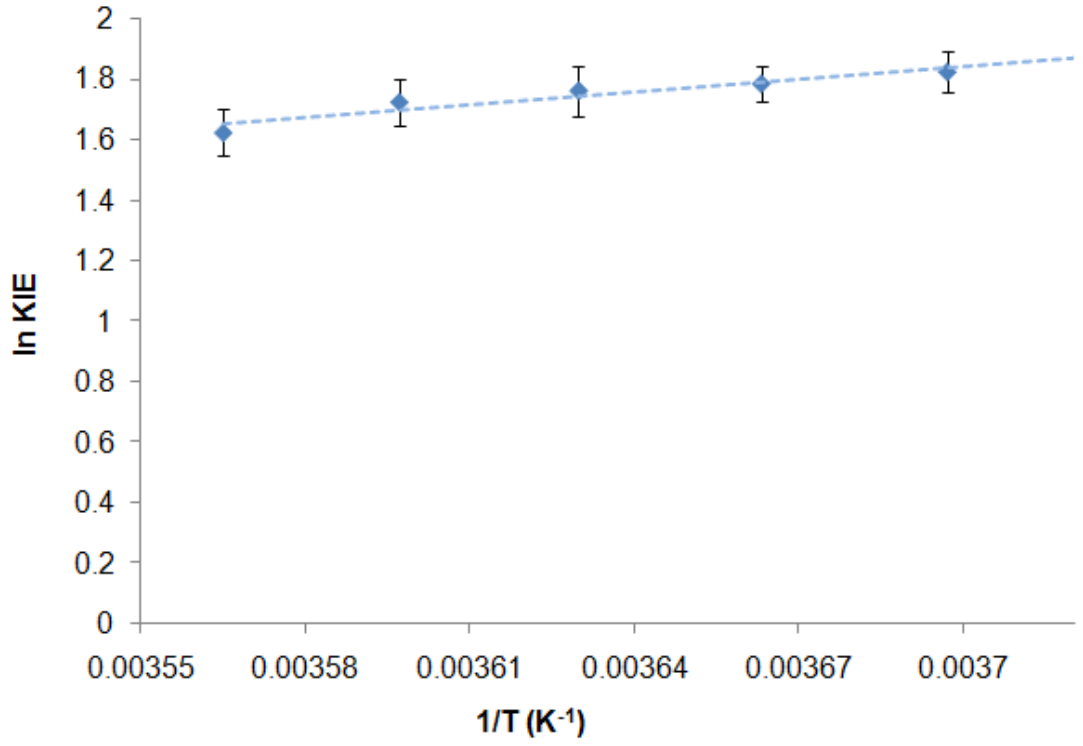

Figure 4.6 Arrhenius logarithm plot: Averaged values from reaction times of 12.9ms, 16.9ms, and 23.6ms at -2.5˚C ~ 7.5˚C

For comparison, data points measured above 7.5˚C were included and data for 11.9ms and 23.6ms were fitted separately to the Arrhenius logarithm plot and A_H/A_D and activation energy differences were obtained (Table 4.2). The plots which including data points above 7.5˚C clearly exhibit more scattering from the linear plot, resulting in quite different values for A_H/A_D and activation energy difference, $\approx 10^{-5}$~10^{-6} and ~7 kcal/mol respectively. However with temperature -2.5˚C ~ 7.5˚C, all the separate or combined data of reaction time 12.9ms, 16.9ms and 23.6ms generate 0.013~0.034 for A_H/A_D ~3 kcal

mol^{-1} for the activation energy difference (Table 4.2). These values are very similar to those of the AdoCbl dependent systems studied previously (Table 4.3).

Temperature (˚C)	time (ms)	A_H/A_D	$\Delta Ea_{(D-H)}$ (kcal/mol)
-2.5 ~ 12.5	12.9	4.00E-06	7.74 ± 1.28
-2.5 ~ 12.5	23.6	1.44E-05	7.05 ± 1.01
-2.5 ~ 12.5	12.9 ~ 16.9	6.00E-06	7.54 ± 1.25
-2.5 ~ 12.5	12.9 ~ 23.6	1.60E-05	6.97 ± 1.14
-2.5 ~ 7.5	12.9	0.0208	3.09 ± 0.89
-2.5 ~ 7.5	23.6	0.0129	3.30 ± 0.67
-2.5 ~ 7.5	12.9 ~ 16.9	0.0265	2.95 ± 0.72
-2.5 ~ 7.5	12.9 ~ 23.6	0.0343	2.80 ± 0.51

Table 4.2 A_H/A_D and activation energy difference obtained from Arrhenius logarithmic plot

Enzyme	**k_H/k_D (0 °C)**	**A_H/A_D**	**ΔEa(kcal/mol)**
Ethanolamine ammonia lyase	~12	0.038	3.1
Methylmalonyl-CoA mutase	~56	0.078	3.4
NpCbl[1]	~42	0.14	3.1
AdoCbl[1]	~40	0.16	3.0
Glutamate mutase	~7	~0.03	~3

Table 4.3 AdoCbl-dependent systems for which moderate tunneling was suggested: calculated from the literature, [1], non-enzymatic model

In particular, extensive hydrogen tunneling in methylmalonyl-CoA mutase has been deduced from the temperature dependence of the deuterium isotope effect on hydrogen transfer and Co-C bond homolysis exhibiting A_H/A_D ~0.08. Moreover, non-enzymatic models of adenosylcobalamin dependent reactions which were studied by

Finke's lab also show relatively a small A_H/A_D ~0.038 value. These values are all below the lower semi-classical limit (A_H/A_D ~ 0.5) which indicates the tunneling of only the light isotope, hydrogen. The activation energy difference between H and D in AdoCbl dependent systems showed very similar value, ~3kcal/mol, which is relatively large among the other enzyme systems for which tunneling have been suggested.

Enzyme	**k_H/k_D (25 °C)**	**A_H/A_D**	**ΔE_a(kcal/mol)**	**Ref.**
Thermophilc ADH	5.3	1.00E-05	7.8	[1]
Thermophilic DHFR	4.8	0.002	4.6	[2]
Ethanolamine ammonia lyase[a]	7.1	0.038	3.1	[3]
Methylmalonyl-CoA mutase[a]	24.7	0.078	3.4	[4]
NpCbl[b]	26.3	0.14	3.1	[5]
AdoCbl[b]	25.4	0.16	3.0	[5]
Galactose oxidase	16.8	0.25	2.5	[6]
Bovine serum amine oxidase	11.5	0.24	2.3	[7]
Monoamine oxidase	9.4	0.25	2.2	[8]
Morphinone reductase	3.9	0.12	2.0	[9]

Table 4.4 Enzyme systems for which moderate tunneling was suggested but show relatively large activation energy differences and large temperature dependences: [a] AdoCbl-dependent enzyme systems, [b] non-enzymatic systems, Calculated from literatures; [1], Kohen and Klinman, 1999; [2], Maglia and Allemann, 2003; [3], Weisblat, and Babior, 1971; [4], Chowdhury and Banerjee, 2000; [5], Doll and Finke, 2003; [6],Whittaker et al, 1998; [7], Grant and Klinman, 1989; [8], Jonsson and Klinman, 1994; [9], Basran and Scrutton, 2003

4.3 Discussion

Doll and Finke have measured the KIE for hydrogen abstraction in non-enzymatic model systems that mimic AdoCbl-dependent enzyme reactions (Doll and Finke, 2003). They measured the kinetics of hydrogen abstraction from ethylene glycol (mimicking the diol dehydrase reaction) either by 5'-dA radical, generated by thermolysis of AdoCbl, or neopentyl radical, generated by thermolysis of neopentylcobalamin. In those systems significant hydrogen tunneling was detected from analysis of Arrhenius plots, and furthermore the KIEs measured were much larger than could be accounted for by semi-classical formulation of KIEs. The isotope effects on Arrhenius pre-exponential factors and activation energies measured in these model systems were very similar to those measured in methylmalonyl-CoA mutase, (Chowdhury and Banerjee, 2000) as were the KIEs when corrected for differences in temperature. These results led to the conclusion that tunneling was an intrinsic property of both the enzyme-catalyzed and non-enzymatic reaction, and that there was no enhancement of tunneling by the enzyme, as has been proposed for some other enzymes where tunneling has been investigated.

Given that the KIEs for hydrogen abstraction in both the model systems and methylmalonyl-CoA mutase are unusually large, it is extremely surprising that the intrinsic KIE in glutamate mutase should be so much smaller. The hydrogen abstraction reactions catalyzed by MMCM and glutamate mutase are chemically identical, and, if anything, the stopped-flow technique used to measure the KIEs in MMCM may under-estimate the intrinsic KIEs. Although d_3-methylmalonyl-CoA and d_4-ethylene glycol were used in the other experiments and therefore the primary KIE is likely inflated by a contribution from the secondary KIE, this effect could not explain such large differences

between the isotope effects. We are not aware of any case where two such similar chemical reactions proceed with such different isotope effects.

Inflated secondary kinetic isotope effects in hydrogen-transfer reactions are diagnostic of coupling to the motion of the secondary hydrogen combined with hydrogen tunneling. Coupled motion occurs when one of the vibrations of the α-hydrogen is part of the reaction coordinate, leading to an increase in the secondary KIE as part of the α-hydrogen's vibrational mode is converted to a translation and the primary KIE is reduced by the coupled motion of the secondary hydrogens (Suhnel and Schowen 1991). This phenomenon is best studied for NAD(P)H dependent dehydrogenases that exhibit primary deuterium KIEs that are also relatively small, being at the upper limit of those expected semi-classically (Nagel and Klinman, 2006).

Recently inflated secondary tritium KIEs associated with the formation of 5'-dA was measured by Mou-Chi Cheng in our laboratory. Both the α-secondary tritium kinetic and equilibrium isotope effects were large and inverse, 0.76 and 0.72, respectively (Cheng and Marsh, 2004). However it was found that introducing a *primary* deuterium kinetic isotope effect on the hydrogen transfer step is to *reduce* the magnitude of the *secondary* kinetic isotope effect to a value close to unity, 1.05, whereas the equilibrium isotope effect is unchanged. The significant reduction in the secondary kinetic isotope effect is consistent with motions of the 5'-hydrogen atoms being coupled in the transition state to the motion of the hydrogen undergoing transfer, in a reaction that involves a large degree of quantum tunneling (Cheng and Marsh, 2007).

Temperature dependence studies on deuterium kinetic isotope effects in glutamate mutase demonstrated a contribution of tunneling in glutamate mutase which is quite

similar to that of other AdoCbl-dependent enzymes studied previously, while the deuterium kinetic isotope effect on glutamate mutase is much smaller than that of methylmalonyl-CoA mutase as quantum tunneling of the primary hydrogen may be coupled to the movement of the secondary hydrogen atoms in the reaction of glutamate mutase.

As mentioned in the introduction chapter, a "Marcus-like" model can explain the system of which temperature dependencies of the reaction rate and of the KIE are separated as the rate for H transfer is governed by an isotope-independent term. The highly temperature-dependent KIE in glutamate mutase can be explained with a Marcus-like model via the incorporation of a distance sampling term into the Franck–Condon expression as shown in equation 7 in the introduction chapter.

$$k = (Const.)\exp[\frac{-(\Delta G^\circ + \lambda)^2}{4\lambda RT}]\int_{r1}^{r0}\exp[\frac{-m_H w_H r_H{}^2}{2\hbar}]\exp[\frac{-E_x}{k_b T}]dx \qquad \text{Eq. 7}$$

Using a model where the initial distance between the H-donor and acceptor is too long for tunneling to take place efficiently, a transient reduction in distance between the donor and acceptor atoms becomes a requisite feature. The larger mass and smaller wavelength of deuterium compared to protium leads to a greater role for distance sampling in the transfer of deuterium transfer, with a concomitant increase in $\Delta E_{a,\,D}$ relative to $\Delta E_{a,\,H}$ and reduction of A_H/A_D to a value that can be much less than unity (Bruno and Bialek, 1992)

4.4 Conclusion

In conclusion, by taking advantage of *intra*-molecular competition between hydrogen and deuterium atoms at the methyl group of methylaspartate, the intrinsic primary deuterium isotope for 5'-dA formation in a B_{12} enzyme was measure for the first time. Remarkably, the KIE is much smaller than expected based on KIE measurements on methylmalonyl-CoA mutase and non-enzymatic model systems which are both of similar magnitude and much larger than the semi-classical limit. Although the intrinsic KIE is within semi-classical limits this result does not rule out hydrogen tunneling in glutamate mutase. This argues strongly for a role for glutamate mutase in modulating the transition state for hydrogen transfer in a manner that reduces the KIE associated with it. Together with temperature dependence studies on deuterium kinetic isotope effects in glutamate mutase and previous studies of inflated secondary KIEs demonstrated the contribution of tunneling with coupled motion in glutamate mutase.

Chapter 5 Conclusions and Proposed Future Work

The intra-molecular isotope competition by d_1-methyl-*threo*-methylaspartate combined with high resolution mass spectrometry allows the amount of non- mono- di- tri-deuterated 5'-dA to be monitored at various reaction times. This would enable us to reinvestigate the time course kinetics in the reaction of glutamate mutase to obtain the rate of each microscopic step. The time course for the formation of 5'-dA was determined previously in the Marsh laboratory when glutamate mutase was reacted with d_5-L-glutamate (Cheng and Marsh, 2005). The reaction with d_5-L-glutamate includes a small, presumably normal, contribution from the secondary isotope effect associated with the presence of deuterium at the C-4 *pro-R* position of glutamate, however by using d_1-methyl-*threo* methylaspartate, those effects from the secondary isotope effect can be overcome. Moreover, the more accurate quantification of mono- di- and tri-deuterated 5'dA can be obtained by high-resolution mass spectrometry.

Although hydrogen tunneling (HT) is well-documented, both in non-enzymatic and in enzymatic reactions, there is little experimental evidence that demonstrates enhanced HT in an enzymatic reaction relative to the corresponding model reaction in solution. Several authors have proposed that enzymes might accelerate hydrogen-transfer reactions by enhancing quantum mechanical tunneling relative to solution, either by inducing tunneling where it did not exist in the solution reaction or by increasing the amount of tunneling already present. Doll and Finke reported that the extent of tunneling

for the non-enzymatic abstraction of a hydrogen atom from ethylene glycol by coenzyme AdoCbl is identical, within error, to that of a similar, but not exactly analogous enzymatic reaction: hydrogen atom abstraction from methylmalonyl-CoA by AdoCbl-dependent methylmalonyl-CoA mutase. This led them to the conclusion that there is no enhanced quantum mechanical tunneling for this enzyme (Doll and Finke, 2003). In contrast, Jonas and Stack have previously reported a model reaction mimicking that catalyzed by soybean loposygenase-1 (SLO-1), proceeds with a KIE of only 2.7 (Jonas and Stack, 1997). This comparison may lead to the conclusion that tunneling is far more significant for SLO-1 than for the model reaction in solution. However, a range of other explanations are possible, beginning with the difficulty of designing a system that mimics the properties of the enzyme active site, followed by the possibility of different rate-limiting steps in the two systems. It is equally likely that extensive tunneling is also occurring in the model reaction but with properties that are different from those in the enzyme reaction. Not only must one find a reaction that occurs by identical mechanisms both in solution and at the active site of the enzyme, but the details of the rate-limiting step(s) must be known, and both systems must be amenable to the measurement of precise KIEs. If it is very difficult design a suitable system for comparison which mimics corresponding enzymatic reaction, it is better to take advantage of computational chemistry. Computational studies provide essential atomic insight into the mechanism of H transfer. Warshel et al. simulated the behavior of the enzyme carbonic anhydrase and incorporated quantum effects such as tunneling (Hwang and Warshel, 1996). They compared their model with one for the same process happening in an enzyme-free solution, and found a similar amount of tunneling in both systems.

Computational simulation can also provide a powerful evidence in support of environmentally coupled H tunneling. Dybala-Defratyka et al. used a mechanical/molecular mechanical potential and semiclassical quantum dynamics calculations to explain the large kinetic isotope effect in hydrogen transfer reactions catalyzed by coenzyme B_{12}-dependent methylmalonyl-CoA mutase. They found multidimensional tunneling increases the magnitude of the calculated intrinsic hydrogen kinetic isotope effect by a factor of 3.6 from 14 to 51, in excellent agreement with experimental results. These calculations confirm that tunneling contributions can be large enough to explain even a kinetic isotope effect >50, not because the barrier is unusually thin but because corner-cutting tunneling decreases the distance over which the system tunnels without a comparable increase in either the effective potential barrier or the effective mass for tunneling (Dybala-Defratyka et al., 2007).

As mentioned in chapter 4, previous secondary deuterium kinetic isotope studies in glutamate mutase suggested a coupled motion in the transition state of the 5'-hydrogen atoms adjacent to the hydrogen that is transferred between substrate and coenzyme in a reaction that involves a large degree of quantum tunneling. Wilde et al. measured secondary kinetic isotope effects for both ketosteroid isomerase (KSI) and its model reaction, acetate-catalyzed isomerizaion to investigate whether KIS enhances HT relative to the nonenzymatic (acetate-catalyzed) and they demonstrated that KSI enhances the CM/HT contribution to the rate acceleration over the solution reaction (Wilde et al., 2007). Therefore, by comparing the tunneling contributions between the model systems (both actual chemical reaction and computational simulation) and enzymatic reaction of glutamate mutase by temperature dependence on primary kinetic isotope effect and

secondary kinetic isotope effects, we can provide the answer whether hydrogen tunneling is an intrinsic feature of enzyme-catalyzed and non-enzymatic reactions, of whether glutamate mutase can actually enhance hydrogen tunneling to speed up biological reaction.

Alternately, the combination of site-specific mutagenesis and the temperature dependence studies on the KIEs can afford us a unique view into the origins of catalytic efficiency in enzymes. Meyer et al. studied the impact of a remote side chain (~15 Å from the active site iron center) mutation in soybean liposygenases-1 on hydrogen tunneling in this enzyme (Meyer et al., 2008). They observed an unexpectedly small temperature dependence of the size of the isotope effects with WT-enzyme while highly temperature dependent KIEs for the distal mutations, which provide some of the strongest evidence in support of a full tunneling process in an enzyme reaction. They reported significant impact of mutagenesis on the efficiency of protium as well as deuterium transfer, illustrating how the judicious placement of proximal hydrophobic side chains within the binding pocket of SLO-1 has created an active site whose properties are optimized for the hydrogen tunneling process. That is, the evolution of the active site has not necessarily made tunneling more prominent. It has, however, made the rate of transfer of hydrogen via tunneling significantly more efficient. They proposed that this property may well be the case for all enzymes that catalyze C–H activation. Kohen et al. compared the nature of the chemical steps catalyzed by the highly evolved and flexible cDHFR and the primitive, rigid R67-DHFR enzymes. The cDHFR appears to have a perfectly pre-reorganized reaction coordinate or, put differently, efficient H-tunneling. In contrast, the R67-DHFR enzyme requires significant gating of its donor–acceptor distance prior to tunneling, or, alternatively, there is no tunneling contribution to its catalyzed reaction.

These findings provide evidence for the notion that enzymes have evolved to optimize their reaction coordinate for efficient tunneling (Kohen et al., 2008).

The crystal structure of glutamate mutase has identified a number of residues that appear to make important hydrogen bonding interactions with the substrate and coenzyme. These include Arg149 and Arg66 that hydrogen bond to the α-carboxyl group of the substrate; Glu171, which makes a hydrogen bond to the amino group of the substrate, and Arg100 that forms a salt bridge with the γ-carboxylate (Madhavapeddi et al., 2002); (Xia et al., 2004). It has been demonstrated that even small mutations to the active site of glutamate mutase can result in quite extensive and unforeseen changes to the mechanism. Mutational studies on glutamate mutase have been focused on the active site mutations to examine how the structural changes affect the catalytic properties. As evidences of the effect of a distal mutation on the active site have been reported as enzyme dynamics is involved in the catalysis (Wang et al., 2006), distal mutational studies on glutamate mutase, KIEs and their temperature dependence studies can provide more information of coupled motion and its relationship to the catalytic efficiency in glutamate mutase. Moreover, previous studies on Glu171Gln mutant revealed that several steps in the kinetic mechanism were altered by this mutation. Thus, substrate binding was weakened, and the apparent rate constants for homolysis of AdoCbl were significantly slowed compared with wild type. Furthermore, the mutation appeared to significantly reduce the kinetic isotope effects on AdoCbl homolysis that are observed when the enzyme is reacted with deuterated substrates. By applying this novel intra competition method with d_1-methyl-*threo*-methylasprtate, the deuterium kinetic isotope

effect on the Glu171Gln mutant can be reinvestigated and temperature dependences on KIE can also be studied to examine the tunneling contribution on the mutant.

REFERENCES

Agrawal, N., Hong, B., Mihai, C., and Kohen, A. (2004) Vibrationally enhanced hydrogen tunneling in the Escherichia coli thymidylate synthase catalyzed reaction, Biochemistry, 43(7), 1998-2006

Bahnson, B. J., Park, D. H., Kim, K., Plapp, B. V., and Klinman, J. P. (1993) Unmasking of hydrogen tunneling in the horse liver alcohol dehydrogenase reaction by site-directed mutagenesis Biochemistry, 32 (21), 5503-5507

Bandarian, V., and Reed, G. H. (1999) Hydrazine cation radical in the active site of ethanolamine ammonia-lyase: Mechanismbased inactivation by hydroxyethylhydrazine, Biochemistry, 38, 12394-12402

Bandarian, V., and Reed, G. H. (2000) Isotope effects in the transient phases of the reaction catalyzed by ethanolamine ammonia-lyase: Determination of the number of exchangeable hydrogens in the enzyme−cofactor complex, Biochemistry, 39 (39), 12069-12075

Banerjee, R. (2001) Radical Peregrinations Catalyzed by Coenzyme B_{12}-Dependent Enzymes, Biochemistry 40, 6191-6198

Banerjee, R. (2003) Radical carbon skeleton rearrangements: catalysis by coenzyme B_{12}-dependent mutases, Chem. Rev., 103, 2083 –2094.

Banerjee, R., and Ragsdale, S. W. (2003) The many faces of vitamin B_{12}: Catalysis by cobalamin-dependent enzymes, Annu. Rev. Biochem. 72, 209-247

Barker, H. A. (1985) β-Methylaspartate-glutamate mutase from Clostridium tetanomorphum, Methods Enzymol., 113, 121-133

Basran, J., Harris, R. J., Sutcliffe, M. J., and Scrutton, N. S. (2003) H-tunneling in the multiple H-transfers of the Catalytic Cycle of Morphinone Reductase and in the Reductive Half-reaction of the Homologous Pentaerythritol Tetranitrate Reductase JBC, 278 (45), 43973–43982

Basran, J., Sutcliffe, M. J., and Scrutton, N. S. (2001) Deuterium isotope effects during carbon–hydrogen bond cleavage by trimethylamine dehydrogenase, JBC, 276(27), 24581–24587

Bothe, H., Darley, D. J., Albracht, S. P., Gerfen, G. J., Golding, B. T., and Buckel, W. (1998) Identification of the 4-glutamyl radical as an intermediate in the carbon skeleton rearrangement catalyzed by coenzyme B_{12}-dependent glutamate mutase from Clostridium cochlearium, Biochemistry, 37, 4105-4113

Bruno, W. J., and Bialek, W. (1992) Vibrationally enhanced tunneling as a mechanism for enzymatic hydrogen transfer, Biophys. J., 63, 689-699

Buchachenko, A. L., and Kuznetsov, D. A. (2008) Magnetic field affects enzymatic ATP synthesis, J. Am. Chem. Soc., 130(39), 12868-12869

Cha, Y., Murray, C. J., and Klinman, J. P. (1989) Hydrogen Tunneling in Enzyme Reactions, Science, 243, 1325-1330

Chen, H. P., and Marsh, E. N. G. (1997) Adenosylcobalamin-dependent glutamate mutase: Examination of substrate and coenzyme binding in an engineered fusion protein possessing simplified subunit structure and kinetic properties, Biochemistry, 36, 14939-14945

Cheng, M. C. and Marsh, E. N. G. (2007) Evidence for coupled motion and hydrogen tunneling of the reaction catalyzed by glutamate mutase, Biochemistry, 46 (3), 883-889

Cheng, M.-C., and Marsh, E. N. G. (2004) Pre-steady state measurement of intrinsic secondary tritium isotope effects associated with the homolysis of adenosylcobalamin and the formation of 5'-deoxyadensosine in glutamate mutase, Biochemistry, 43, 2155-2158

Cheng, M.-C., and Marsh, E. N. G. (2005) Isotope Effects for Deuterium Transfer between Substrate and Coenzyme in Adenosylcobalamin-Dependent Glutamate Mutase, Biochemistry, 44, 2686 –2691

Chih, H. W., and Marsh, E. N. G. (1999) Pre-steady-state kinetic investigation of intermediates in the reaction catalyzed by adenosylcobalamin-dependent glutamate mutase, Biochemistry, 38, 13684 – 13691

Chih, H.-W., and Marsh, E. N. G. (2000) Mechanism of glutamate mutase: Identification and kinetic competence of acrylate and glycyl radical as intermediates in the rearrangment of glutamate to methylaspartate, J. Am. Chem. Soc., 122, 10732-10733

Chih, H.-W., and Marsh, E. N. G. (2001) Tritium partitioning and isotope effects in adenosylcobalamin-dependent glutamate mutase, Biochemistry, 40, 13060-13067

Chih, H.-W., Roymoulik, I., Huhta, M. S., Madhavapeddi, P., and Marsh, E. N. G. (2002) Adenosylcobalamin-dependent glutamate mutase: Pre-steady-state kinetic methods for investigating the reaction mechanism, Methods Enzymol., 354, 380-399

Chowdhury, S. and Banerjee, R. (2000) Evidence for quantum mechanical tunneling in the coupled cobalt−carbon bond homolysis−Substrate radical generation reaction catalyzed by methylmalonyl-CoA mutase, J. Am. Chem. Soc., 122 (22), 5417-5418

Cleland, W. W., (1982) Use of isotope effects to elucidate enzyme mechanisms, CRC Crit. Rev. Biochem., 13, 385 –428

Cleland, W. W., in Isotopes in Organic Chemistry, Vol. 7 (Ed.: Buncel, E., Lee, C. C.), Elsevier, Amsterdam 1987

Clough, S., and Hill, J. R. (1974) Temperature dependence of methyl group tunneling rotation frequency, J. Phys. C: Solid State Phys., 7, L20 – L21

Cook, P. F., Oppenheimer, N. J., and Cleland, W. W., (1981) Secondary deuterium and nitrogen-15 isotope effects in enzyme-catalyzed reactions: Chemical mechanism of liver alcohol dehydrogenase, Biochemistry, 20 (7), 1817-1825

Cui, Q., and Karplus, M. (2002) Quantum Mechanics/Molecular Mechanics Studies of Triosephosphate Isomerase-Catalyzed Reactions: Effect of Geometry and Tunneling on Proton-Transfer Rate Constants J. Am. Chem. Soc., 124 (12), 3093-3124

Doll, K. M., and Finke, R. G. (2003) A compelling experimental test of the hypothesis that enzymes have evolved to enhance quantum mechanical tunneling in hydrogen transfer reactions: The β-neopentylcobalamin system combined with prior adocobalamin data, Inorg. Chem., 42, 4849 –4856

Doll, K. M., Bender, B. R., and Finke, R. G. (2003) The first experimental test of the hypothesis that enzymes have evolved to enhance hydrogen tunneling, J. Am. Chem. Soc., 125, 10877 –10884

Dybala-Defratyka, A., Paneth, P., Banerjee, R., and Truhlar, D. G. (2007) Coupling of hydrogenic tunneling to active-site motion in the hydrogen radical transfer catalyzed by a coenzyme B_{12}-dependent mutase, Proc. Natl. Acad. Sci. USA, 104(26) 10774-10779

Francisco, W. A., Knapp, M. J., Blackburn, N. J., and Klinman, J. P. (2002) Hydrogen Tunneling in Peptidylglycine α-Hydroxylating Monooxygenase J. Am. Chem. Soc., 124 (28), 8194-8195

Frey, P. A. (1997) Radicals in enzymatic reactions, Current Opinion in Chemical Biology, 1, 347-356

Frey, P. A. (2001) Radical mechanisms of enzymatic catalysis, Annu. Rev. Biochem. 70, 121-148

Frey, P. A., Hegerman, A. D., and Reed, G. H.(2006) Free radical mechanisms in enzymology, Chem. Rev., 106, 3302 –3316

Garcia-Viloca, M., Alhambra, C., Truhlar, D. G., and Gao J. (2002) Quantum Dynamics of Hydride Transfer Catalyzed by Bimetallic Electrophilic Catalysis: Synchronous Motion of Mg2+ and H- in Xylose Isomerase J. Am. Chem. Soc., 124 (25), 7268-7269

Goldanskii, V. I. (1979) Facts and hypotheses of molecular chemical tunneling, Nature 279, 109 - 115

Goldstein, H., Poole, C. P., Jr., and Safko, J. L. (2002) Classical Mechanics, 3rd ed., Addison Wesley, San Francisco

Grant, K. L., and Klinman, J. P. (1989) Evidence that both protium and deuterium undergo significant tunneling in the reaction catalyzed by bovine serum amine oxidase Biochemistry, 28 (16), 6597-6605

Grissom, C. B. (1995) Magnetic Field Effects in Biology: A Survey of Possible Mechanisms with Emphasis on Radical-Pair Recombination, Chem. Rev., 95, 3 –24

Gruber, K., and Kratky, C. (2002) Coenzyme B_{12} dependent glutamate mutase, Curr. Opin. Chem. Biol., 6, 598-603

Gruber, K., Reitzer, R., and Kratky, C. (2001) Radical shuttling in a protein: Ribose pseudorotation controls alkyl-radical transfer in the coenzyme B-12 dependent enzyme glutamate mutase, Angew. Chem., Int. Ed., 40, 3377-3381

Hammes-Schiffer, S. (2006) Hydrogen Tunneling and Protein Motion in Enzyme Reactions Acc. Chem. Res., 39 (2), 93-100

Harkins, T. T., and Grissom, C. B. (1994) Magnetic field effects on B_{12} ethanolamine ammonia lyase: evidence for a radical mechanism, Science, 263, 958 –960

Hay, S., Pang, J., Monaghan, P. J., Wang, X., Evans, R. M., Sutcliffe, M. J., Allemann, R. K., and Scrutton, N. S. (2008) Secondary kinetic isotope effects as probes of environmentally-coupled enzymatic hydrogen tunneling reactions, ChemPhysChem., 9, 1536-1539

He, F., Hendrickson, C. L., Marshall, A. G. (2001) Baseline mass resolution of peptide isobars: a record for molecular mass resolution, Anal. Chem., 73, 647-450

Holloway, D. E., and Marsh, E. N. G. (1994) Adenosylcobalamin-dependent glutamate mutase from Clostridium tetanomorphum. overexpression in Escherichia coli, purification, and characterization of the recombinant enzyme, J. Biol. Chem., 269, 20425-20430

Holloway, D. E., Harding, S. E., and Marsh, E. N. G. (1996) Adenosylcobalamin-dependent glutamate mutase: properties of a fusion protein in which the cobalamin-binding subunit is linked to the catalytic subunit, Biochem. J., 320, 825-830

Huhta, M. S., Ciceri, D., Golding, B. T., and Marsh, E. N. G. (2002) A novel reaction between adenosylcobalamin and 2-methyleneglutarate catalyzed by glutamate mutase, Biochemistry, 41, 3200-3206

Huskey, W. P. and Schowen, R. L., (1983) Reaction-coordinate tunneling in hydride-transfer reactions, J. Am. Chem. Soc., 105, 5704.

Hwang, J.-K., Warshel, A. (1996) How Important Are Quantum Mechanical Nuclear Motions in Enzyme Catalysis?, J. Am. Chem. Soc., *118* (47), pp 11745–11751

Iyengar, S. S., Sumner, I., and Jakowski, J. (2008) Hydrogen tunneling in an enzyme active site: A quantum wavepacket dynamical perspective, J. Phys. Chem. B, 112 (25), 7601-7613

Iyer, K. R., J. P. Jones, Darbyshire, J. F., and Trager, W. F. (1997) Intramolecular isotope effects for benzylic hydroxylation of isomeric xylenes and 4,4'-dimethylbiphenyl by cytochrome P450: relationship between distance of methyl groups and masking of the intrinsic isotope effect, Biochemistry, 36, 7136 –7143

Jonas, R. T. and Stack, T. D. P. (1997) C−H bond activation by a ferric methoxide complex: A model for the rate-determining step in the mechanism of lipoxygenase J. Am. Chem. Soc., 119 (36), 8566-8567

Jonsson, T., Edmondson, D. E., and Klinman, J. P. (1994) Hydrogen tunneling in the flavoenzyme monoamine oxidase B, Biochemistry, 33(49), 14871-14878

Jonsson, T., Glickman, M. H., Sun, S., and Klinman, J. P. (1996) Experimental Evidence for Extensive Tunneling of Hydrogen in the Lipoxygenase Reaction: Implications for Enzyme Catalysis J. Am. Chem. Soc., 118 (42), 10319-10320

Kohen, A., and Klinman, J. P. (1998) Enzyme catalysis: Beyond classical paradigms. Acc. Chem. Res., 31, 397-404

Kohen, A., and Klinman, J. P. (1999) Hydrogen tunneling in biology, Chemistry & Biology, 6, R191–R198

Kohen, A., Cannio, R., Bartolucci, S., and Klinman, J. P. (1999), Enzyme dynamics and hydrogen tunnelling in a thermophilic alcohol dehydrogenase, Nature, 399(3), 496-499

Kohen, A., and Klinman, J. P. (2000) Protein flexibility correlates with degree of hydrogen tunneling in thermophilic and mesophilic alcohol dehydrogenases. J. Am. Chem. Soc., 122 (43), 10738-10739

Kohen, A. (2003), Kinetic isotope effects as probes for hydrogen tunneling, coupled motion and dynamics contributions to enzyme, Progress in Reaction Kinetics and Mechanism, 28, 119–156

Kurz, L. C., and Frieden, C. (1980) Anomalous equilibrium and kinetic α-deuterium secondary isotope effects accompanying hydride transfer from reduced nicotinamide adenine dinucleotide,
J. Am. Chem. Soc., 102 (12), 4198-4203

Lee, H.-Y., Yoon, M., and Marsh, E. N. G. (2007) Synthesis of Mono- and Di-deuterated (2S, 3S)-3-methylaspartic Acids to Facilitate Measurement of Intrinsic Kinetic Isotope Effects in Enzymes. Tetrahedron, 63, 4663 –4668

Leutbecher, U., Albracht, S. P., and Buckel, W. (1992) Identification of a paramagnetic species as an early intermediate in the coenzyme B_{12}-dependent glutamate mutase reaction, FEBS Lett., 307, 144-146

Liang, Z.-X., and Klinman, J. P. (2004) Structural bases of hydrogen tunneling in enzymes: progress and puzzles Current Opinion in Structural Biology, 14, 648–655

Licht, S. S., Gerfen G., J., and Stubbe, J. (1996) Thiyl radical in ribonucleotide reductases. Science, 271, 477- 481

Licht, S. S., Booker, S., and Stubbe, J. A. (1999) Studies on the catalysis of carbon-cobalt bond homolysis by ribonucleoside triphosphate reductase: Evidence for concerted carbon-cobalt bond homolysis and thiyl radical formation, Biochemistry, 38, 1221-1233

Madhavapeddi, P., Ballou, D. P., and Marsh, E. N. G. (2002) Pre- Steady State Kinetic studies on the Gly171Gln Active Site Mutant of Adenosylcobalamin-dependent Glutamate Mutase, Biochemistry, 41, 15802-15809

Maglia, G., and Allemann, R. K. (2003) Evidence for Environmentally Coupled Hydrogen Tunneling during Dihydrofolate Reductase Catalysis J. Am. Chem. Soc., 125 (44), 13372-13373

Majer, P., Jackson, P. F., Delahanty, G., Grella, B. S., Ko, Y. S., Li, W. X., Liu, Q., Maclin, K. M., Polakova, J., Shaffer, K. A., Stoermer, D., Vitharana, D., Wang, E. Y., Zakrzewski, A., Rojas, C., Slusher, B. S., Wozniak, K. M., Burak, E., Limsakun, T., and Tsukamoto, T. (2003) Synthesis and biological evaluation of thiolbased inhibitors of glutamate carboxypeptidase II: Discovery of an orally active GCP II inhibitor, J. Med. Chem. 46, 1989-1996

Mansoorabadi, S. O., Padmakumar, R., Fazliddinova, N., Vlasie, M., Banerjee, R., and Reed, G. H. (2005) Characterization of a succinyl-CoA radical-cob(II)alamin spin triplet intermediate in the reaction catalyzed by adenosylcobalamin-dependent methylmalonyl-CoA mutase, Biochemistry, 44, 3153-3158

Marsh, E. N. G. (1995) Tritium isotope effects in adenosylcobalamin-dependent glutamate mutase: Implications for the mechanism, Biochemistry, 34, 7542-7547

Marsh, E. N. G., and Ballou, D. P. (1998) Coupling of cobaltcarbon bond homolysis and hydrogen atom abstraction in adenosylcobalamin-dependent glutamate mutase, Biochemistry, 37, 11864-11872.

Marsh, E. N. G. (2000) Coenzyme- B_{12}-dependent glutamate mutase, Bioorganic Chemistry, 28, 176–189

Marsh, E. N. G., and Drennan, C. L. (2001) Adenosylcobalamindependent isomerases: New insights into structure and mechanism, Curr. Opin. Chem. Biol. 5, 499-505

Masgrau, L., Roujeinikova, A., Johannissen, L. O., Hothi, P., Basran, J., Ranaghan, K. E., Mulholland, A. J., Sutcliffe, M. J., Scrutton, N. S. (2006) Atomic description of an enzyme reaction dominated by proton tunneling, Science, 312, 237 –241

Masuda, J., Shibata, N., Morimoto, Y., Toraya, T., and Yasuoka, N. (2000) How a protein generates a catalytic radical from coenzyme B_{12}: X-ray structure of a diol-dehydratase–adeninylpentylcobalamin complex, Structure, 8, 775–788

Meyer, M. P., Tomchick, D. R., and Klinman, J. P. (2008) Enzyme structure and dynamics affect hydrogen tunneling: The impact of a remote side chain (I553) in soybean lipoxygenase-1, Proc. Natl. Acad. Sci. USA, 105(4), 1146-1151

Nagel, Z. D., and Klinman, J. P. (2006) Tunneling and dynamics in enzymatic hydride transfer, Chem. Rev., 106, 3095 –3118

Padmakumar, R., and Banerjee, R. (1997) Evidence that cobalt-carbon bond homolysis is coupled to hydrogen atom abstraction from substrate in methylmalonyl-CoA mutase Biochemistry, 36, 3713 –3718

Pudney, C. R., Hay, S., Sutcliffe, M, J, and Scrutton, N. S., (2006) α-Secondary isotope effects as probes of "Tunneling-ready" configurations in enzymatic H-tunneling: Insight from environmentally coupled tunneling models, J. Am. Chem. Soc., 128 (43), 14053-14058

Reitzer, R., Gruber, K., Jogl, G., Wagner, U. G., Bothe, H., Buckel, W., and Kratky, C. (1999) Structure of coenzyme B_{12} dependent enzyme glutamate mutase from Clostridium cochlearium, Structure, 7, 891-902

Roymoulik, I., Chen, H.-P., and Marsh, E. N. G. (1999) The reaction of the substrate analog 2-ketoglutarate with adenosylcobalmin-dependent glutamate mutase, J. Biol. Chem., 274, 11619-

Roymoulik, I., Moon, N., Dunham, W. R., Ballou, D. P., and Marsh, E. N. G. (2000) Rearrangement of L-2-hydroxyglutarate to L-threo-3-methylmalate catalyzed by adenosylcobalamin-dependent glutamate mutase, Biochemistry, 39, 10340-10346

Sandala, G. M., Smith, D. M., Marsh, E. N. G., and Radom, L. (2007) Toward an improved understanding of the glutamate mutase System, J. Am. Chem. Soc., 129 (6), 1623-1633
Schramm, V. L. (2001) Transition state variation in enzymatic reactions, Curr. Opin. Chem. Biol., 5, 556 –563

Shantanu Chowdhury and Ruma Banerjee (2000) Evidence for Quantum Mechanical Tunneling in the Coupled Cobalt−Carbon Bond Homolysis−Substrate Radical Generation Reaction Catalyzed by Methylmalonyl-CoA Mutase. J. Am. Chem. Soc., 122, 5417 – 5418

Shi, S. D. H. , Hendrickson, C. L., Marshall, A. G. (1998) Counting individual sulfur atoms in a protein by ultrahigh-resolution Fourier transform ion cyclotron resonance mass spectrometry: experimental resolution of isotopic fine structure in proteins, Proc. Natl. Acad. Sci. USA, 95, 11532 –11537.

Sikorski, R. S., Wang, L., Markham, K. A., Rajagopalan, P. T. R., Benkovic, S. J., and Kohen, A. (2004) Tunneling and coupled motion in the Escherichia coli dihydrofolate reductase catalysis, J. Am. Chem. Soc., 126 (15), 4778-4779

Suhnel, J., and Schowen, R. L. in Enzyme mechanism from isotope effects (Ed.: Cook, P.F.), CRC, Boca Raton, FL, 1991, pp. 3 –35

Sutciffe, M. J., and Scrutton, N. S. (2002) A new conceptual framework for enzyme catalysis. Hydrogen tunnelling coupled to enzyme dynamics in flavoprotein and quinoprotein enzymes,
Eur. J. Biochem., 269, 3096 –3102

Tang, K.-H., Casarez, A. D., Wu, W and Frey, P. A. (2003) Kinetic and biochemical analysis of the mechanism of action of lysine 5,6-aminomutase, Archives of Biochemistry and Biophysics, 418, 49–54

Toraya, T. (2000) The structure and the mechanism of action of coenzyme B_{12}-dependent diol dehydratases, Journal of Molecular Catalysis B: Enzymatic, 10, 87–106

Toraya, T. (2003) Radical catalysis in coenzyme B_{12}-dependent isomerization (eliminating) reactions, Chem. Rev. 103, 2095- 2127

Tsai, S. C., and Klinman, J. P. (2001) Probes of hydrogen tunneling with horse liver alcohol dehydrogenase at subzero temperatures, Biochemistry, 40(7), 2303-2311

Tsukamoto, T. (2003) Synthesis and biological evaluation of thiolbased inhibitors of glutamate carboxypeptidase II: Discovery of an orally active GCP II inhibitor, J. Med. Chem., 46, 1989-1996

Turro, N. J. (2000) From boiling stones to smart crystals: supramolecular and magnetic isotope control of radical-radical reactions in zeolites, Acc. Chem. Res., 33, 637 –646

Yoon, M., Patwardhan, A., Qiao, C., Mansoorabadi, S.O., Menefee, A. L., Reed, G. H., and Marsh, E. N.G. (2006) Reaction of adenosylcobalamin-dependent glutamate mutase with 2-thiolglutarate, Biochemistry, *45(38),* 11650-11657

Yoon, M., Kalli, A., Lee, H.-Y., Håkansson, K., and Marsh, E. N. G. (2007) Intrinsic Deuterium Kinetic Isotope Effects in Glutamate Mutase Measured by an *Intra*-molecular Competition Experiment, Angewandte Chemie International Edition, 46(44), 8455-8459

Wang, L., Tharp, S., Selzer, T., Benkovic, S. J., and Kohen, A. (2006) Effects of a distal mutation on active site chemistry, Biochemistry, 45 (5), 1383-1392

Warncke, K. (2005) Characterization of the product radical structure in the Co-II-product radical pair state of coenzyme B_{12}-dependent ethanolamine deaminase by using three-pulse H-2 ESEEM spectroscopy, Biochemistry 44, 3184-3193

Weisblat, D. A., and Babior, B. M. (1971) The mechanism of action of ethanolamine ammonia-lyase, a B 12 -dependent enzyme. 8. Further studies with compounds labeled with isotopes of hydrogen: identification and some properties of the rate-limiting step, J. Biol. Chem., 246, 6064 –6071

Whittaker, M. M., Ballou, D. P., Whittaker, J. W. (1998) Kinetic isotope effects as probes of the mechanism of galactose oxidase Biochemistry, 37 (23), 8426-8436

Wilde, T. C., Blotny, G. and Pollack, R. M. (2007) Experimental evidence for enzyme-enhanced coupled motion/quantum mechanical hydrogen tunneling by ketosteroid isomerase, J. Am. Chem. Soc., 130 (20), 6577-6585

Wolthers, K. R., Rigby, S. E. J., and Scrutton, N. S. (2008) Mechanism of radical-based catalysis in the reaction catalyzed by adenosylcobalamin-dependent ornithine 4,5-aminomutase, JBC, 283(50), 34615–34625

Wu, W. M., Lieder, K. W., Reed, G. H., and Frey, P. A. (1995) Observation of a second substrate radical intermediate in the reaction of lysine 2,3-aminomutase: A radical centered on the β-carbon of the alternative substrate, 4-thia-L-lysine, Biochemistry, 34, 10532-10537

Xia, L., Ballou, D. P., and Marsh, E. N. G. (2004) The role of Arg100 in the active site of adenosylcobalamin-dependent glutamate mutase, Biochemistry, 43, 3238-3245

Yahashiri, A., Howell, E. E., and Kohen, A. (2008), Tuning of the H-transfer coordinate in primitive versus well-evolved enzymes, ChemPhysChem, 9, 980–982

Yang, J., Mo, J. J., Adamson, J. T., and Hakansson, K. (2005) Characterization of oligodeoxynucleotides by electron detachment dissociation fourier transform ion cyclotron resonance mass spectrometry, Anal. Chem., 77, 1876 –1882